



Norwegian University of
Science and Technology

Testing of large-scale CNF synthesis reactor

Pablo Saz Perez

Chemical Engineering

Submission date: Januar 2012

Supervisor: Magnus Rønning, IKP

Co-supervisor: Fan Huang, IKP



MASTER'S THESIS 2011-2012

Title: Testing of large-scale CNF synthesis reactor	Key words: Large scale reactor; CNF synthesis; Ni; Carbon felt
Author: Pablo, Saz Pérez	Carried out through: August, 2011 January, 2012
Supervisor: Magnus, Rønning Co-supervisor: Fan, Huang	Number of pages Report: 63 Appendixes: 55
ABSTRACT Aim of work: This thesis consists of up-scaling and performing a CNF synthesis reactor from previous small scale works. CNFs were synthesized on supports to develop structured catalysts for water treatments. The supports are made up of carbon felt exchanged with Nickel as active clusters. The catalysts obtained had to be characterized by means of gravimetric, SEM, TPO and BET surface analysis. Estimation tasks of reactants and electrical power needs were accomplished. Moreover, checking of catalysts obtained was accomplished to validate the results released here.	
Conclusions: Similitude model has been a useful tool to establish previous conditions in scaling up. CNF deposition on CF was high despite the short times of reaction employed, whose yields of deposition ranged 70-130%. CNF deposition did not depend on the position in support, up to 4 hours of t_{batch} the crystallinity, size, shape and distribution of CNF were satisfactory. But as from 6 hours encapsulation phenomenon is present, reducing its quality. TGA provided that the thermal stability of CF-CNF was not modified in scaling up. BET surface analysis concluded that specific surface increased according to CNF deposition, even in presence of encapsulation. ITQ tests of CF-CNF synthesized at 4 in t_{batch} gave satisfying results for BrO_3^- removal. The activity of catalysts was high, since the yield of BrO_3^- elimination reached 100% in batch tests.	
Affirmation: I affirm that this master thesis has been carried out by myself, and the given references and appendixes are the only extern sources that I have been employing to finish this thesis.	
Signature:..... 23 rd , January, 2012	

Acknowledgements

Firstly, I would like to thank my supervisor Magnus Rønning, my co-supervisor Fan Huang and the professor De Chen; whose patience, explanations, advice, assistance with the appliances and comprehension, enlightened me at the beginning of my stay in NTNU. They have provided me the tools without which I could not have accomplished my project.

I would like to mention it was a pleasure to work in NTNU, especially in the catalysis group. I have spent a great time there, enjoying a good work environment. I expect to come back again.

Finally, I would like to thank my family, Erasmus program, and the international offices of NTNU and UPV for giving me the opportunity of carrying out my project abroad. It let me know a country such as Norway, which I will always carry in my heart.

Pablo.

List of abbreviations and symbols

Ai	Inner circular area of reactor i
BET	Brunauer-Emmett-Teller
(C)CVD	(Catalytic) chemical vapor deposition
CF	Carbon felt
CF-Ni	Carbon felt exchanged with Ni
CF-CNF	Carbon nanofiber/Carbon felt, composite
CF-CNF-Pd	Composite exchanged with Palladium
CNF	Carbon nanofibers
CNT	Carbon nanotubes
GTR	Gas phase heterogeneous tubular reactor
MFC	Mass Flow Controller
MWNT	Multi-walled nanotube
P	Pressure
P_i	Partial pressure of i
PSD	Pore size distribution
Q_T	Volumetric total flow
Re	Reynolds number
$rate_{CNF}$	rate of CNF growth
SEM	Scanning Electron Microscope
T, temp.	Temperature
t	Time
tbatch	Time of CNF synthesis reaction
τ	Spatial time of gaseous current inside reactor
τ_{CF}	Spatial time of gaseous current inside CF bed
TEOM	Tapered element oscillating microbalance
TGA	Thermo-gravimetric analysis
TPO	Temperature programmed oxidation
X_{CNF}	Fraction of CNF in CF-CNF
Y-CNF	Yield of carbon nanofibers deposition on support
% set	Percentage of deviation from maximum value
%CNF	Fraction of CNF in catalyst (after synthesis)

Table of contents

Acknowledgements	i
List of abbreviations and symbols	ii
Index of figures and tables	v
1. Introduction	1
1.1. Evolution and importance of CNF	1
1.1.1. Carbon nanofibers	1
1.1.2. Catalysts based on CNF structures	2
1.1.3. Type of packaging	3
1.2. Towards scale up	4
1.2.1. Situation	4
1.2.2. Different scales	5
1.3. Aim and scope	6
1.3.1. Presentation of this project	6
1.3.2. Objectives to achieve	7
1.3.3. Application	7
2. Literature review	8
2.1. Previous works in CNF synthesis	8
2.1.1. Synthesis (CCVD)	8
2.1.2. Gas phase heterogeneous tubular reactor, GTR	11
2.1.3. Synthesis reactants and catalytic supports	11
2.1.4. Operational variables	14
2.2. Scaling up method: similitude model	16
2.2.1. Overview	16
2.2.2. Scaling rules	17
2.3. Methods of analysis and characterization	17
2.3.1. Scanning electron microscope (SEM)	17
2.3.2. Thermo-gravimetric analysis (TGA)	18
2.3.3. Calculation of BET surface area by gas adsorption/desorption	18
3. Experimental	20
3.1. Scaling up accomplished	20
3.1.1. Hypothesis and limitations	20
3.1.2. Application of similarity model	21

3.1.3. Setup considered	22
3.2. Preparation of catalytic supports	24
3.2.1. Acid washing	24
3.2.2. Nickel impregnation	26
3.3. Synthesis of CNF	26
3.3.1. Previous settings	26
3.3.2. Reduction step	27
3.3.3. CNF synthesis step	28
3.4. Palladium deposition	29
3.5. Analysis and characterization of obtained catalysts	30
3.5.1. Scanning electron microscope (SEM)	30
3.5.2. Temperature programmed oxidation (TPO)	31
3.5.3. BET surface area and pore size distribution	32
4. Results and discussion	33
4.1. CNF content	33
4.1.1. Small scale test	33
4.1.2. Large scale experiments	34
4.2. Microscopic analysis	36
4.2.1. Small scale test	35
4.2.2. Differences according to time of reaction	39
4.2.3. Differences according to position in support	42
4.2.4. Estimation of mean CNF diameter	44
4.3. Temperature programmed oxidation (TPO)	46
4.4. BET surface area and pore size distribution	48
4.5. Deviations from similitude model	51
4.6. Electrical power needs	52
4.7. Gas requirements	53
4.8. Testing of catalysts obtained	55
5. Conclusions	57
References	59
Appendixes	63

Index of figures and tables

Figure 1: Scheme of converter package	4
Figure 2: Visualisation of current CNT growth mechanisms	9
Figure 3: CH ₄ , C ₂ H ₆ /H ₂ and C ₂ H ₄ decomposition on Ni catalyst at 823 K	13
Figure 4: Influence of temperature about CNF deposition rate, time of reaction and CNF deposition yield	15
Figure 5: Small scale scheme	23
Figure 6: Large scale scheme	24
Figure 7: Photography of large scale installation	24
Figure 8: Scheme of the setup of acid wash	25
Figure 9: SEM and TPO equipments employed for the characterization of catalysts	32
Figure 10: In relation to batch time, the tendency of: Y-CNF, XCNF in catalyst, Superficial and volumetric density	35
Figure 11: Y-CNF from laboratory tests	36
Figure 12: SEM pictures of CF-CNF interior, synthesized in the small-scale test	37
Figure 13: SEM pictures of CF-CNF surface, synthesized in the small-scale test	38
Figure 14: SEM pictures of CF-CNF, at X1.00K in zoom	39
Figure 15: SEM pictures of CF-CNF, at X5.00K in zoom	40
Figure 16: SEM pictures of CF-CNF, at X20.00K in zoom	41
Figure 17: SEM pictures of CF-CNF, at X1.00K in zoom, for tbatch of 4 hours	43
Figure 18: SEM pictures of CF-CNF, at X5.00K in zoom, for tbatch of 4 hours	44
Figure 19: Tendency of weight loss according to heating temperature	47
Figure 20: Pore size distribution for large scale experiments	49
Figure 21: Pore size distribution from laboratory tests	50
Figure 22: Results from ITQ experiments carried out in batch reactor	56
Figure 23: Results from ITQ experiments carried out in continuous plug flow reactor	56

Table 1: Design variables for both scales	22
Table 2: Operational variables for both scales	22
Table 3: Schedule of synthesis reactions	29
Table 4: Gaseous flows and % max set employed in each part of CNF synthesis	29
Table 5: Pd-salt requirements	30
Table 6: Characteristic parameters of CF-CNF obtained from small scale test	33
Table 7: Several properties measured from samples in large scale tests	34
Table 8: Characterization parameters of CF-CNF obtained from large scale tests	34
Table 9: Statistical parameters of the CNF diameter estimation for 2 hours and 4 hours of tbatch	45
Table 10: Statistical parameters of the CNF diameter estimation in relation to the position in CF-CNF composite	46
Table 11: Mass of sample employed, oxidation temperature of CNF and CF; for each analysis	48
Table 12: BET surface area data	48
Table 13: Mean volume of pore per gram	51
Table 14: Ratios of deviation referring to each type of similitude: dimensional, kinetic and dynamic	52
Table 15: Electrical potency required for heating stage	53
Table 16: Electrical potency required for reaction stage	53
Table 17: Argon needs per batch in CCVD stage	54
Table 18: Synthesis gases needs during CCVD reaction per CNF deposited. For a total flow of 1000ml/min (75%H₂/25%C₂H₆)	54
Table 19: Gas needs per batch in reduction stage	54

1. Introduction

1.1. Evolution and importance of CNF

1.1.1. Carbon nanofibers

The discovery of Buckminsterfullerene C_{60} [1], together with the recent discoveries of CNTs [2, 3] has involved intense research efforts with the expectation that these materials may have many unique properties and potential applications. These CNFs are structurally similar to fullerenes and they can have potential applications in fields such as composite materials science, hydrogen storage, electrochemistry, catalyst supports technology, field emission devices, etc. [4, 5].

Fullerenes consist of a large closed cage of carbon clusters and have several special properties that were not found in any other compound before. Before the first synthesis and characterization of the smaller fullerenes C_{60} and C_{70} , it was generally accepted that these large spherical molecules were unstable. However, in some Russian works had already calculated that C_{60} in the gas phase was stable and had a relatively large band gap [6, 7].

As is the case with numerous, important scientific discoveries, fullerenes were accidentally discovered. In 1985, Kroto and Smalley [8] found strange results in mass spectra of evaporated carbon samples. Enclosed, fullerenes were discovered and their stability in the gas phase was demonstrated. The researching of fullerenes had started.

Since their discovery in 1991 by Iijima and co-workers, carbon nanotubes have been investigated by many researchers all over the world. Their large length (order of microns) and small diameter (several nanometres) result in a large aspect ratio. They can be seen as the nearly one-dimensional form of fullerenes. Therefore, these materials are expected to possess additional interesting electronic, mechanic and chemical properties.

Especially in the beginning, all theoretical studies on carbon nanotubes focused on the influence of the nearly one-dimensional structure on molecular and electronic properties [9]. Afterwards, as it could be observed, the surface reactivity of these nano-structured fibrous carbons was found to be strongly dependent on their edge terminal structures, [10] and thereby the different physicochemical properties. During the last decades, it has been demonstrated that CNFs have great potential as novel catalyst supports in heterogeneous catalysis [10-12].

1.1.2. Catalysts based on CNF structures

In order to achieve a controlled growth of CNF besides a desired structural resistance, the researching in structured supports, due to its easy handling and utilization for desired applications, they can be more simply realized by means of theoretical production of well controlled nanostructure of carbon composites as they are also presented elsewhere [13, 14].

Towards history, different types of structural supports for CNF have been emerging, among which ones are included monolithic, membrane and arranged supports. Being the most widely employed ceramic monolithic supports in hydrocarbons conversions typical of CNF. Although initially, the unique use for these support was for catalytic conversions in combustion processes. [15]

Monolithic materials usually have been lifetimes relatively short related to their extreme operating and synthesis conditions. Such situation leaded Corning Inc. to develop monoliths made from cordierite, which seems to present an almost zero thermal expansion coefficient causing it essentially to be insensitive to temperature changes. Being increased its efforts in an advanced extrusion technology for the manufacture of monoliths giving a broad field of application. Monoliths made up of other ceramic and mixed materials were necessary to other applications have been developed and have become commercially available (e.g.: α - and γ -alumina, mullite, titania, zirconia, silicon de, silicon carbide). Taking into account all of them, they could be doped with other compounds so as to achieve and activity and selectivity, mainly metal crystallites are the active phase in many catalysts .Bulk metals can be fabricated into shapes suitable to go into a reactor, and although a low surface area of metal is provided, if reaction rates are high; since with operation at high temperature, then attractive conversions can be achieved. Diffusion effects can be reduced, and with short contact times conditions are ideal for selective oxidations/reductions, but products are usually limited to species thermally stable. Less thermally stable molecules require reaction at lower temperatures with compensating higher active phase surface areas to achieve economic reaction rates [15].

According to monolith shapes, structures with hexagonal channels became more popular due to the major distribution of the wash-coat around the channel, with a potential improvement in largely catalyst activity. Moreover, monoliths with hexagonal channels (also called honeycomb) have 7% lower thermal mass than square cells of similar hydraulic diameter [15].

In the last decades, the great progress in CNF synthesis field has been possible to be able to control the carbon nanostructures in addition to its growth, being promising to reach high

yields of productions and the distribution of clusters desired. Applying hydrotalcite supports in CNF or CNT synthesis is a relatively new idea and has only been reported for a limited number of studies [16–20].

Currently, last studies have been mostly involved in the development of hydrotalcite monoliths derived $\text{FeO}_3/\text{NiCu}/\text{Al}_2\text{O}_3$ in hydrocarbons decomposition [21–22].

More and more catalyst are submitted to extreme conditions, therefore several operative problems results in the formation of fine powder and its structural instability mainly at high temperature (e.g. phase transformation). That makes necessary the use of other types of supports. CNF have recently been reported to be suitable active phase supports for heterogeneous catalytic reactions, either in liquid or in gas phases. [23–25]. Such new catalytic materials displayed unusual behaviours as compared to generally used supported catalysts, due to their peculiar interactions and/or their high external surface area. Thus it was necessary the use of new catalytic supports more stables structurally and with properties closers to CNF, such as Graphite felt [26]. Several reports have provided great improvement in which surface area and mechanical strength of the composite were significantly enhanced when they were compared to its parent material [13, 14].

1.1.3. Type of packaging

In most reports, due to configuration and composition (as fibrous carbon nanostructures), CNF are synthesized as powders. That means these powders have to be collected in pellets, monoliths or felts. Therefore their applications are limited in fixed-bed, fluidized bed, and even slurry-bed reactors where a certain mechanical resistance and metallic bulk density are required as well [15, 27, 28].

In small scale is more common to obtain CNF directly as powder. Nevertheless in higher scales, the supports have to be more resistant in order to bear the increasing weight. This type of reactors can be approximated to a cylinder in which catalytic support is disposed; longitudinally synthesis reactants pass through it, behaving this flow approximately uniform unlike CNF production inside support.

A typical converter package, shown in Fig. 1, consists of a flexible mounting material (also called support) in order to hold the substrate; besides preventing gas leakage. Besides, a stainless steel can be mounted in order to protect the support and substrate, and a heat shield to protect adjacent components from excessive thermal radiation [15]. In contrast, a much bigger converter package (generally ceramic reinforced with metallic wires) provides positive investment pressure on the support. Such suport promotes symmetric entry of inlet gas, giving

thermal insulation to the substrate (thereby heating the substrate rapidly and keeping its exothermic heat for catalytic activity while minimizing the radial temperature gradient), and provides adequate frictional force at the substrate/support interface to resist vibrational and back pressure loads, otherwise this would result in a glide of the substrate inside the can [29].

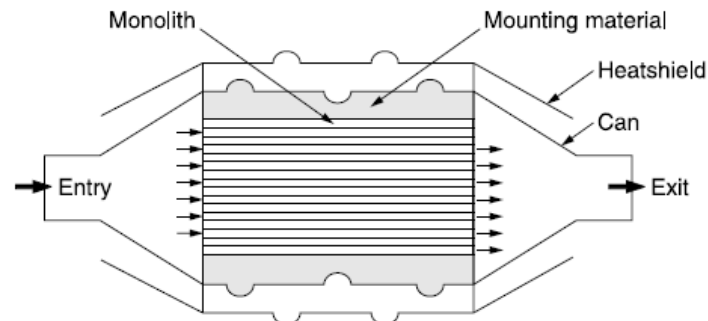


FIGURE 1: Scheme of converter package [15].

Classic fixed-bed catalytic reactors present several disadvantages: such as non homogeneous distribution of reactants, temperature (resulting in non uniform access of reactants to the catalytic surface and non optimal local process conditions), large pressure drop over the bed, and sensitivity to fouling by powder formation. Due to the random and chaotic behaviour of a fixed bed, scale up modelling and design of conventional reactors is very narrow having a limited number of degrees of freedom in its sized, testing and final implementation. An example of this problem can be shown studying the particle diameter. On the one hand, it should be small in general in view of catalytic activity and selectivity. On the other hand, the smaller the particle the greater the pressure drop is. [15]

1.2. Towards scale up

1.2.1. Situation

Often choosing between innovation and invention can be turned complicated, a good idea can involve good results in laboratory scale but later it can be very difficult to achieve a satisfactory industrial implementation in addition to obtaining business profitability. I.e. scale up must be a process in which the continuous innovation of the process has to be carried out.

In chemical engineering, this means to focus efforts on optimizing the process and putting it into practice rather than the invention of new products. The improvement of process, conversion and selectivity can be increase in order to get a better production, being the main

aim pretended by chemical industry business. In that situation, scale up methods play a main role in order to adapt lab-scale reactor into ones large enough to satisfy a production demand [30].

That is why reactors scaling is the principal task in which, with a well defined chemical synthesis in the laboratory, a determined valuable product can be obtained in an efficient way (e.g. maximizing reactor volume in order to reduce energy requirements per unit of product, changing the value of operating parameters for this new reactor disposition...)

Scale up development consists of “know how” synthesis learned in previous activities of researching such as: design of laboratory experiments, kinetic modelling... employing fluid dynamic experiments, mathematical models and testing in pilot/industrial plant. All these actions also have to be studied by an economical point of view. Some problems are present in whole this procedure [30]:

- Kinetic data are most of times inaccurate for other conditions and they cannot be extrapolated ensuring total control of results (e.g. in heterogeneous reactions, they can be masked by mass transport phenomena or changes of fluid regime)
- Laboratory equipment has rarely a direct correspondence to pilot plant and industrial technologies; in addition to devices such as: reactive beds, pipelines, columns of extraction and distillation; besides stirring systems, reactants, refrigeration units...
- And other problems which are worsened according to reactor size: corrosion, deactivation of catalysts, safety risk, waste treatments...

1.2.2. Different scales

Different ways exist to approach a scale up process depending on what is pretended to achieve and in which development degree it is [30].

- Laboratory experiments: they do not have to be exact replicas of industrial unit in order to obtain satisfactory results. They are usually employed mainly to check fluid dynamics models and mass transport properties, to obtain kinetic results and ranges of operation variables, check results and hypothesis.
- Pilot scale plants: they consist of obtaining testing results in order to be able to reach the industrial scale subsequent. That is why much more expensive devices and setups are necessary in that degree of scale. Pilot plants must be approximated as much as possible to industrial unit, because in strict sense a pilot plant is similar to industrial

unit; except that in the pilot scale are necessary an additional investigation and demonstration procedure.

Economically this scale is the most costly; it is not involved in industrial business, since it is a mean of testing previous laboratory works of a later industrial use. Hereby in a pilot plant can have decreased its tasks in order to saving resources (i.e. the use of mock-ups followed by a mathematical reasoning, separate studies in smaller pilot plants so as to join results later)

- Industrial units: they are mainly focused on computing and automation employment in order to collect data in real time by means of computing programs. The main goal of this scale is get a better understating of industrial process in order to be able to improve the control and optimization of operation parameters of the plant. It is very important to say that industrial facility is not modified since production would be interrupted and the purpose solutions would be very expensive.

1.3. Aim and scope

1.3.1. Presentation of this project

This project is part of a bigger project subsidized by European Union called *MONACAT*. It is carried out by several universities and companies of Europe.

Project: EU-FP7 (FP7/2007-2013), Grant Agreement No. 226347.

The actors implied in this master thesis are:

- NTNU (Norwegian University of Science and Technology), in whose facilities this thesis was carried out.
- Veolia Environmental Services: this company is a partner of NTNU interested in testing the structured catalysts obtained from this project to be employed in its own reactors. Veolia establishes several parameters according to its reactor specifications shown in *Appendix A*.
- UPV (Universidad Politécnica de Valencia): where the catalysts synthesized in NTNU are proved, specifically in ITQ (Instituto de Tecnología Química), references in *Appendix B*.

To get more information about *MONACAT* visit: www.monact.eu

1.3.2. Objectives to achieve

The main purposes of this project are to scale up and perform a CNF synthesis reactor from previous small scale works. CNFs are synthesized on a support to develop structured catalysts for water treatments.

It is required to synthesize CNF on carbon felt exchanged with Nickel at 2%w. Moreover, it is necessary to obtain the CNF as fish-bone shape according to Veolia specifications, *appendix A*. For those tasks, a literature review was necessary to determinate what dimensional and operational variables should be fixed.

The influence of reaction time (t_{batch}) and the distribution of CNF deposition had to be studied, besides establishing the optimum t_{batch} in function to the quality of CF-CNF.

This quality was characterized from gravimetric, SEM, TGA and BET surface analysis. It was required good quality in fibbers, homogeneity, high active surface, high chemical resistance... more than achieving large yields of deposition.

As secondary objectives were aimed: estimate electrical power and reactive needs from the operating conditions more satisfactory.

1.3.3. Application

These catalysts have to be able to remove several pollutants from water; such as bromates, atrazines... A palladium deposition 0.3%w had to be done to obtain catalysts for this task, obtaining CF-CNF-Pd. Their activity was tested in ITQ (UPV), in order to remove bromates from water and check how active the catalysts are.

Once these tests were accomplished and the results were satisfactory, CF-CNF synthesized would be ready to work in Veolia's facilities.

In *Appendix A* the Veolia's pilot plant is exposed. Moreover an interview with Veolia's crew shows which the specifications of catalysts are pretended.

2. Literature review

2.1. Previous works in CNF synthesis

2.1.1. Synthesis (CCVD)

In this part the different methods of CNFs obtaining will be explained in addition to their mechanism of growth, making emphasis in the way of synthesis considered as the most feasible and profitable one in order to achieve a synthesis scaled up of CNFs.

The reaction mechanism of CNFs is not very known continuing still as a subject of controversy. Initially a first mechanism was postulated consisting of three steps in which single CNTs are formed constituting a whole set called commonly CNFs. First a precursor to the formation of CNTs (generically called C_xH_y) is decomposed on the surface of the metal particle dispersed in catalyst support (metallic cluster). Then is formed an instable carbide particle, a rod like carbon (CNT) is formed rapidly. Secondly, a slow graphitisation occurs on its surface. This mechanism was purposed thanks in-situ TEM observations. The exact conditions depend on the technique used, which will be explained below [30]. That first analysis gives that it is necessary to take into account catalytic support and synthesis reactants composition once type of synthesis was chosen.

The current theory of CNF growth seems to be the same for any techniques of synthesis, even though several theories have appeared to explain the exact growth mechanism for CNFs. The most important theory postulates that metal catalyst particles are floating or are supported on graphite or another substrate. In which is presumed that the catalyst particles are spherical or flat-shaped, in which case the deposition will take place on only one half of the surface. The carbon diffuses along the concentration gradient and precipitates on the opposite half, around and below the bisecting diameter. However, it does not precipitate from the apex of the hemisphere, which accounts for the hollow core that is characteristic of these filaments.

Depending on growth direction, two mechanisms can be differentiated. By the base growth (extrusion) the CNT grows upwards from the metal particle that remains attached to the substrate. By the tip growth the metallic particle is detached and stays on the top of the growing CNT. Depending on the size of the catalyst particles, single-walled or multi-walled CNT are grown [31, 32]. Both ways of growth are shown in fig. 2.

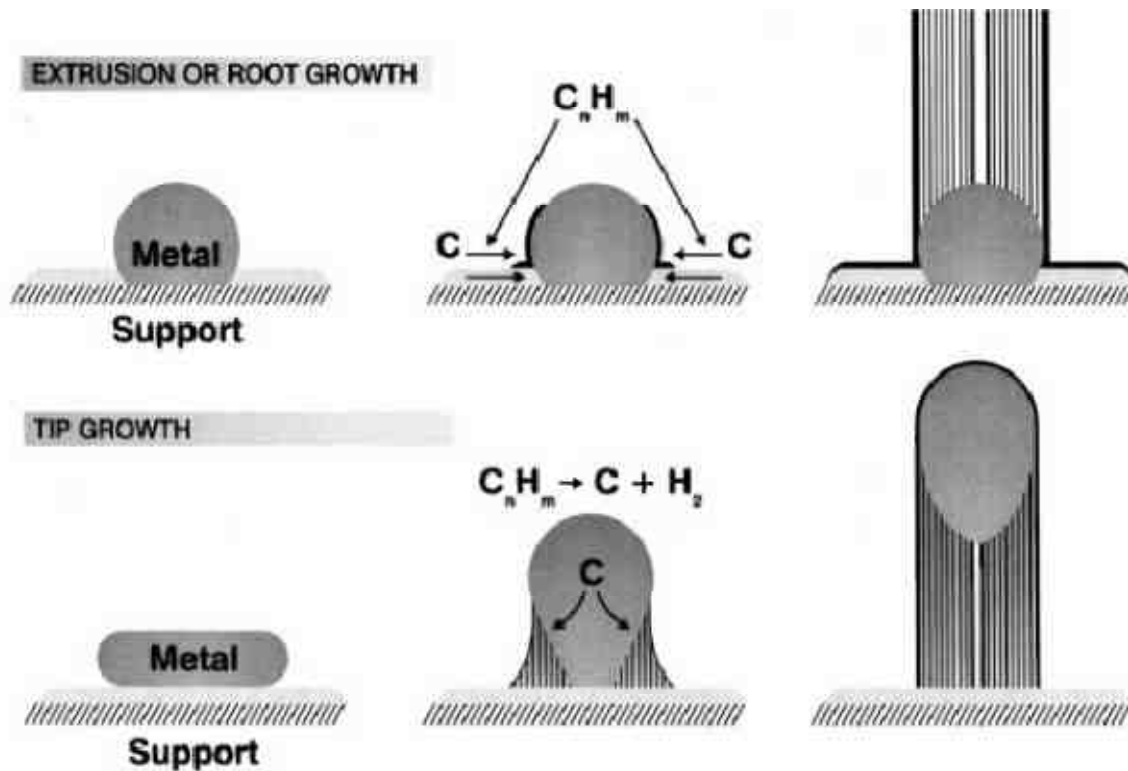


FIGURE 2: Visualisation of current CNT growth mechanisms [31, 32].

CNF are generally produced by three main techniques; arc discharge, laser ablation and chemical vapour deposition, although researchers are always innovating in more economic ways to produce these structures.

The carbon arc discharge method, initially used for producing C_{60} fullerenes, is the most common and perhaps easiest way to produce CNT of singled walled whose mechanism is very simple. This method creates CNT through arc-vaporisation of two carbon rods placed end to end, in an enclosure that is usually filled with inert gas (helium, argon) at moderate pressure [33]. A difference in potential creates a high temperature discharge between the two electrodes. The discharge vaporises one of the carbon rods and forms a small rod shaped, which is deposited on the other rod [34]. However, it is a technique that produces a mixture of components and requires separating CNT from the crap and the catalytic metals present in the crude product, besides the growth of CNT is very low obtaining low productions. Big amounts of energy would be necessary in a possible scaling up in order to increase CNT production [34]. Due to these reasons, this technique is discarded for that purpose.

In 1995, Smalley's group [35] at Rice University reported the synthesis of CNT by laser vaporisation. A pulsed [36, 37], or continuous [38, 39] laser is used to vaporise a graphite target in an furnace at 1200 °C. The main difference between continuous and pulsed laser is that the pulsed laser demands a much higher light intensity. The furnace is filled with helium

or argon gas in order to keep the pressure under-atmospheric. A very hot vapours plume forms, then expands and is cooled rapidly. Due to this, small carbon molecules and atoms quickly condense to form larger clusters, possibly including fullerenes. The reaction products obtained are quite pure with satisfactory properties [40]. Nevertheless this method has a high cost, which requires expensive lasers and high power requirement, which is not applicable at industrial scale at all.

Chemical vapour deposition (CVD) synthesis is carried out by putting a carbon source in the gas phase and using an energy source, to transfer energy to a gaseous carbon molecule. Commonly hydrocarbons are used as carbon sources. The energy source is used to “crack” the molecule into reactive atomic carbon. Then, the carbon diffuses towards the substrate (generally and structural support coated with an active metal). It is a technique with a wide versatility, thus a well known study of the process besides the operating variables being necessary. CVD consists of two-step process consisting of a catalyst preparation step followed by the factual synthesis of the CNT. Thermal annealing processes are required to obtain the active support resulting in the formation of metallic clusters on the substrate, from which the CNT will grow. That method may be employed so scale up at industrial scale, since an admissible production is obtained as well as it is a simple process in which the product aimed is quite pure. Mainly multi-walled CNTs are obtained and often riddled with defects; therefore a high study of process is essential in order to optimize it correctly being possible to control CNT diameter, length and shape. [41-44].

Summarising this last method is superior to laser ablation and arc discharge in terms of selectivity, yield, cost and energy requirements [45].

Catalytic CVD was first introduced and patented in 1979 [46]. Currently, CCVD is commonly used for the industrial purposes because the method has already been well investigated and it offers acceptable results at industrial scale [47, 48].

This technique was further studied by Doyle et al [49] and Matsumura [50, 51] showing a high deposition rate as its prominent feature. The synthesis production yield, which indicates the amount of CNT in the converted carbon, reached 90% [52].

Many groups have made extensive research efforts on the large-scale synthesis of CNFs and CNTs with controlled structures by (C)CVD, such as Ismagilov and co-workers [16, 53, 54], Baker and co-workers [55–60], B. Nagy and co-workers [61,62], Ledoux and co workers [63–65] and de Jong and co-workers [11,66,67]. These authors obtained desired carbon nanostructures acting in reaction conditions and gaseous feed mainly.

2.1.2. Gas phase heterogeneous tubular reactor, GTR

As it has been exposed previously, a tubular fixed bed reactor fed by gaseous reactants seems the best reaction system in order to achieve CNF growth since a large volume increment is produced from CNF formation in longitudinal direction (flow path) and these reactors enhance such volume change [70]. Besides it is feasible to scale up [68].

Unsupported catalysts are very efficient to achieve a high carbon yield, but they have a little or no control over the eventual CNF diameter or morphology [72, 73]. The use of supported catalysts returns in the growth of smaller structured carbon materials, and improve control over the structure of the catalysts during carbon growth; besides providing structural resistance to catalytic bed so important in large scale reactors. However, the supported catalysts have the disadvantage of a tedious removal of the support, in addition to a low productivity, possibly due to the low active metal loadings [73]. Thus in most cases, a compromise has to be found between the CNF quality and productivity.

In large scale, the main skills of fixed bed are to give a structural stability to support in order to achieve a controlled growth of CNF with a determinative shape according to its final employment, i.e. supported catalyst are the best option.

From laboratory-scale reports can be appreciated the most popular configuration is as tubular quartz reactor working at atmospheric pressure [69, 21, 22]; either employing CF [69, 71] or a ceramic compound [22, 21, 70] as catalytic support. Their dimensions were around 5 cm in diameter and 50 cm in bed length. Moreover experiments by TEOM [70] reactors validates the kinetics of this synthesis reaction (catalytic decomposition of hydrocarbon) in order to be scaled up.

Besides, it is exposed as an important condition a high temperature of synthesis ranging from 600°C to 1000°C, thus a furnace will be necessary to ensure those conditions.

2.1.3. Synthesis reactants and catalytic supports

In the first instance the possible reactants employed in synthesis of CNF on catalytic supports, fall into three groups: an inert gas, the gas containing carbon atoms and a chemical reducer. This election also depends on which bulk metallic particle is employed because the type of CNFs growth depends on the combination among the active metal, the type of carbon containing gas and the operating conditions. The CNF filament produced is associated with the physical dimensions of the metal particle [74]. The most suitable metals used for CNF growth are Fe, Co and Ni. It is suggested that morphology changes of metal surfaces at increased temperature with reactive gases can facilitate CNF growth. CNF growth stops when

the catalyst particle is deactivated, which usually takes place when carbon deposition is faster than carbon diffusion [74]. On the contrary, metal powders will produce large amount of CNFs, but provide little or no control over the final CNF diameter or structure [60, 70], thus they are not very suitable for CNFs synthesis for concrete aims.

Due of its abundance and low cost, methane is usually considered the best carbon feedstock for CCVD. Methane decomposition has also been considered as an alternative method to produce H₂ with CNFs as an additional product [75–78], that is why much effort has been dedicated to develop this mechanism in order to optimize the synthesis process of CNFs.

Ceramic catalysts (e.g. hydrotalcite) have been considered a viable choice for large-scale synthesis of CNF, since their structure makes it possible synthesize a high loading catalyst with a high dispersion and a narrow particle size distribution besides they have a high surface areas and high thermal stability [79, 63].

Mostly the studies related to CNF synthesis on hydrotalcites have been involved to Ni/Cu metallic clusters and performed CNF synthesis from methane decomposition, which have produced fishbone shape [16-19], whose structure forms typically an angle from 20° to 45°, between the fibre axis with the cluster.

To produce different carbon nanostructures, it is necessary to employ other metallic catalysts and gas precursors. Apart from fishbone structure, the most common ways to synthesise CNF's are platelet (angle of 90°) and tubes (angle of 0°), being this last one either multi-walled or single-walled. These structures provide different catalytic properties to the final CNF composite [80-82], depending on their final employment within catalysis field.

In several reports CO, CH₄, C₂H₄ and C₂H₆ have been employed as gases containing carbon [21, 22, 70], providing satisfactory results regarding process optimization, structure control and scaling up viability study.

The mixture C₂H₄/CO is very interesting for increase Y-CNF being employed with Fe/Ni-ceramic supports [21]; C₂H₄ is involved in CNF synthesis and CO permitting C=C bonds rupture increasing C₂H₄ decomposition. Unlike iron 100%, the higher nickel proportion is the more fish-bone structure is enhanced; moreover it provides temperature stability and a satisfactory dispersion on support. Although the deactivation appears earlier compromising Y-CNF [21, 22] but since it is not the main aim, nickel is considered as a good active metal according to Veolia's requirements. When nickel is employed with C₂H₄ or C₂H₆ yield problems decrease [21, 22] giving better results than iron in terms of production.

Other important gas for CNF growth is the hydrogen employed mainly as a chemical reducer, which is also the by-product of CNFs synthesis by decomposition of hydrocarbons. On one

hand, the higher hydrogen partial pressure is the more suppression of hydrocarbon dissociation there is, and P_{H_2} also increases the rate of gasification. On the other hand, an increase of hydrogen partial pressure helps prevent metal encapsulation of metals and it saturates the dangling bonds of graphite for preparing certain nanostructures [83]. That is why their concentration will have to be very accurately defined in order to find a relationship of compromise. Besides, H_2 serves as reducer in supports preparation passing from oxidized to reduced form of the metal, because in metallic exchange of support often are employed their salts.

Inert gases which can be used are mainly He, Ar and N_2 ; they are employed in tasks such as heating/cooling the reactor, support's activation, previous reductions of metallic bulks, and to adjust partial pressures of the other gases involved in the synthesis [21].

Summarising, depending on the type of metallic bulk ratio CNFs growth can change; due to its dispersion on the surface, proportion (or ratio, in metallic mixtures) and the size of cluster formed. This choice is more determinative in CNFs growth [21] than reactants election, which ones will be elected as a consequence.

Regarding to scaling up, it has no influence about CNFs shape, diameter and/or structure; thus catalytic support and synthesis gases have it [22].

Due to all these reasons, Nickel was chosen and the appropriate synthesis gases mixture. Figure 3 shows CH_4 , C_2H_6/H_2 and C_2H_4 decomposed on Ni catalyst at 823 K, it leads to an increased chemical reactivity of these molecules in chemical conversions [74]. When t_{batch} is a critical parameter (more vital than total CNF production) within large-scale; C_2H_6/H_2 is the best election, since higher productions of CNFs are achieved than with the other gases; at the beginning of synthesis. Although for long t_{batch} , C_2H_6/H_2 does not obtain a big production.

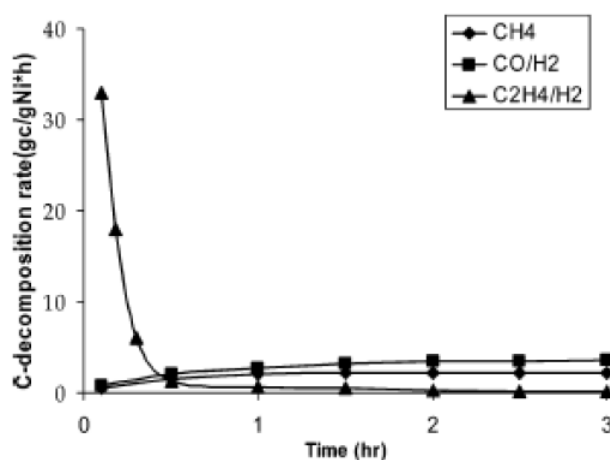


FIGURE 3: CH_4 , C_2H_6/H_2 and C_2H_4 decomposition on Ni catalyst at 823 K [74].

CNF formation on CF as support increases its mechanical strength and the surface area which can become two magnitudes higher, being also possible to deposit Nickel on its surface. The pore volume of the CF increases dramatically after forming CNFs on the felt and the pore density increases due to the higher surface area. The high pore density makes CNF interesting as a catalyst support [32] and its thermal conductivity allows the user to heat the reaction system internally by the Joule effect [84] and improving the heating compared to the unique external heat sources employment. That is why these types of catalytic supports are so interesting to Veolia Co.

2.1.4. Operational variables

The optimization of operational parameters for CNF growth is an important step towards economically feasible large-scale production. That is why; the most important conclusions of operational variables influence are presented here.

Operational variables considered to study are: $P_{H_2}/P_{C_xH_y}$ ratio, hydrogen content, spatial time of the gaseous inlet, temperature, batch time, total pressure and total pressure [22, 70]; either to be set or changed.

The dependence of Y-CNF on the $P_{H_2}/P_{C_xH_y}$ ratio inside reactor has been studied through both mechanistic [85–88] and experimental studies [89–96], that is why it is a parameter to take into account.

The control of hydrogen partial pressure is vital to control the growth from the carbon sources which depends on inlet hydrogen flow and C_xH_y decomposition inside reactor. High H_2 partial pressures were used for the synthesis with C_2H_6 which resulted in MWNTs with good quality and crystallinity. It has been suggested that the presence of hydrogen is needed in order to initiate nucleation of CNTs and thereby avoid the formation of onion-like structures [97]. However, some tubes are disposed at a small angle respecting to the fibre axis, which is most likely because H_2 is able to saturate the dangling bonds of the graphite sheets [98]. H_2 is also believed to influence the surface orientations of the catalysts by mesh restructuring [98]. Thus this parameter has to be fixed considering the support employed so as to obtain a determinative CNF structure. An optimum hydrogen partial pressure is given with respect to $rate_{CNF}$, over which the rate decreases significantly [70].

Total flow of synthesis gases is a parameter closely related to batch time. By increasing the space velocity, the hydrogen level is decreased and the $rate_{CNF}$ is increased; such CNFs could be synthesized faster at high t_{batch} for the low space velocity. However, a higher carbon formation rate (as a result from the higher space velocity and lower t_{batch}) leads to more

polymerization of surface carbon and thereby faster deactivation causing less total production of CNFs [70]. That involves t_{batch} cannot be decreased as much as it was pretended by increasing the total flow of synthesis gases.

A short spatial time resulted in a lower H_2 partial pressure in the catalyst bed through a lower C_xH_y decomposition conversion, leading to a higher rate_{CNF} , but improving the future deactivation of that catalyst [70].

Deactivation is a phenomenon which appears in function flow rate employed and hydrogen inlet flow, due to the saturation of active centres at a t_{batch} determined. Therefore observing that time of deactivation is obtained being able to establish t_{batch} [70].

As in each chemical reaction, temperature plays an important role within kinetics in addition to power requirements.

Typically on supported Ni catalysts, MWNTs are obtained at higher temperatures (700–1000 °C), while CNFs (Fishbone and platelet) are obtained at lower temperatures (400–700 °C) [22].

The effect of operating temperature in the rate_{CNF} of methane (C_xH_y) over Ni catalyst is shown in Fig. 4a [74]. It influences directly in CNFs formation rate being improved the higher temperature is; besides the higher temperature is the shorter deactivation times appear [74]. Y-CNF in function temperature is shown in Fig. 4b [70], in which is indicated an optimal one exists, where deactivation effect is countered by a high CNF deposition rate.

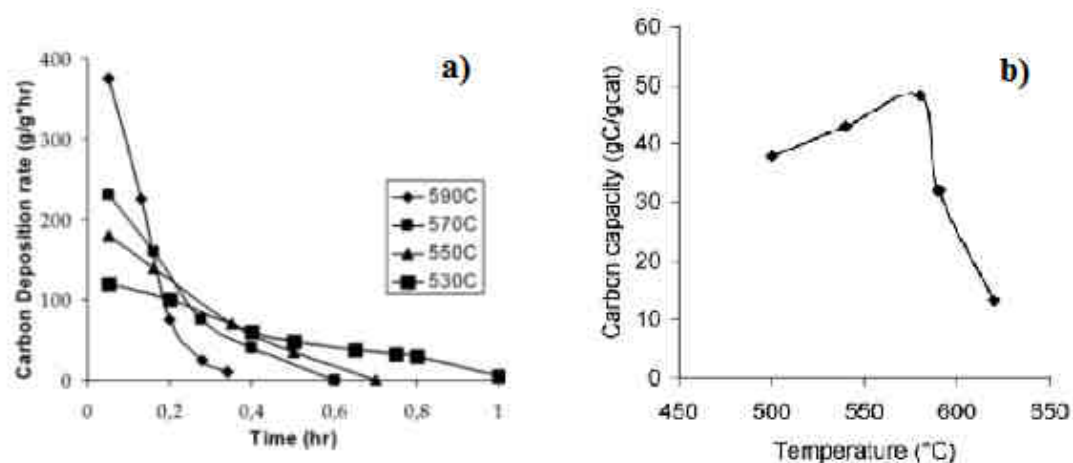


FIGURE 4a [74] and 4b [70]: Influence of temperature about CNF deposition rate, time of reaction and CNF deposition yield.

Total pressure effect is not studied since atmospheric pressure is fixed as design variable. The reason obeys to the principle of safety and economy. Pressurized reactors would involve

possible leakages increasing explosion risk by reactants which are very flammable. Besides pressurized reactors are much more expensive being necessary higher thicknesses and better materials. Moreover it has been demonstrated at atmospheric pressure the synthesis can be carried out [70].

2.2. Scaling up method: similitude model

2.2.1. Overview

Main applications of similitude model in engineering are focused on testing fluid flows conditions by means of scaled models, being the primary theory behind many textbook formulas in fluid mechanics. In this case, it comes to approach such knowledge in chemical reactors testing field treating to reproduce faithfully fluid conditions inside reactor in both scales: such as flow movement, transport and adsorption phenomena...

Engineering models are used to study complex fluid dynamics problems when calculations and computer simulations aren't profitable. Models are usually smaller than the final design, but not always. Scale models allow the testing of a previous design in mounting stages, and in many cases is a critical step in the development process [99].

The construction of a scale model, however, must be accompanied by an analysis to determine what conditions are tested under. While the geometry may be simply scaled, other parameters, such as pressure, temperature or the velocity and type of fluid may need to be altered if safety tasks if required [99].

The following criteria are required to achieve similitude:

- Geometric similarity – The model has the same shape as the application, usually scaled. In GTRs, dimensions considered are: inner diameter, length and thickness of the catalytic bed, total length, thickness and volume of reactor. Although this type of similarity is not usually employed in scaling up in which laboratory reactors are different in shape and composition from pilot and industrial scale.

$$D_1/D_2 = L_1/L_2 = L_{CF1}/L_{CF2}$$

- Kinematic similarity – Fluid flow of both the model and scaled up application must undergo similar time rates of change motions. (Fluid streamlines are similar) It is usually achieved keeping space velocity constant (in pug flow) or spatial time (in entire mixed flow)

$$vel_1 = vel_2 = Q_1/A_1 = Q_2/A_2 \text{ (plug flow)} \quad \tau_{CF1} = \tau_{CF2} \text{ (entire mixed flow)}$$

- Dynamic similarity – Ratios of all forces acting on corresponding fluid particles and boundary surfaces in the two systems are constant. In most cases, maintaining Reynolds number constant is normally enough, in testing works.

$$Re = (L_1 \cdot vel_1 \cdot \rho_1) / \mu_1 = (L_2 \cdot vel_2 \cdot \rho_2) / \mu_2$$

It is often impossible to achieve strict similitude during a scaling up. The greater the deviation from the application of operating conditions is, the more difficult to achieve similitude is. In these cases some aspects of similitude may be neglected, focusing on only the most important parameters. Such as temperature, total flow, material composition, gas current composition, type of catalytic support... [100]

2.2.2. Scaling rules

The process is carried out to satisfy the conditions above exposed, following these rules [99]:

1. All parameters required to describe the system are identified using principles from continuum mechanics.
2. Dimensional analysis is used to express the system with as few independent variables and as many dimensionless parameters as possible.
3. The values of the dimensionless parameters are held to be the same for both the scale model and application. This can be done because they are dimensionless and will ensure dynamic similitude between the model and the application. The resulting equations are used to derive scaling laws which dictate model testing conditions.

2.3. Methods of analysis and characterization

2.3.1. Scanning electron microscope (SEM)

SEM is a type of electron microscope that images a sample by scanning it with a beam of high-energy electrons in which it can be focused on the sample scanned by a set of deflection coils. As the electron beam is scanned over the specimen surface, both secondary and backscattered electrons are detected. The raster of the electron beam is synchronized with that of a cathode ray tube, and the detected signal then produces an image on the tube. Thus a fine electron beam is generated and electrons signals are registered efficiently making possible obtain high resolution. [101]

It covers a wide range of magnification from X10 to X1000K. The electrons interact with the atoms that make up the sample producing signals that contain information about either CNFs distribution in catalytic support or their general shape. Besides being able to distinguish their inner structure of CNFs, it is possible to detect the metallic bulk deposited on the support. [101]

For this project, this measurement allowed quantifying the structure of catalyst produced: surfacing texture, morphology, diameter of CNF, its homogeneity of CNFs in addition to its distribution on the support.

2.3.2. Thermo-gravimetric analysis (TGA)

Thermo-gravimetric analysis (TGA) is a type of test carried out on samples which are submitted on temperature variations which result in a weight change. Such analysis relies on a high degree of precision in three measurements: weight, temperature, and temperature change. A derivative weight loss curve can identify the point where weight loss is more apparent.

The analyzer usually consists of a high-precision balance with a pan (generally made up of platinum) plenty of the sample aimed. The sample is placed in a small electrically heated oven with a thermocouple to measure accurately the temperature. The sample is put in contact to a gas that will cause it a reaction, in which a weight loss depending on temperature is present. The atmosphere may be purged with an inert gas to prevent undesired reactions. A computer is used to control the instrument [102].

For this project, temperature of oxidation is the variable pretended to measure, in which the sample will be oxidized with air. This type of TGA is called TPO (Temperature programmed Oxidation)

2.3.3. Calculation of BET surface area by gas adsorption/desorption

Surface area and porosity are important characteristics of a catalyst, because they determine the capacity to hold active sites, the accessibility of them to reactants, and the level to transport of products from the catalyst surface to the bulk fluid which is facilitated too.

The most widely used method for determining the internal surface area (from $1\text{m}^2/\text{g}$ - $1200\text{m}^2/\text{g}$) is based on the adsorption and condensation of nitrogen at liquid nitrogen temperature using static vacuum procedures [103]. By measure the nitrogen molecules absorbed at monolayer coverage, the internal surface area can be calculated by BET equation [104]:

$$\frac{1}{V \cdot \left(\frac{P}{P_0} - 1\right)} = \frac{c - 1}{V_m \cdot c} \cdot \left(\frac{P}{P_0}\right) + \frac{1}{V_m \cdot c} \quad [69]$$

Where: P represents the partial pressure of nitrogen; P_0 represents the saturation pressure at the experimental temperature; V is the volume adsorbed at P ; V_m is the volume adsorbed at monolayer coverage; and c is a constant [104].

The assumptions for BET method are [105]:

- Gas adsorption at the flat and uniform surface
- No lateral interaction between the adsorbed molecules
- Multi-molecular adsorption

The total pore volume and pore size distribution (PSD) can be calculated by Barret-Joyner-Halenda (BJH) method. The BJH scheme can be summarized in the formula [106]:

$$v_{ads}(P_k) = \sum_{i=1}^k \Delta V_i(r_i \leq r_c(P_k)) + \sum_{i=k+1}^n \Delta S_i \cdot x_i(r_i \leq r_c(P_k)) \quad [69]$$

In this formula, $v_{ads}(x_k)$ is the volume of adsorbate (liquid nitrogen) at relative pressure P_k ; V is the pore volume; S is surface area and x is the thickness of adsorbed layer.

3. Experimental

3.1. Scaling up accomplished

3.1.1. Hypothesis and limitations

Most of this previous study has been focused on the development of synthesis conditions through empirical studies, with more effort put into kinetic studies in order to set t_{batch} and total flow according to deactivation time and deposition rate; moreover in this synthesis there is an optimum temperature.

As it has been shown previously, TEOM studies of this kind of process have provided that operating variables have no significant effect in a scaling up, regarding to pretended shape, yield... [70]. Thus the best values of variables from small-scale reports can be chosen for large-scale synthesis.

The catalytic support purposed is carbon felt disposed in discs which are perpendicular to gas flow direction, which supports good structural and chemical resistance as well as it is easier to shape than for other supports.

From *Appendix C* given by Carbon Lorraine Co. shows the conditions to deposit CNF-fishbone on CF the active metal is Nickel (2% in weight) and the synthesis gases are hydrogen and ethane. The synthesis was carried out at atmospheric pressure at 650°C. Despite having operational conditions established, a small scale test had to be performed to validate if the quality of CNF deposition was the suitable one or it was not.

Due to its availability, Argon was the inert gas used in this project.

The reactive flows are mainly limited by the mass flow controllers employed, whose maximum flows are:

- H_2 (MFC for CO) 1000ml/min.
- C_2H_6 (MFC for CH_4) 1000ml/min
- Ar (MFC for CO) 300ml/min.

As the gases employed were not the same as pretended gas of MFC, these devices were only used as volumetric flow controllers.

This limitation determines the total flow inside reactor.

The reactors supplied for both experiments were already prefixed, giving the deviation from a scaling up process which satisfied of total similarity.

Since the reactors in this type of experiments are big in relation to fixed bed and total flow; complete mixed reactor may be considered being the same composition of gases inside reactor and in outlet current. In the only design variables in which could be elected are the length of fixed bed (total and active), each disc of CF had 0.6cm which active part is the same in both experiments. However in large scale, 2 discs only washed with acid have been disposed ahead and behind active disc; for the purpose of homogenizing the flow across bed to achieve turbulence increment, improving CNF deposition in all disc part equally.

The variable to study is time of reaction, being a batch process because in each reaction the fixed bed has to be replaced.

3.1.2. Application of similarity model

From the three scale-up rules explained in point 2.2 it has been worked out the three relations that our model must to accomplish, according to the conditions of this case. The whole process has been developed in *Appendix D*, here are presented its results:

- Dimensional similitude: $(D_1/D_2) = (L_{CF1}/L_{CF2})$
- Kinematic similitude: $(D_1^2 \cdot L_{CF1})/(Q_1) = (D_2^2 \cdot L_{CF2})/(Q_2)$
- Dynamic similitude: $(Q_1/Q_2) = (D_1/D_2)$

Where: Q is the total flow of gaseous current which pass across reactor; D is the inner diameter of reactor besides the diameter of fixed bed; and L_{CF} is the length of fixed bed (active carbon felt and non active)

In Table 1 are presented the main dimensions of both reactors besides both beds; the scale relation presented gives the division between large-scale and small scale measure.

In Table 2 are shown the variables of operation according to the restrictions and *Appendix C* already exposed. They are only presented the 2 main reactions of this synthesis: the previous reduction of CF and the reaction CVD of CNFs. The election of the operational variables will be developed in the point 3.3.

The variables related to chemical reactions, such as T, P, gas composition...; have been kept constant according to scale change. Only physical parameters have been considered to be changed. That is why this test is suitable for compare mass transport and deposition of CNF in CF (which is a physical phenomenon) because flow mechanics is the only one compared in relation geometry of model and other physical properties.

Summarising, the analysis of similarity is based on fluid dynamics theory, since chemical reaction is pretended being equal in both scales.

Design variable	Small scale test	Large scale	Scale relation
D (cm)	4.0	10.0	2.50
L (cm)	45.0	135.0	3.00
LCF (cm)	0.6	1.8	3.00
LCF ACTIVE (cm)	0.6	0.6	1.00
Reactor/bed area (cm ²)	12.6	78.5	6.25
Active bed volume (cm ³)	7.5	47.1	6.25
Reactor volume (cm ³)	565.5	10602.9	18.75

TABLE 1: Design variables for both scales.

Operational variable	Small scale test	Large scale	Scale relation
Total pressure (atm)	1	1	
Heating gradient (°C/min)	20	20	
Time of heating (min)	31.6	31.6	
Reduction temperature (°C)	650	650	
Reduction time (min)	120	120	
Total flow in reduction (ml/min)	100	400	4
% Hydrocarbon in reduction (% vol)	0	0	
% Argon in reduction (% vol)	75	75	
% Hydrogen in reduction (% vol)	25	25	
Reaction temperature (°C)	650	650	
Total flow in reaction (ml/min)	100	1000	10
% Hydrocarbon in reaction (% vol)	25	25	
% Argon in reaction (% vol)	0	0	
% Hydrogen in reaction (% vol)	75	75	
Residence time in reaction (min)	5.65	10.60	1.88

TABLE 2: Operational variables for both scales.

3.1.3. Setup considered

In both models, mass flow controllers and gas bottles were the same type.

Flow controllers “El-Flow” and the flow controlling interface “Hi-Tech” supplied by Bronkhorst were used for establish the gas flows. The model was: *RS232 INTERFACE FOR DIGITAL MASS FLOW / PRESSURE INSTRUMENTS* [107].

EL-FLOW® Select Series Mass Flow Meters/Controllers are thermal mass flow meters of modular construction for laboratory works, generally controlled by pc-board housing. Control valves can either be integrally or separately mounted, to measure and control gas flows. [107].

Gas bottles have a regulator valve which adjusts the outlet flow of each gas. They are connected to MFCs by means of a pressure-reducer appliance, this system consist of 2 manometers and 2 valves. The working of the dosage system is the following: the gas bottle’s valve regulates the flow until achieve a pressure in the first manometer of the system around

100atm; the first valve of the pressure-reducer appliance decreases the pressure down to 5atm, which can be seen by the second manometer; finally the last valve is opened totally supplying gas at 5 atm whose flow is controlled by MFCs. Later, gas currents are mixed before entering to the reactor; which is controlled by a valve.

Small-scale setup is an installation already fixed. The oven is integrated to a quartz reactor. The heating rate is controlled by a PID controller, a “Eurotherm – Thermostat”.

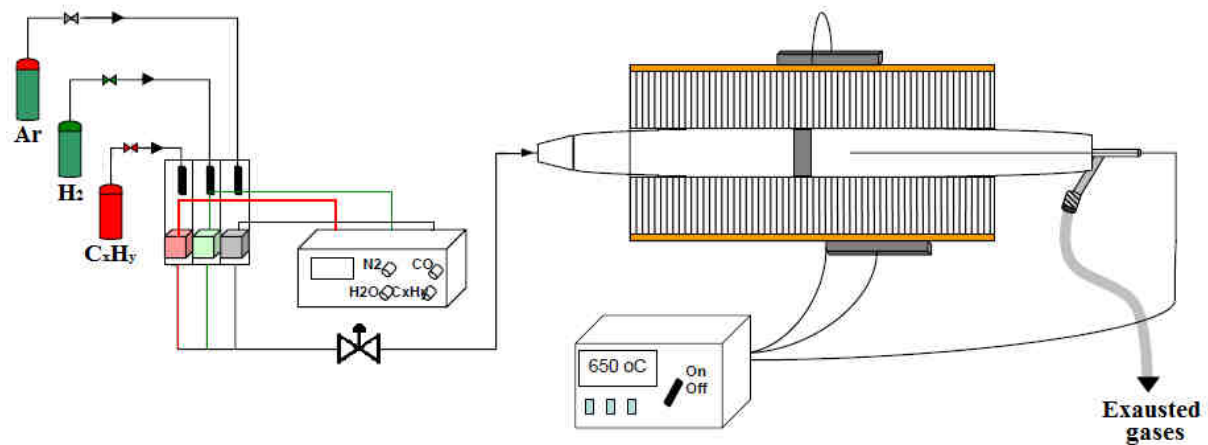


FIGURE 5: Small scale scheme.

In large scale, the reactor considered is tubular made up of refractory ceramics reinforced with metallic wires transversally and longitudinally.

Mass flow control setup is a flow bus (Type RS232) Hi-Tech; managed digitally by means of a computer. The large scale oven is: *1200°C 3 Zone Horizontal Split-Hinge Tube Furnace (maximum potency: 4500W) model: HZS 12-900 [108]* It consists of three PID controllers (Eurotherm controls) to keep a temperature constant or modify it changing temperature profile.

- 1 central PID temperature controller: model 2416. (Main PID controller)
- 2 entrance/exit PID temperature controllers: model 2132. (Control by difference from main PID)

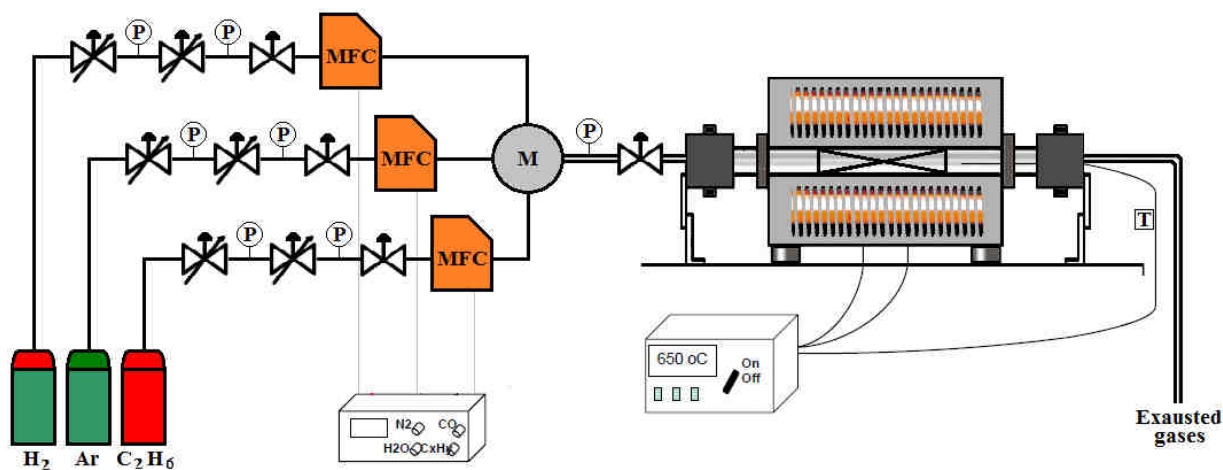


FIGURE 6: Large scale scheme.

In fig. 7 large scale setup can be seen, in which its different zones can be distinguished:



FIGURE 7: Photography of large scale installation.

3.2. Preparation of catalytic supports

3.2.1. Acid washing

The purpose for this step was to become rougher CF surface by addition of CO_3^- in order to increase CF activity. Besides it was also achieved the removal from CF of all impurities

containing in addition to cleaning it to enhance a correct subsequent deposition. The acid considered was nitric acid (HNO_3) with a purity of 65% in volume.

This wash was carried out at 100°C and 1atm, thus a refrigerating coil was necessary so as to avoid acid evaporation which was condensed on the inner walls of the coil before it could reach its top part. A vessel was employed for this aim in which CF supports and acid are introduced. It was connected directly to the refrigerating coil, apart from being sunk in a bath of silica-oil heated and stirred by a thermal-magnetic agitator. The temperature of bath was controlled by means of a thermocouple connected to the magnetic agitator.

Whole mounting is shown in fig. 8:

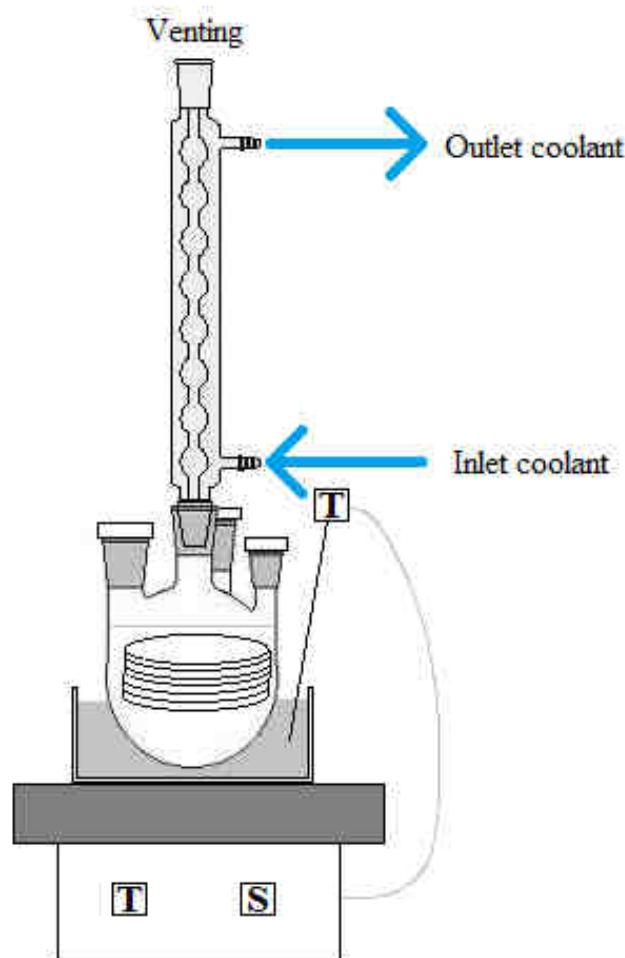


FIGURE 8: Scheme of the setup of acid wash.

This operation lasted 1 hour; afterwards the vessel was cooled by turning off the heating device. Once room temperature was reached, CF supports were neutralized by distilled water until achieve 6 pH, removing acid dissolution from vessel and introducing new distilled water, as many times as necessary.

At last, wet CF supports were introduced into an oven for 12 hours at 100°C to remove all water remaining.

3.2.2. Nickel impregnation

The following step consisted of achieving the deposition of 2%w of active metal (Nickel) on CF supports to can be put in the reduction and synthesis reactions. The method was carried out by pouring of a salt Ni containing dissolved in ethanol on CF support.

The salt employed was $\text{Ni}(\text{NO}_3)_2 \cdot 6\text{H}_2\text{O}$ which was weighted the following amount in relation to mass of CF, according to *Appendix E*: $m_{\text{SaltNi}} = (m_{\text{CF}}) \cdot 0.1042$. Thus each CF support had to be weighted too.

Salt weighted was dissolved in approximately 40ml of ethanol (96%) employing a magnetic stirred to improve its dissociation. This dissolution was poured on CF directly.

Wet supports were put in venting room so as to let evaporate ethanol, having only the salt on a uniformly distributed way in CF.

The whole procedure was provided by Lorraine Carbon Co. shown in *Appendix C*.

3.3. Synthesis of CNF

3.3.1. Previous settings

The calibration of volumetric flow controllers is a task which had to be considered, since always a drift of flow measured appears due to flow meters employment. This discrepancy usually is lineal; hence working out calibration curves at different flows this error can be calculated.

In small-scale tests, calibration curves are given in advance as shown in *Appendix F*.

The calibration of large scale plant was done by soap-bubble flow meter in which the ascension time of a soap-bubble across it was measured in accordance with its volume path. Therefore set-flow (or percentage of max set-flow) versus measured flow was plotted. All data and graphics are put in *Appendix F* as well.

Before any planed reactions safety checks must be carried out. Previous, load test employing argon would determinate if there was any leakage throughout installation; in addition to cleaning inner reactor from possible initial dust. Leakage detector fluid was applied on over joint in whole pipeline watching any possible bubble. The used flow of argon was the highest

possible, i.e. 100% about max flow. In general, joints, nuts, valves, sections changes, manometers were inspected in order to minimize the accident possibility due to leakages.

In each CF loading/unloading in reactor, the reactor had to be clean from hydrogen and ethane as well as all joints manipulated had to be checked again.

Either reduction or synthesis step, high temperatures were submitted to CFs which could lead it to degradation in oxidant atmosphere. For this reason, there had to ensure most of initial air inside reactor had been displaced by inlet argon waiting for a time long enough. In *Appendix GI* was calculated that around 65min of cleaning with argon would remove 90% of air from reactor, which was enough long to avoid possible reactions of oxidation during heating period.

Providing hydrogen is used, a H₂ detector must be placed close to reactor, taking special care in outlet part because the hottest and richest in hydrogen current pass across it.

For this project a risk assessment was carried out by the researcher Fan Huang, this report is shown in *Appendix I*.

3.3.2. Reduction step

The purpose of this step was to reduce the Nickel salt from Ni⁺² to Ni⁰, removing the other elements of the salt. Since it is aimed the support is mostly made up of CF and metallic Nickel clusters, which makes possible CNF formation on them. The reduction of supports is divided into 3 stages: heating, reduction and cooling down. The procedure in order to perform it at small scale has been provided by Lorraine Carbon Co.; which is totally exposed in *Appendix C*. For this thesis Fishbone procedure was chosen, because it is the shape of CNF pretended.

The reducer gas was a mixture of H₂ and Ar.

From that appendix, large scale conditions were established modifying only total flow according to the limitations of volumetric flow controllers.

This reaction was carried out at atmospheric pressure; the temperature profile and flow ratios are the following:

- Heating: (from room temp. to 650°C) at a heating rate of 20°C/min. Employing pure Argon as gaseous current. The time for this stage was 31.6 min. The flow was around %SET (Ar)=100%.
- Reduction: at 650°C for 2 hours. Using 75% (vol) of Ar and 25% (vol) of H₂.
- Cooling down: natural cooling down (from 650°C to room temp.) Employing around 30ml/min of pure Argon as gaseous current of cleaning for all night, around 14 hours.

In small scale tests, total flow was the same as *Appendix C*: 100ml/min.

In large scale the flow limitation is given by Ar flow meter (300ml/min max.) thus the reduction flow was $(300/0.75)$ 400ml/min. For heating stages the flow was around %SET (Ar)=100%.

3.3.3. CNF synthesis step

The aim of this step was to deposit CNFs on CF exchanged with Nickel, by means of CCVD mechanism. This reaction is divided into 3 stages: heating, reaction and cooling down. The operational conditions were submitted by *Appendix C*, as fish-bone structure.

For large scale, inlet flows were worked out according to the limits of volumetric flow controllers.

This reaction was carried out at atmospheric pressure; the temperature profile and flow ratios were the following:

- Heating: (from room temp. to 650°C) at a heating rate of 20°C/min. Employing pure Argon as gaseous current. The time for this stage is 31.6 min. The flow was around %SET (Ar)=100%.
- Reduction: at 650°C during the time of batch. Using 75% (vol) of H₂ and 25% (vol) of C₂H₆ in large scale and C₂H₄.
- Cooling down: natural cooling down (from 650°C to room temp.) Employing around 30ml/min of pure Argon as gaseous current of cleaning for all night, around 14 hours.

In small scale tests, total flow was the same as *Appendix C*: 100ml/min. The gas carbon carrier has been ethylene because there was not availability of ethane in small scale setup. This change of gas is not so important due the fact that the aim of large scale test is only validate laboratory works in relation with distribution of CNF and quality.

In large scale the total synthesis flow was 1000 ml/min; limited for the maximum flow hydrogen (1000ml/min). For heating stages the flow was around %SET (Ar)=100%.

Since small scale test had not as a purpose to achieve a great deposition of CNFs, the t_{batch} considered were relatively low, 2 hours [69].

Regarding time of batch in large scale synthesis, the previous works had given as result that in small scale 20 hours of reaction provide yields of CNF deposition around 90-110% for our conditions [69]. As our large-scale reactor is bigger in relation to gas flow and CF load, it was predictable that t_{batch} optimum were shorter than 20hours. As an increase of CNF deposition is not a main objective short t_{batch} were considered, thereby reducing head loss caused by CNF deposition is much more important in large scale in addition to CNF quality improvement. Because of these reasons, the times of reaction were 2, 4, 6 and 10 hours.

In summary, in Table 3 is presented the schedule of each synthesis carried out besides their mass of CF, batch time and mass of Ni-salt used for Ni impregnation related to the mass of CF (mass before):

Reaction date	N° Sample	Test	Mass before (g)	Batch time (h)	Mass salt (g)
04/11/2011	1	Small scale test	0.7728	2.00	0.0805
28/11/2011	2	Large scale 1	4.0209	6.00	0.4190
30/11/2011	3	Large scale 2	4.2311	10.00	0.4409
01/12/2011	4	Large scale 3	3.9460	4.00	0.4112
05/12/2011	5	Large scale 4	4.0714	2.00	0.4242

TABLE 3: Schedule of synthesis reactions.

In Table 4: according to the calibration curves, they are presented the flows of each gas employed and their % set already calculated, for both reactions.

Gas of the current	Hydrocarbon		Argon		Hydrogen	
Parameters	Flow (ml/min)	%SET	Flow (ml/min)	%SET	Flow (ml/min)	%SET
Small scale test (red)	0.0	0.0	75.0	6.3	25.0	11.0
Small scale test (synt)	25.0	0.9	0.0	0.0	75.0	32.4
Large scale (red)	0.0	0.0	300.0	79.4	100.0	9.2
Large scale (synt)	250.0	33.8	0.0	0.0	750.0	58.5

TABLE 4: Gaseous flows and % max set employed in each part of CNF synthesis.

3.4. Palladium deposition

The purpose of this step was to deposit palladium on CF-CNF already synthesized to be tested as catalyst for bromites/bromates removal, in aqueous effluents. The CF-CNF exchanged with Pd is sent to ITQ (UPV) Valencia (Spain) in order to validate its capability as catalyst.

This deposition consisted of achieving the deposition of 0.3%w of active metal (Palladium) on CF-CNF. The method used was a pouring of a salt pd containing dissolved in ethanol on CF-CNF.

The salt employed was $(\text{N}_2\text{O}_8\text{Pd}) \cdot 2\text{H}_2\text{O}$ which was weighted the following amount in relation to mass of CF-CNF, according to *Appendix J*: $m_{\text{SaltPd}} = (m_{\text{CF-CNF}}) \cdot 0.007523$.

Thus each CF-CNF supports had to be weighted before deposition.

Salt weighted was dissolved in approximately 20ml of ethanol (96%) employing a magnetic stirred to improve its dissociation. This dissolution was poured on CF directly.

Wet supports were put in venting room so as to let evaporate ethanol and consequently have only salt on uniformly distributed way.

The whole procedure was planned by the researcher Fan Huang, according to ITQ requirements.

In Table 5 are shown which samples are obtained from support, to be exchanged (4 and 6 hours), besides its weight, CNF content and mass of Pd salt required.

N° Sample	From test	mCF_CNF (g)	Mass CNF (g)	Mass salt (g)
2A	Large scale 1A	1.1231	0.6361	0.0084
4A	Large scale 3A	1.5194	0.7310	0.0114

TABLE 5: Pd-salt requirements.

The sample, which finally would be sent, would depend on its quality according to its analysis in chapter 4.

3.5. Analysis and characterization of obtained catalysts

3.5.1. Scanning electron microscope (SEM)

The appliance used was *ZEISS SUPRA-55VP FESEM [109]*.

For the CF-CNF obtained from small scale test 2 samples were extracted, one from surface and other from inner part. Thus the comparison between the surface and interior would give information about the homogeneity of deposition, being more critical in large scale. The resolutions employed are the following:

- X248 and X1K: their employment permits us to evaluate CNF distribution on CF besides check if the deposition is uniform throughout support, if there was places on CF in which deposition have not carried out.
- X5K: with this zoom can be studied the homogeneity of CNFs, if there was a high difference in density of CNFs.
- X20K: in which CNF can be appreciated, it was used to check if the fibbers are so different between them and see if the shape was tubular or not. In case, diameter size could be estimated.

For CF-CNF synthesized from large scale experiments, the samples to be analyzed were extracted from the central inner part of the CF-CNF; thus 4 samples of central part were analyzed for 2, 4, 6 and 10 hours of t_{batch} . Besides, 3 samples more would be obtained from

the support with better characteristics; these samples were extracted at 33mm, 67mm from centre and at its edge, all of these from the inner part. The purpose of this was to evaluate the distribution of CNF on CF, its homogeneity besides finding out the mean diameter of fiber.

The resolutions employed for each of 4 samples were the same as small scale analysis: X248, X1K, X5K and X20K; whose criteria were the same as well.

Therefore 28 images were obtained in total, 20 for large scale and 8 for small scale. It should be pointed that big zooms were not used, hence fish-bone shape could not be checked, which was already presupposed according to conditions chosen.

3.5.2. Temperature programmed oxidation (TPO)

The device employed was a TGA, *NETZSCH STA 449C [110]*. This type of analysis is based on the measurement of weight loss by the oxidation of the sample at high temperature using air.

The temperature profile was:

- Heating at 10°C/min from room temperature to 800°C, in whose period weight loss was registered in a file.
- Natural cooling down from 800°C to room temperature.

As oxidant current was employed 20ml/min of air and as protective current was employed 25ml/min of Argon.

Carefully, from 10mg to 20mg of sample were added to precision balance by the help of tweezers.

TPO was accomplished after pre-treatment on the CF in addition to each catalyst obtained (2, 4 and 6 hours of t_{batch}) to identify the effect of CNF formation.

From this analysis were obtained several values of the weight loss of the sample versus temperature in heating stage. It is expected that there is significant decrement of weight close to reach the temperature of oxidation and just in this temperature two inflexion points could appear, the first one of CNF oxidation and the other one of CF oxidation. That is why; the temperature of oxidation can be calculated by means of the method of first derivative, in which a maximum/minimum can appear if first derivative of weight loss is represented versus temperature of heating.

These data can give information about: how much degradability is gained due to synthesis, in CF support and how resistant the CNF formed are.

In summary, in fig. 9 are shown both equipments, SEM and TPO analysis:

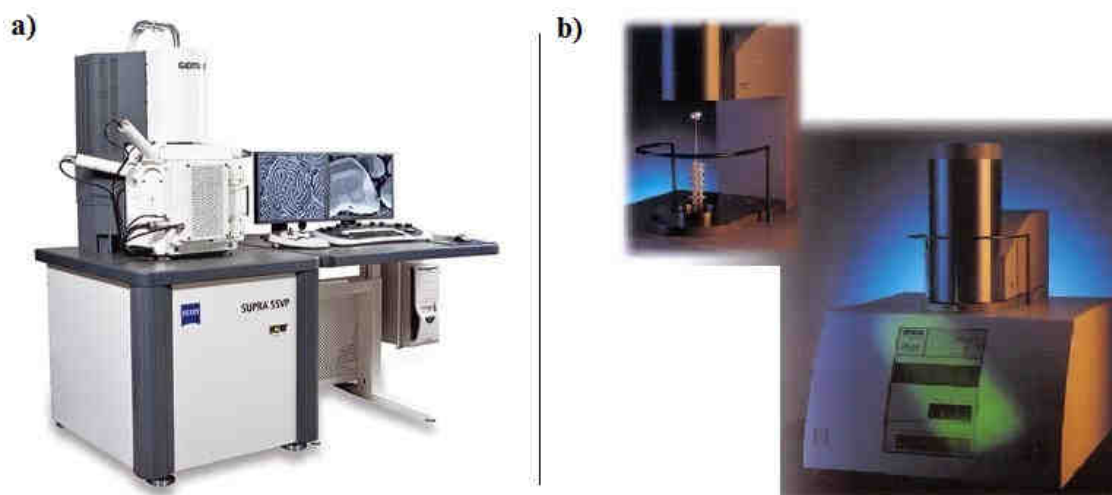


FIGURE 9a and 9b: SEM and TPO equipments employed for the characterization of catalysts.

3.5.3. BET surface area and pore size distribution

This analysis does not belong directly to this project; their data were collect from the study included in *MONACAT* project, which is carried out by the researcher Fan Huang.

The data required are:

- Specific BET surface of CF-CNF synthesized (in m^2/g)
- Pore size distribution, whose data are relative pore volume ($\text{cm}^3/\text{g}\cdot\text{\AA}$) versus pore diameter (\AA).

From pore size distribution, relative porosity can be estimated as the area below curve, according to the integration method of trapezoids. This area can be directly related to relative porosity of each catalyst, establishing a way of comparison.

4. Results and discussion

4.1. CNF content

CNF content is determined by gravimetric way, all samples analyzed were weighted before Ni exchange and after CVD reaction. (Note: mass of support before synthesis has been shown in 3.3.3 point of this project)

4 parameters are calculated for each sample analyzed from large scale experiments:

- Yield of CNF deposition: it is defined as the percent in weight of CNF deposited on catalytic support (in this case it is the mass of CF plus Nickel deposited), this parameter is calculated for small scale test as well. From *Appendix K1*, this is the formula of its calculation:

$$\%Y\text{-CNF} = (100 \cdot (m_{\text{after}} - 0.9241 \cdot m_{\text{before}})) / (0.9241 \cdot m_{\text{before}}) \quad (\text{for small scale})$$

$$\%Y\text{-CNF} = (100 \cdot (m_{\text{after}} - 1.02 \cdot m_{\text{before}})) / (1.02 \cdot m_{\text{before}}) \quad (\text{for large scale})$$

- Fraction of CNF in catalyst: it is defined as the mass of CNF deposited per the mass of total catalyst synthesized. Its formula was calculated in *Appendix K2*, which is the following:

$$X_{\text{CNF}} = (m_{\text{after}} - 1.02 \cdot m_{\text{before}}) / (m_{\text{after}})$$

- Superficial density: it makes reference to the mass of CNF deposited on transversal surface of carbon felt. It is calculate as the quotient between mass of carbon deposited and the area of CF discs.
- Volumetric density: it makes reference to the mass of CNF deposited in whole carbon felt. It is calculate as the quotient between the mass of carbon deposited and the volume of CF discs after synthesis. That is considering the thickness of CF supports after synthesis.

4.1.1. Small scale test

First small scale test was carried out, from which following data were obtained shown in Table 6:

Test	Mass after (g)	Yield_CNf (%)	Mass of CNF (g/u.)
Small scale test	0.7338	2.75	0.02

TABLE 6: Characteristic parameters of CF-CNF obtained from small scale test.

Foremost the yield obtained could seem too low, but it is because it has been employed at a time of reaction too short, 2 hours, compared to other small scale tests in which these times were around 20 hours [69]. As the aim of this test is to check synthesis conditions in relation to CNF formation, this value is not taken into account.

However, the deposition of CNF is demonstrated due to the weight increase of the sample. Therefore synthesis conditions are validated for a scaling up. Afterwards a SEM analysis will be presented to check the homogeneity and quality of CNF deposition.

4.1.2. Large scale experiments

In large scale, the following properties were measured for the characterization of CF-CNF obtained here:

Batch time (h)	Mass after (g)	Final thickness (cm)	Volume CF-CNF (cm ³)
6.00	9.4575	0.65	51.05
10.00	9.415	0.65	51.05
4.00	7.7569	0.6	47.12
2.00	7.2198	0.6	47.12

TABLE 7: Several properties measured from samples in large scale tests.

CF-CNFs synthesized were weighted after CCVD reaction besides being submitted to a cleaning by means of a brush to remove the dust and sub-products deposited on their surface. Afterwards, their thickness was measured to check if there was an increase due to either CNF deposition or bulking, mainly. The volume of each CF-CNF was calculated considering it as a disk of 10cm in diameter with the thickness measured after CCVD.

The main characterization parameters of CF-CNF composites synthesized are presented in Table 8:

Batch time (h)	Yield_CNF (%)	Mass of CNF (g/u.)	Fraction of CNF (g/g)	Density (mg/cm ²)	Density (mg/cm ³)
6.00	130.60	5.36	0.57	68.20	104.92
10.00	118.16	5.10	0.54	64.93	99.89
4.00	92.72	3.73	0.48	47.52	79.20
2.00	73.85	3.07	0.42	39.05	65.08

TABLE 8: Characterization parameters of CF-CNF obtained from large scale tests.

Theoretically, the tendency of these parameters is to increase according to time of batch proportionally, since the longer t_{batch} is the more deposition of CNF occurs. Moreover, this deposition is related to the difference between $m_{\text{after}} - m_{\text{before}}$ which is present in each formula of these parameters.

On the contrary, the test at 6 hours of t_{batch} gives the highest yield of deposition. This discrepancy can be involved by the noise of the data considering that the saturation of CF has happened around this point, since the difference of CNF mass between 6 hours and 10 hours is not too high.

In fig. 10 is presented the tendency of these parameters related to t_{batch} , whose vertical asymptote can determine their exactly saturation value:

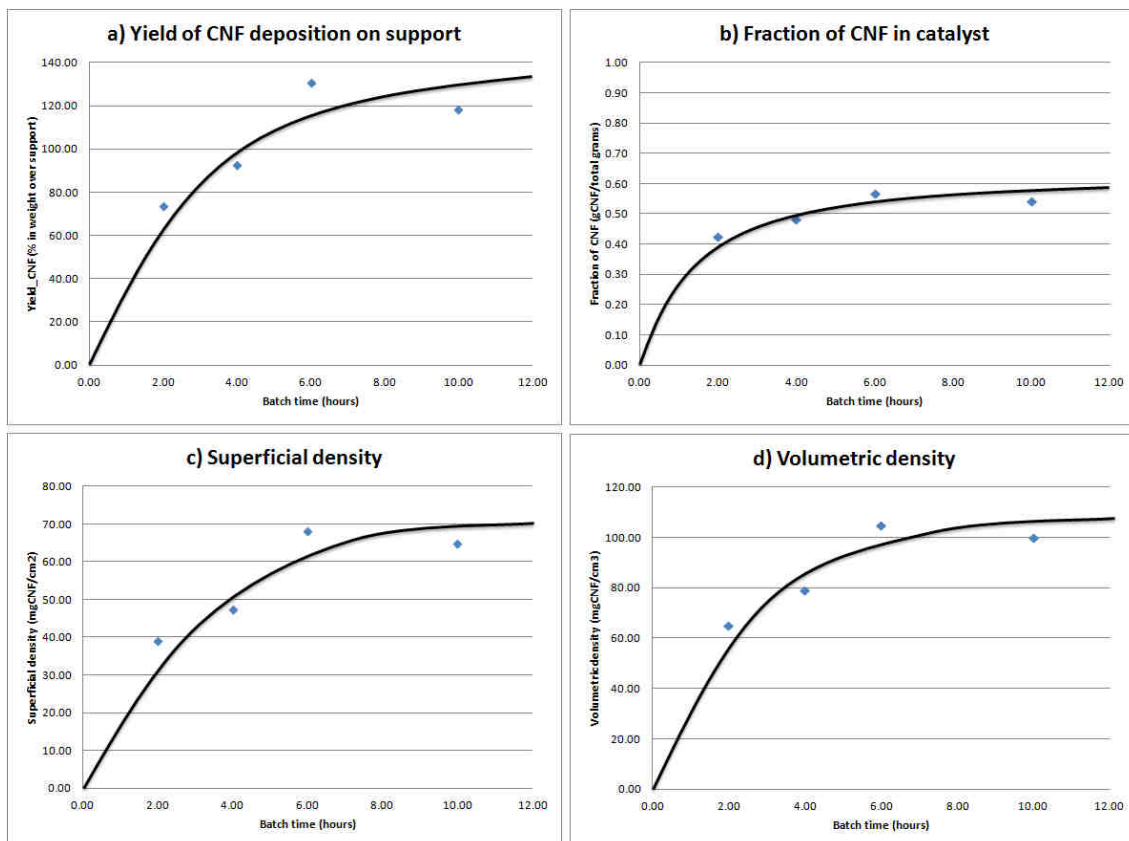


FIGURE 10: In relation to batch time, the tendency of: a) CNF deposition yield, b) the fraction of CNF in catalyst, c) Superficial density, d) volumetric density.

Regarding to yield of CNF deposition, it is going to be compared to other laboratory work to check if the values are satisfactory.

From the project of *Specialisation Topic* carried out by the researcher Ye Zhu, figure 2.4, fig. 11 was taken [69]; whose values of CNF yield are presented. Its t_{batch} were 20 hours, and the supports tested were CF exchanged with Nickel in which ethane and hydrogen were employed as synthesis gases.

Ni₂-C₂H₆:40 is the test more similar test to our experiments (the other conditions are the same as our small-scale test), which presents values from 90% to 110%, approximately the same range obtained. However, the t_{batch} of this project are shorter: from 10 times to 2 times

shorter. The reason of this result could be the high time of residence of gases whose relation between both scales is 1.88 (information obtained for table 2 in point 3.1.2.). As a higher amount of ethane remains more time inside large-scale reactor, C-C decomposition is enhanced besides CNF yield is favoured.

It could be a great result because employing t_{batch} shorter the same results are obtained in large scale, but this might be caused by a quality loss or a bad synthesis of CF-CNF. The microscopic analysis and TGA will contribute to check the quality of CNFs.

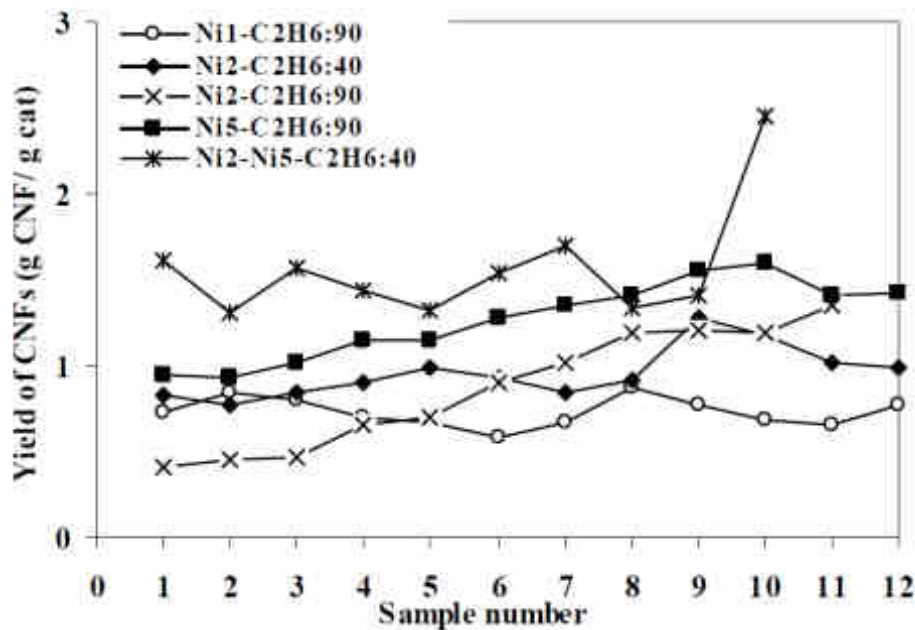


FIGURE 11: Ni1-C₂H₆:90, Ni1-C₂H₆:40, Ni2-C₂H₆:90, Ni5-C₂H₆:90 indicate that the CNFs grew on Ni catalyst for 20h, using C₂H₆/H₂ mixture as reactant in different rate (90ml/min/150ml/min and 40ml/min/150ml/min) at 923 K. Ni2- Ni5-C₂H₆:40 represents the CNFs first grew on 2 wt% Ni catalyst for 20h and then grew on 5 wt% Ni for 20h, using C₂H₆/H₂ (40ml/min/150ml/min) mixture as reactant at 923 K [69].

4.2. Microscopic analysis

4.2.1. Small scale test

The SEM analysis of small-scale test has as aim to check the general distribution and homogeneity of CNFs on CF, their quality, in addition to comparing differences between the surface and the interior of CF-CNF. All pictures taken are in *Appendix L*.

In fig. 12 and fig.13 are shown the different pictures taken from inside and the surface of CF-CNF, respectively.

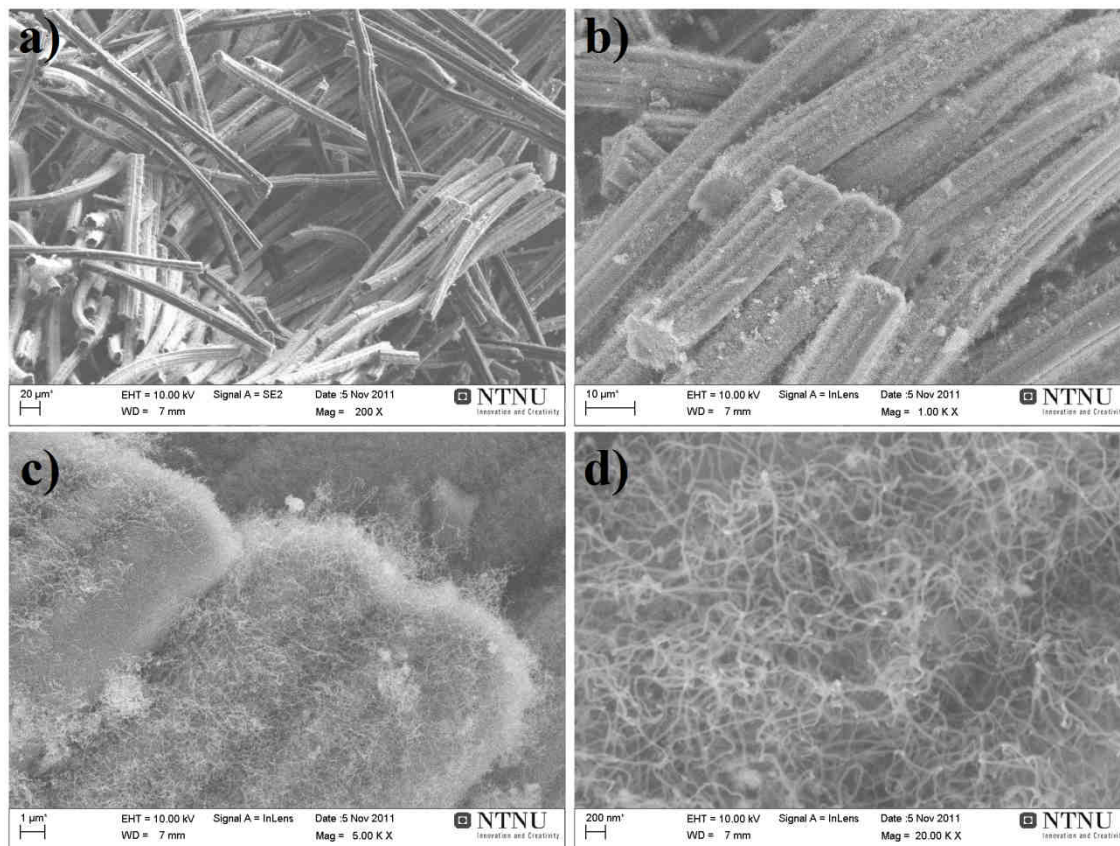


FIGURE 12: SEM pictures of CF-CNF interior, synthesized in the small-scale test.

Zoom values: 12a: X200; 12b: X1.00K; 12c: X5.00K; 12d: X20.00K.

In fig. 12a and fig. 13a the deposition can be appreciated, mostly in all CF fibers equally. In fig. 12b and fig. 13b CNFs can be distinguished on CF seeing a uniform distribution throughout CF.

Little zones of encapsulating can be appreciated in sectors very dispersed.

In figs. 12c, 12d, 13c and 13d the CNFs are checked their shape is satisfactory. CNFs have tubular shape with a size quite uniform regardless what sample is.

This analysis gives the proof necessary to validate the literature review and *Appendix C*, thus scale up tests could be carried out.

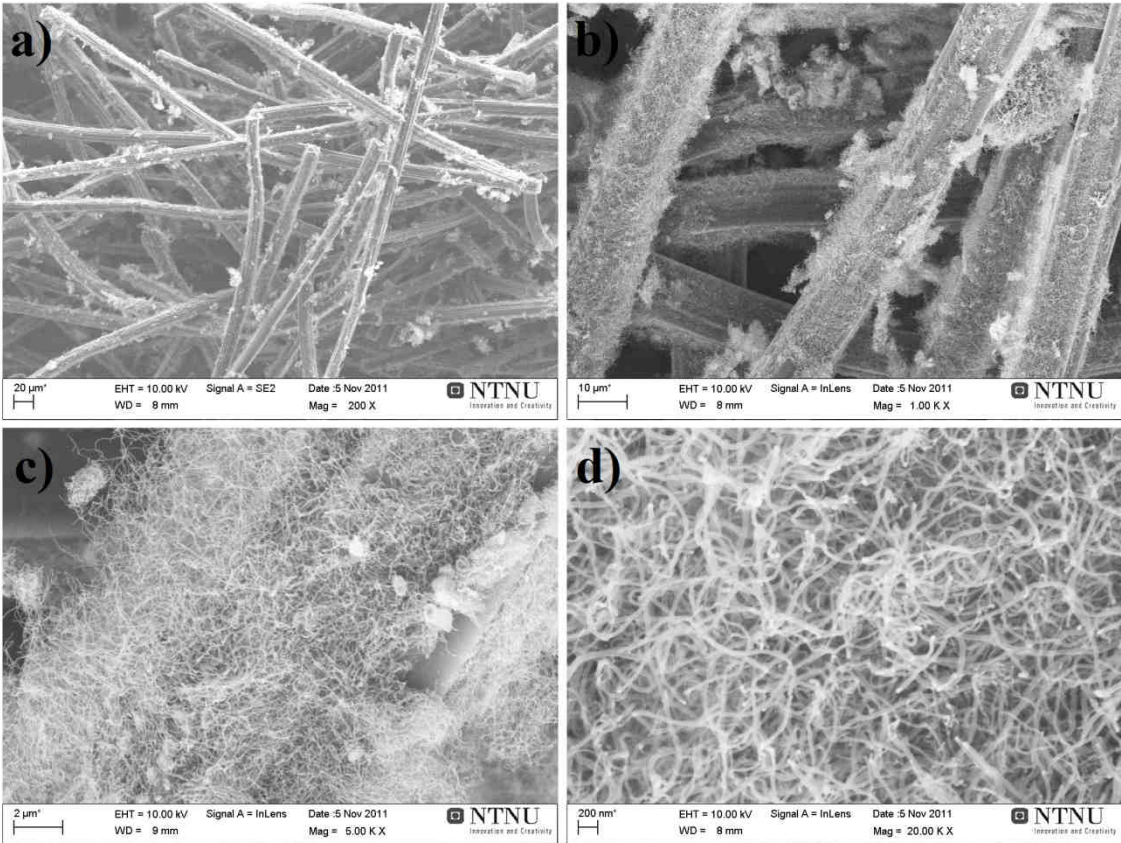


FIGURE 13: SEM pictures of CF-CNF surface, synthesized in the small-scale test.

Zoom values: 13a: X200; 13b: X1.00K; 13c: X5.00K; 13d: X20.00K.

The SEM analysis of large-scale tests has as aim to check the quality of CF-CNF composites and complement the results obtained from gravimetric analysis.

4.2.2. Differences according to time of reaction

In fig. 14 are shown the images of different samples for each t_{batch} , in which an increase of CNF density on CF can be appreciated according to t_{batch} increase. Except “the test of 6 hours”, in which has a higher density than “10 hours test”. These pictures are in accordance with the data of Y_{CNF} shown in point 4.1.2., Table 8.

In general the distribution of CNF on CF is quite uniform.

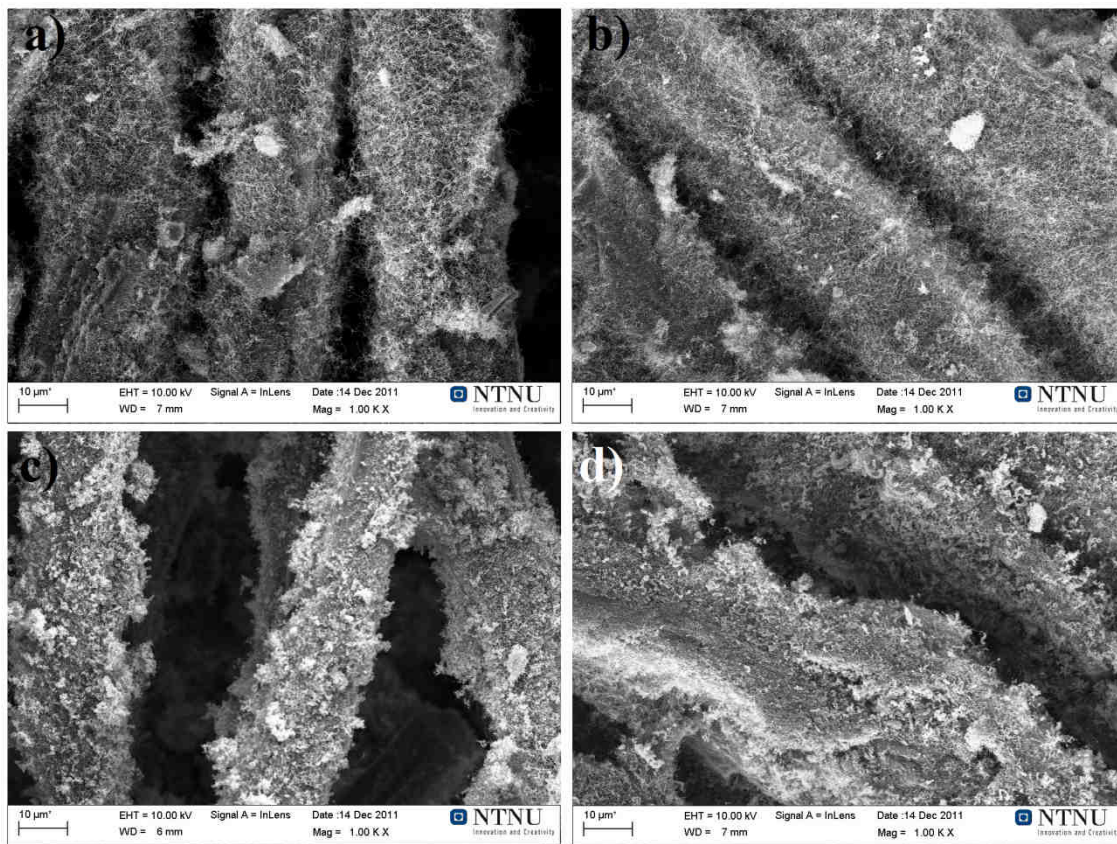


FIGURE 14: SEM pictures of CF-CNF, at X1.00K in zoom.

15a: for t_{batch} of 2 hours; 15b: for t_{batch} of 4 hours; 15c: for t_{batch} of 6 hours; 15d: for t_{batch} of 10 hours.

In fig. 15 for time of 2 and 4 hours, the quality and homogeneity of samples is pretty satisfactory, CNF shape is tubular and their size is uniform in whole picture. Both samples seem quite similar, thus the quality in this range is constant.

In 6 and 10 hours of t_{batch} the structure of fibbers is amorphous in most of CNF, this seems an encapsulation of Ni clusters has happened making CNF growth irregular and surrounding the fibbers.

This encapsulation is present in entire images; therefore it is a problem in the whole CF-CNF for t_{batch} as from 6 hours.

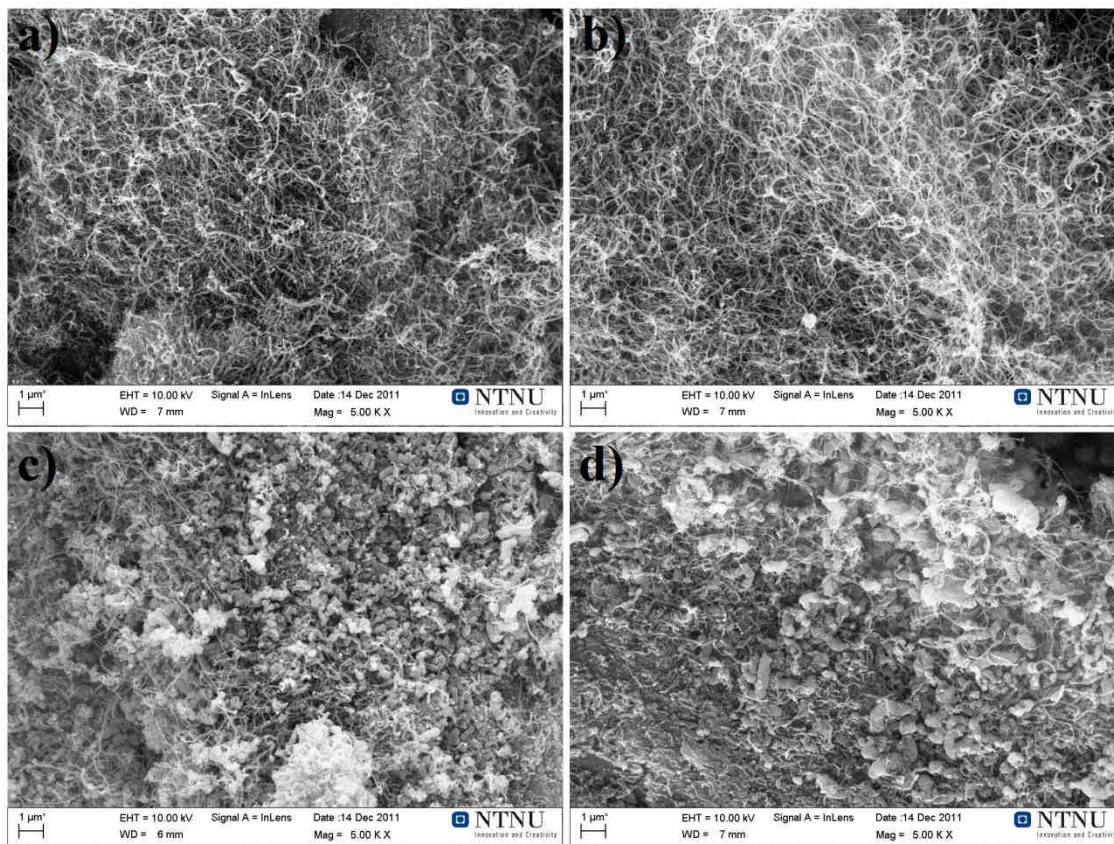


FIGURE 15: SEM pictures of CF-CNF, at X5.00K in zoom.

15a: for t_{batch} of 2 hours; 15b: for t_{batch} of 4 hours; 15c: for t_{batch} of 6 hours; 15d: for t_{batch} of 10 hours.

In fig. 16 a clearer comparison is easy to see. In which the amorphous shape is still more remarkable shown in figs. 16c and 16d. Between 4 and 6 hours of t_{batch} , the beginning of

encapsulation seems to take place; from which the quality of synthesis required is compromised.

The emergence of encapsulation coincides with the deactivation of catalytic supports as it has presented in point 4.1.2., table 8; which is probably that it is related. The saturation of support results in an irregular adsorption of C atoms.

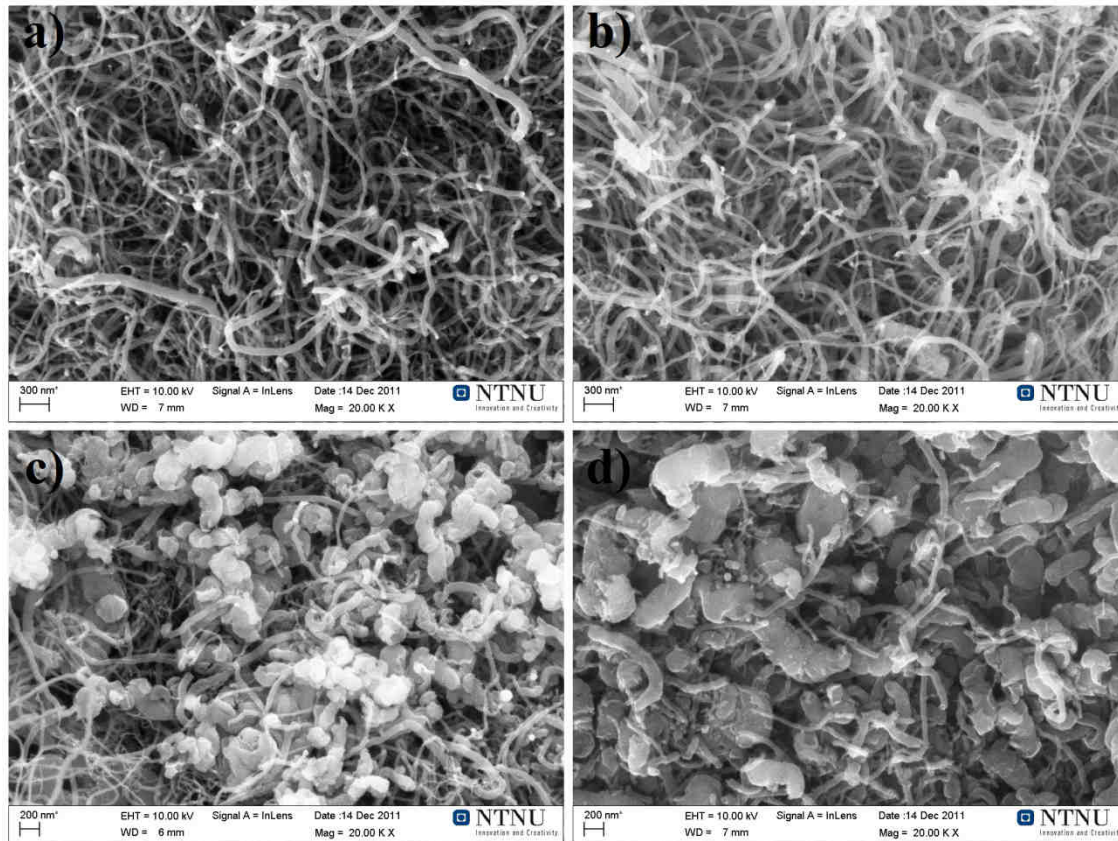


FIGURE 16: SEM pictures of CF-CNF, at X20.00K in zoom.

16a: for t_{batch} of 2 hours; 16b: for t_{batch} of 4 hours; 16c: for t_{batch} of 6 hours; 16d: for t_{batch} of 10 hours.

2 reasons might be the cause of encapsulation for t_{batch} as from 4-6 hours:

- Hydrogen concentration decreases inside reactor, which is related to encapsulation emergence (as it has been explained in point 2.1.3.). This hydrogen diminution may be caused by:
 - High head loss rising due to yield increase, as well as the thickness of CF-CNF increases from 4-6 hours of t_{batch} . If the head loss increases inner gas is harder to pass through fixed bed, being easily for smaller gases as H_2 . Therefore H_2 is removed easily than ethane, decreasing its concentration.
 - As it can be checked in point 3.1.2., table 2; the quotient: volume of reactor divided into fixed bed volume in large scale is bigger than in small scale. Thus

in this model there is much more concentration of ethane than H_2 , inside reactor. Therefore, less proportion of ethane is decomposed due to the fact that there is less active surface.

- A sudden cooling down of reactor just to finish the synthesis might be other cause. When the reaction is finished, the reactor is cooled and the flow is changed from synthesis gas to pure argon. The problem is that at low temperatures the synthesis, which takes place, is CNF of amorphous shape. If gas synthesis is still remained during this cooling, then these undesired reactions might appear.

The question is: why only does this problem appear as form 4-6 hours of reaction? Probably, because as from this moment the support is already saturated, improving the encapsulation of Ni clusters more than CNF growth. Moreover the higher head loss there is due of CNF deposition, the easier H_2 removal is across fixed bed.

One solution for this problem is to keep the temperature of reactor for a moment; meanwhile the Argon is removing the synthesis gas from reactor. In *Appendix G2* this time of waiting is calculated, considering 90% in Argon inside reactor as the final state. The time obtained is **9.5 min** at 100% set in Argon flow.

4.2.3. Differences according to position in support

The relation between the quality of CNF synthesized and their position in CF is going to be explained bellow. The experiment elected for this analysis has been “large scale 3” submitted to a t_{batch} of 4 hours, since it is a catalyst with a high yield (as shown in point 4.1.2., table 8) as well as it has good quality CNFs (as shown in point 4.2.2.).

In fig. 17 is presented the comparison among the 4 samples according to their position in CF for a X1.00K zoom. In which, similar distribution of CFNs can be appreciated, some clusters appear due to an isolated encapsulation, but it is inconsiderable. The distribution is quite good and uniform, independently the position in CF-CNF of catalyst obtained.

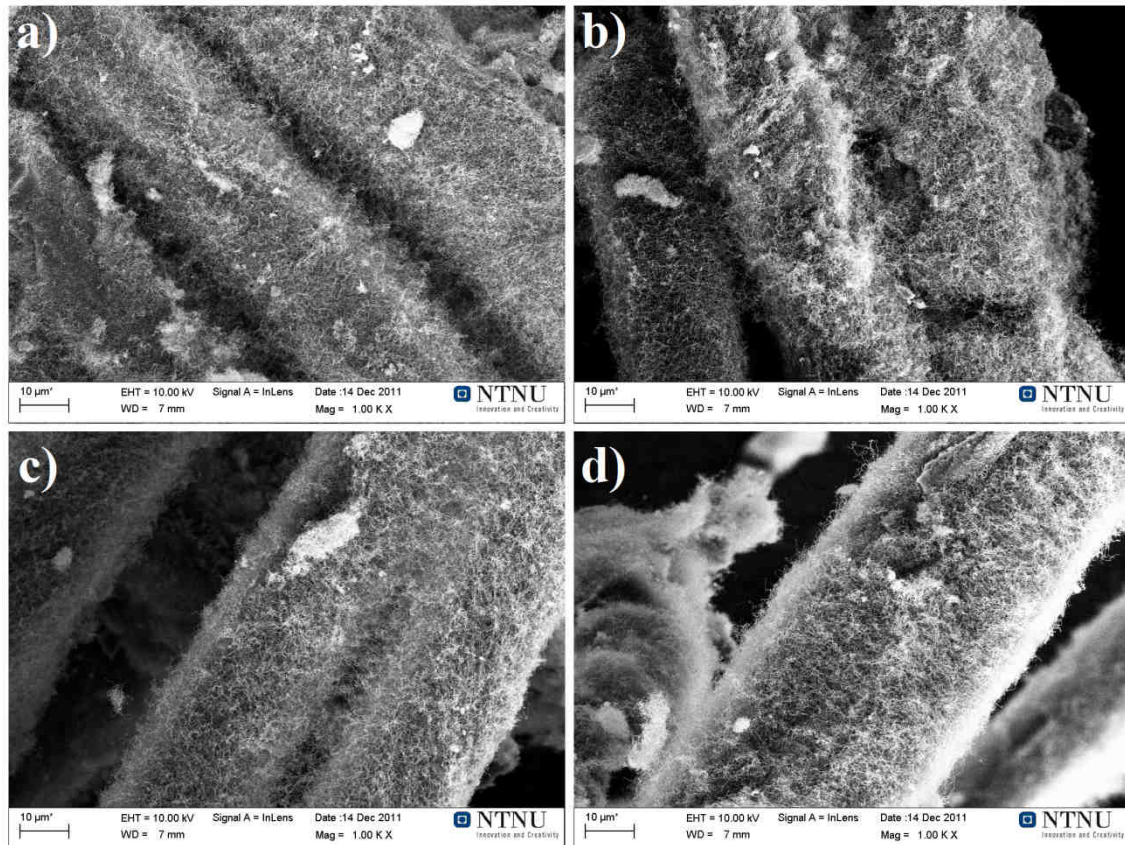


FIGURE 17: SEM pictures of CF-CNF, at X1.00K in zoom, for t_{batch} of 4 hours.

17a: centre, 17b: 1.67cm from centre; 17c: 3.33cm from centre; 17d: edge.

In fig. 18 the comparison among the 4 samples according to their position in CF for a X1.00K zoom is presented. Thanks for this zoom their shape and homogeneity of CNFs can be studied.

In 4 samples the CNF are very homogeneous in whole pictures can be appreciated; besides they look quite similar among them. There is not any sign of encapsulation in any sample.

The quality of fibbers seems quite good, since their shape is pretty tubular and there is not much variation among CNF sizes.

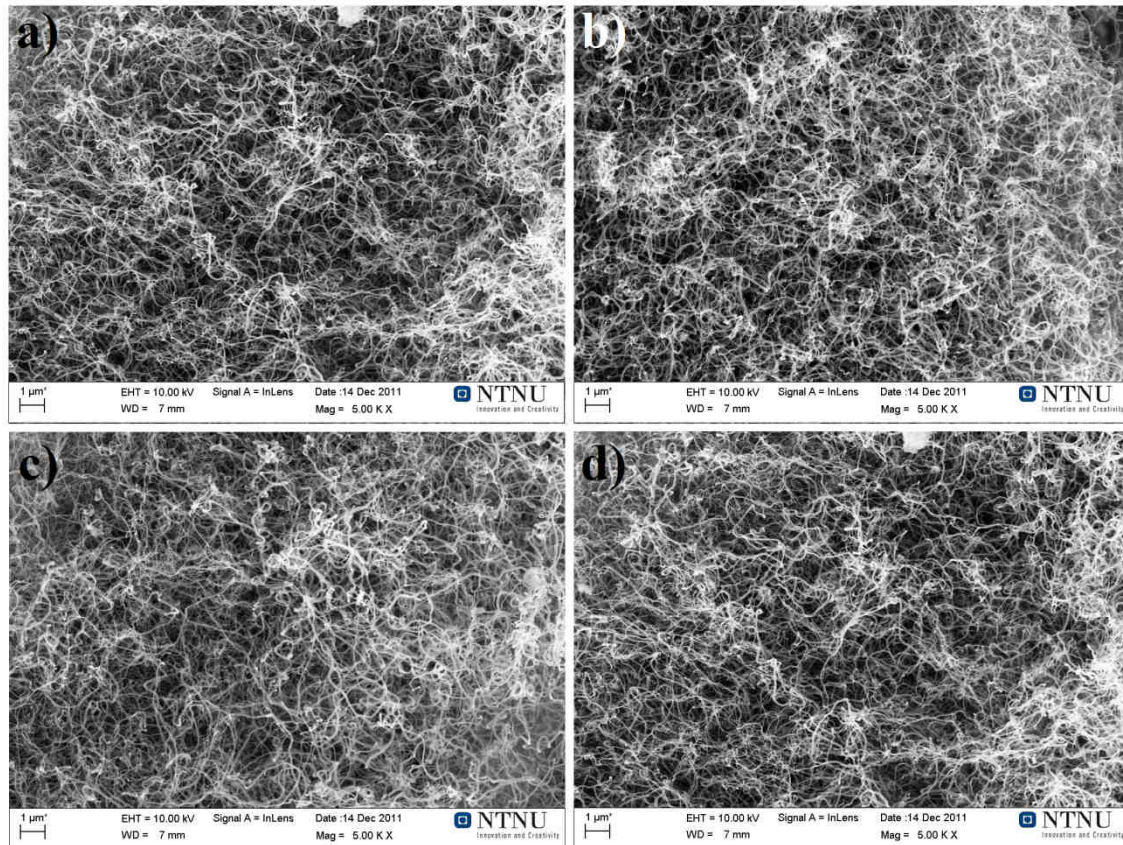


FIGURE 18: SEM pictures of CF-CNF, at X5.00K in zoom, for t_{batch} of 4 hours.

18a: centre; 18b: 1.67cm from centre; 18c: 3.33cm from centre; 18d: edge.

In general the pictures are quite similar, therefore it is concluded that there is no influence of position referred to CNF deposition.

The employment of 2 supports in the front and back part of each support for synthesis has been a success. They homogenized the flow at the entrance and exit of CF-Ni supports, minimizing the effect of flow mixture in large scale size.

4.2.4. Estimation of mean CNF diameter

The mean diameter of CNF can be estimated by means of SEM pictures with more resolution, X20K. Only large-scale test referring to 2 hours and 4 hours have been considered, because in amorphous (6 hours and 10 hours) structures there is no a properly diameter to measure.

These pictures are placed in *Appendix L*:

The procedure consists of a random sampling from each picture:

- For 2 hours of t_{batch} (*image L3d* from *Appendix L*): 100 measurement points have been taken.

- For 4 hours of t_{batch} (images: *L4d*, *L5d*, *L6d* and *L7d* from *Appendix L*): 25 measurement points from each picture have been taken, 100 in total. With this sampling, the effect of CF radio can be studied, in addition to obtaining the general results for 4 hours of t_{batch} .

Each point has been measured by a ruler over a printed photography, trying to obtain the transversal length of fibbers, considering them as the CNF diameters. From the direct values of ruler measures were obtained the real values of CNF diameters, by applying the scale of photography.

All data of this study have been collected and presented in *Appendix M* from each group of data. Its arithmetic mean and standard deviation have been found out, according to their formulae:

$$mean = \frac{1}{n} \cdot \sum_{i=1}^n x_i \quad \sigma = \sqrt{\frac{1}{n} \cdot \sum_{i=1}^n (x_i - mean)^2}$$

Where: n is the number of measurement points and x_i are each point taken randomly from SEM pictures already cited above.

In Table 9 are shown the results to compare the CNF diameter among t_{batch} considered.

Test:		
2 hours	scale	300nm/41mm
	mean diameter (nm)	44.5
	standard deviation (nm)	24.5
4 hours	scale	300nm/41mm
	mean diameter (nm)	49.3
	standard deviation (nm)	20.5

TABLE 9: Statistical parameters of the CNF diameter estimation for 2 hours and 4 hours of t_{batch} .

The mean diameter ranges from 44.5 to 49.3 nm, increasing its value in accordance with t_{batch} rise. This may be due to multilayer formation by the increase of t_{batch} , which makes thicker CNFs. Although it is a difference quite small, hence it could be considered as sampling noise. Standard deviation is referred to variation of values because there is a distribution of CNF diameters. Given that their values are approximately half of CNF diameter, the variation of mean CNF diameter among the different tests can be considered as noise.

Considering that the magnitude degree of CNF size is of nm, such variation between points taken is not so wide.

In summary, the size of CNF diameter is quite homogeneous according to the time of reaction (t_{batch}).

In Table 10 are presented the results in order to compare the CNF diameter to the distance from the centre of CF-CNF.

Test: "4 hours of batch time"		
center	scale	300nm/41mm
From 1	mean diameter (nm)	44.8
to 25	standard deviation (nm)	20.9
r=33mm	scale	200nm/27mm
From 26	mean diameter (nm)	52.6
to 50	standard deviation (nm)	19.5
r=67mm	scale	300nm/41mm
From 51	mean diameter (nm)	50.4
to 75	standard deviation (nm)	22.7
r=100mm	scale	300nm/41mm
From 76	mean diameter (nm)	49.5
to 100	standard deviation (nm)	19.0

TABLE 10: Statistical parameters of the CNF diameter estimation in relation to the position in CF-CNF composite.

The distribution of CNF diameters and their possible variation seem to be constant to the position in CF-CNF composite.

Since, in the analysis of "4 hours sample", several samples were taken from different positions to estimate CNF diameter, this is the CNF diameter purposed:

49.5±20.5 nm (for 4 hours of synthesis)

4.3. Temperature programmed oxidation (TPO)

From this study, the pairs of data weight loss and temperature were obtained for the following samples: CF washed with acid, CF-CNF obtained at 2, 4 and 6 hours in t_{batch} . 10 hours in t_{batch} was not considered because as from 6 hours of t_{batch} encapsulation was present and its analysis was important for one sample. Thus oxidation resistance is studied only in one sample with encapsulation.

All data obtained from this analysis are presented in *Appendix N*.

In fig. 19 is shown the tendency of weight loss according to heating temperature for each sample considered, which is directly related to the oxidation suffered by samples at temperature given. Carbon felt is loosing less weight than any sample submitted to CNF

deposition throughout analysis, since mainly CNF presents less oxidation resistance than CF. Initially, the weight lost by CF-CNF is due to CNF oxidation.

It is supposed that CF is decomposed regardless which sample is, but a degradation of CF may be due to t_{batch} . This question will be solved with the determination of oxidation temperature. The degradation of CNF seems to be increased in accordance with t_{batch} .

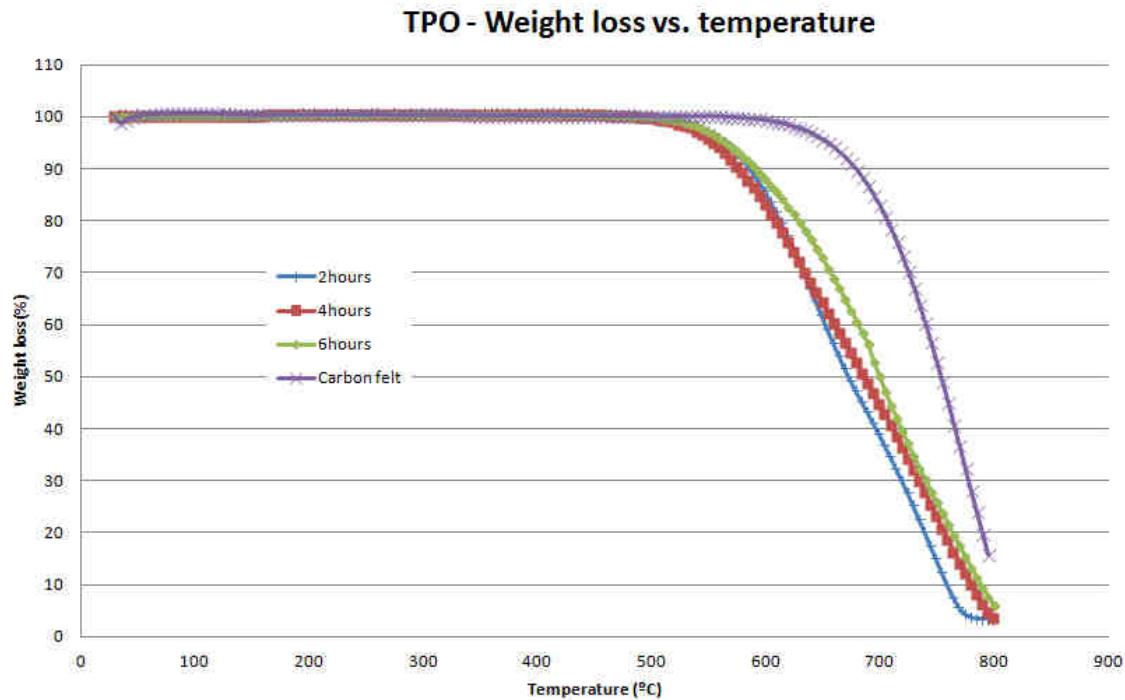


FIGURE 19: Tendency of weight loss according to heating temperature.

Given that the oxidation of each compound starts when an inflexion point appears in previous graphic, the method of first derivative is employed.

This method takes for each interval of data its discrete derivative; and it is represented versus the mean temperature of each interval considered.

The formula for discrete derivative between 2 points is the next:

$$f(x_{\text{mean}_i})'_{i+1,i} = \frac{f(x_{i+1}) - f(x_i)}{x_{i+1} - x_i} \quad x_{\text{mean}_i} = \frac{x_{i+1} + x_i}{2}$$

Applied for this case, $f(x_i)$ is the weight loss of sample and x_i is the temperature at which this loss occurs.

An inflexion point of a function is a local maximum/minimum of its derivative. As CF is more resistant than CNF to oxidation, the first peak is referred to CNF oxidation and the second one to CF.

The data obtained from the application of this method are presented in *Appendix N*, as well. In table 11 are shown the oxidation temperature of CNF and CF for the experiments tested:

Sample	Mass (mg)	Temp. Oxid. CNF (°C)	Temp. Oxid. CF (°C)
CF	10	--	777
2 hours	13.9	646	751
4 hours	20.3	641	741
6 hours	21.6	691	691

TABLE 11: Mass of sample employed, oxidation temperature of CNF and CF; for each analysis

As it can be seen, the longer t_{batch} is the more the degradation of CF is, in accordance with the temperature increase. It is checked CF has suffered an inner transformation during a CVD reaction, decreasing its oxidation resistance.

Other interesting result is that the oxidation temperature of CNF is approximately the same in the range of well CNF deposition (for a t_{batch} of 2 hours and 4 hours). Their values are at the same range from other tests [111].

However for the interval in which the encapsulation is present (as from t_{batch} of 6 hours), a unique oxidation temperature appears. Because a sole phase is formed among: CF, CNF already formed and the amorphous new structure. Moreover, its oxidation temperature is placed between the predictable oxidation temperature of CNF and the CF's one.

4.4. BET surface area and pore size distribution

For this analysis, BET surface area and mean pore volume were obtained to study how much active surface and free volume each CF-CNF has. These parameters give information about the general quality of catalysts.

Only one sample of both with encapsulation was analyzed to study its influence.

In Table 12 are put the BET surface areas obtained directly from the analyzer, carried out by the researched Fan Huang.

Time of batch	BET surface area (m ² /g)
2 hours	32.2
4 hours	44.4
6 hours	71.6

TABLE 12: BET surface area.

Surface area increases according to t_{batch} , because the yield of CNF deposition rises as well. The more CNFs deposited there are, the more specific surface there is.

From laboratory experiments BET surface ranges from 100 to 200m²/g whose t_{batch} is 20 hours [69]. Therefore it is concluded that the values obtained in our experiments are quite low than small scale tests. It means that a loss of catalytic activity is produced, because the mean size of CNF is bigger than laboratory experiments, besides give that the yields obtained by us are similar.

For a t_{batch} of 6 hours, the BET surface area increases even more than expected. An amorphous structure has less specific surface than a tubular fiber. Thus in this encapsulation there is no specific surface loss, otherwise the formation of amorphous structures is given on the CNF already formed as new structures. Other cause of BET surface increase might be the bulking of sample by thickness increment, shown in point 4.1.2., Table 7.

Moreover the pore size distribution of our experiments were obtained, which are presented in *Appendix O*. Their plots are represented in Fig. 20, for all samples analyzed. Furthermore pore size distributions from laboratory tests carried out by the researcher Ye Zhu [69], are presented in Fig. 21 to their comparison.

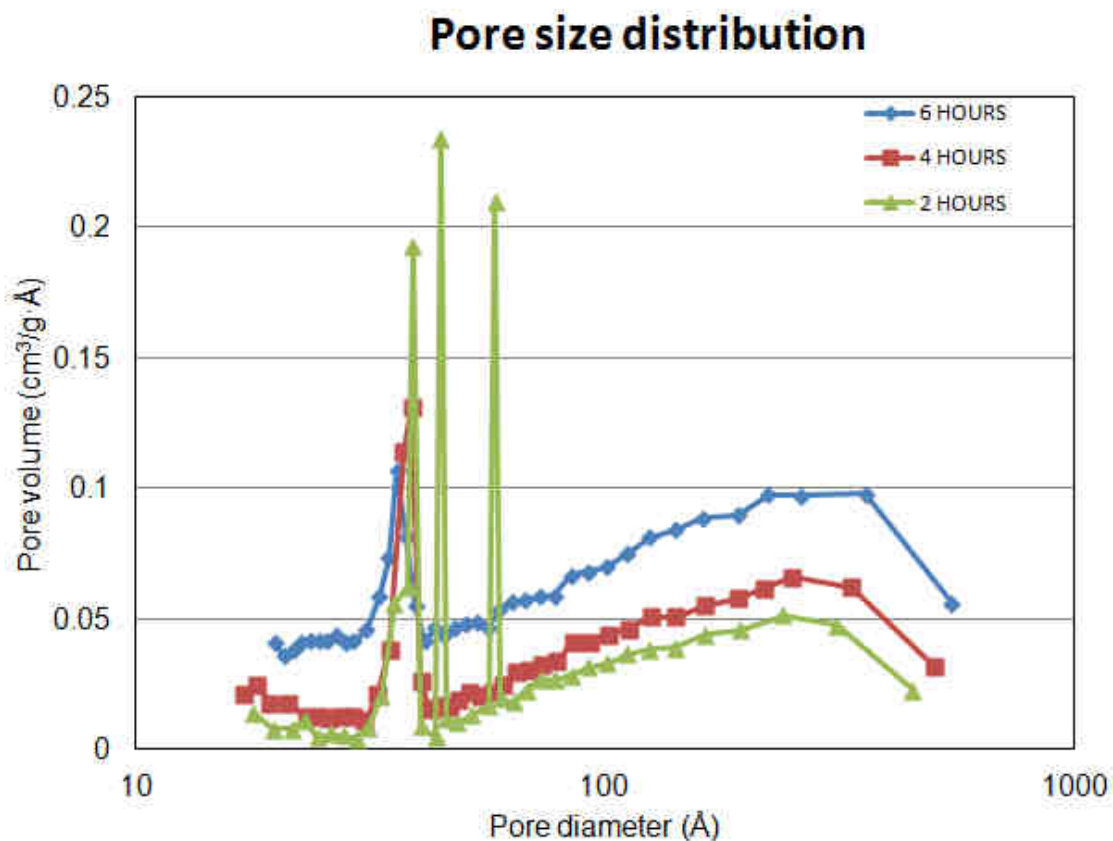


FIGURE 20: Pore size distribution for large scale experiments.

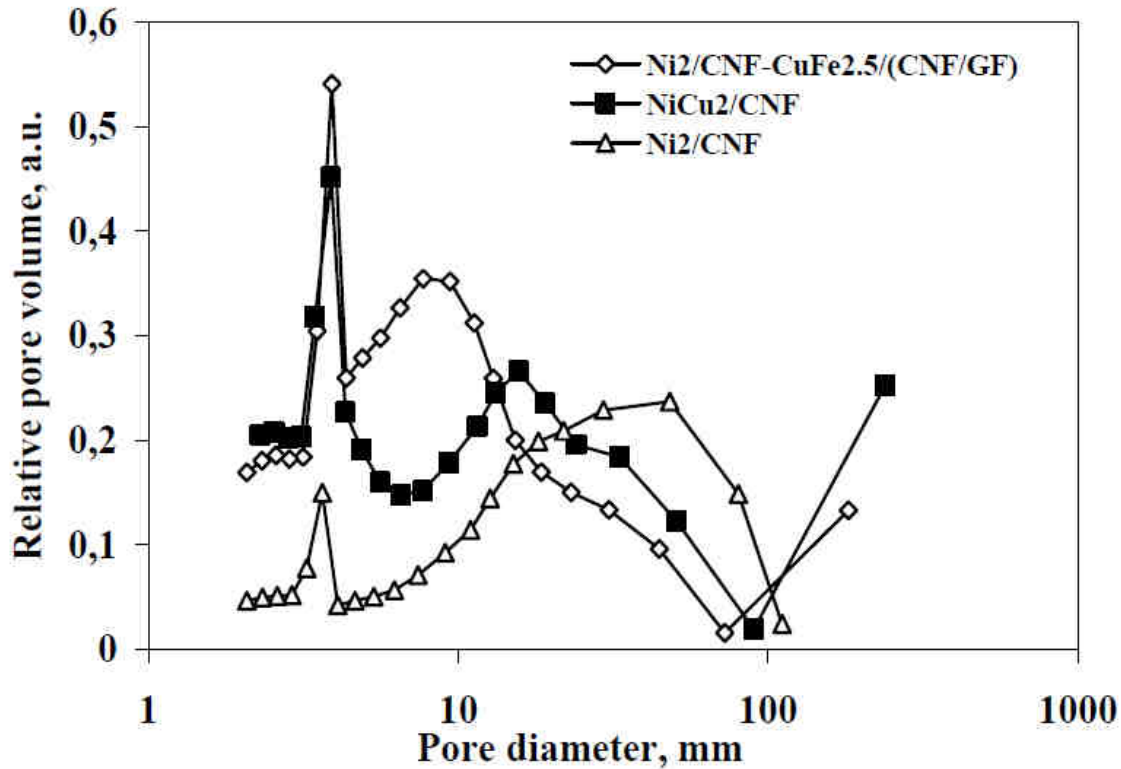


FIGURE 21: Pore size distribution from laboratory tests [69].

Firstly, in Fig. 20 the distribution of pore size increases in relation to t_{batch} . If these curves are compared to the Plot: Ni2/CNF in fig. 21, small scale test has higher pore size distribution due to the fact that its t_{batch} is longer than in large-scale tests.

The curves of pore size distribution are quite hard because it is difficult to establish a value for a comparison; therefore a calculation of the area below the curve had to be carried out. This area is directly related to the porosity of each sample, thus its assessment is easy to do. The area was calculated according to trapezoid method of integration from the pair of data: pore diameter and specific pore volume. Its formula is presented below:

$$\int_{a_1}^{a_n} f(x) \cdot dx \approx \sum_{i=1}^n (a_{i+1} - a_i) \cdot \frac{f(a_{i+1}) + f(a_i)}{2}$$

Where: a_i are the data of pore diameter and $f(a_i)$ are the data of specific pore volume; n represents the number of points registered in the interval of pore sizes from a_1 to a_n .

All data obtained from this method are exposed in *Appendix O*.

In Table 13 are presented the different areas below the curve, for the 3 samples.

Time of batch	Pore volume per gram (cm ³ /g)
2 hours	17.08
4 hours	24.35
6 hours	42.84

TABLE 13: Mean volume of pore per gram.

According to the rise of BET surface area, the porosity increases; which involves in better the activity of CF-CNF. Between 4 and 6 of t_{batch} the difference in pore volume per gram is higher than expected, as BET surface area. Therefore both parameters are directly related, because they follow the same tendency respect to t_{batch} .

4.5. Deviations from similitude model

This study is focused on the comparison between large scale model and laboratory models. As chemical conditions have been kept constant^{*1} in order to obtain the same type of CNF on CF, physical parameters are the ones modified to achieve the scaling up.

^{*1}In fact, as the residence times of gaseous currents are not the same in both scales and the active surface of support changes as well; then it is supposed that the hydrogen concentration inside reactor is not the same in both scales. Gases concentration inside reactor is not a parameter which could be measured and controlled, because a gases analyzer was not available in this project. This control lack might be the reason why the encapsulation of metallic clusters is present from a certain t_{batch} in large scale.

To an easier comparison, the rules of similitude model have been transformed into deviation ratios whose values give the degree of deviation.

These ratios are defined as the quotient of large scale factor divided into a small scale factor:

Ratio = f_2/f_1 , where 2 is referred to large scale and 1 to small scale.

From *Appendix D*, the following factors have been defined according to their similitude rules:

- Dimensional factor: $f_i = (D_i/LCF_i)$
- Kinetic factor: $f_i = (D_i^2 \cdot LCF_i)/(Q_i)$
- Dynamic factor: $f_i = (Q_i/D_i)$

In Table 14 are shown all factors calculated besides their ratios of deviation:

Similitude	Small scale	Large Scale	Ratio
Dimensional	6.67	5.56	0.83
Kinetic	0.10	0.18	1.88
Dynamic	25.00	100.00	4.00

TABLE 14: Ratios of deviation referring to each type of similitude: dimensional, kinetic and dynamic.

The following observations have been taken into account from each ratio of deviation:

Dimensional similitude: This ratio is less than 1, which means that the scaled-up model has a fixed bed longer than the small scale one. A better CNF distribution in whole transversal surface can be produced, because there is less bed diameter in relation to its length. Moreover, its faster saturation involves higher head loss by CNF deposition throughout fixed bed.

Kinetic similitude: This ratio is more than 1, which means that there is a longer time of residence in CF large model (bed size is bigger in relation to gas flow). This enhances the CNF deposition which explains the higher Y-CNF obtained in large scale experiments.

Dynamic similitude: This ratio is more than 1, which involves large model to have more turbulent flow inside; due to the fact that reactor diameter is smaller in relation to flow. As it is more turbulent, gas mixture is improved enhancing CNF distribution inside fixed bed. Besides, the reactor has a gaseous composition more homogeneous than small scale tests.

4.6. Electrical power needs

Only in the synthesis reaction of CNF deposition electrical power needs have been calculated, in which there are 2 stages where heating power is necessary:

- A heating stage in which the temperature is increased from room temperature (18°C) to 650°C passing a current of argon at 20°C per minute. The furnace must supply heat to: heat up the current of argon, overcome the heat lost in the stainless steel lids place in the top and bottom of reactor, and heat the reactor (considered as refractory ceramics).
- A stage of reaction in which the mixture of synthesis gases is passed at constant temperature of 650°C. In this stage the furnace must heat the synthesis gases inlet and overcome the heat loss in reactor lids.

It is considered that the reactor is thermally isolated, thus there is no heat loss due to reactor. The pressure of process is the atmospheric one.

In *Appendix P* all calculation procedure is explained, carried it out by the software MathCAD 14. In *Appendix H* are placed the thermodynamic graphics employed for this estimation.

In Table 15 and 16 are shown the data referring to the electrical potency necessary for both stages.

Heating stage	
Process	Electrical potency necessary (W)
Caseous current heating	0.0018
Heat loss	183.817
Reactor heating	1308
Total	1491.8

TABLE 15: Electrical potency required for heating stage.

Reaction stage	
Process	Electrical potency necessary (W)
Caseous current heating	2.296
Heat loss	753.081
Total	755.4

TABLE 16: Electrical potency required for reaction stage.

It is checked that the potency necessary in these experiments can be supplied, since the furnace employed has a nominal potency of 4500W.

Reactor heating is the part in which more potency is needed, because it has high density and specific heat coefficient. A correct isolation of this part is fundamental to save energy consumed.

As it may be seen, heating any gaseous current does not require so much potency. Optimization efforts must also be put into reducing heat loss of this setup, placed in the top and bottom of reactor.

4.7. Gas requirements

In tables 17, 18 and 19 are presented the quantity of gases needed in CCVD and reduction stages. Post-cleaning step was only carried out in CCVD stage because in reduction stage was not necessary.

Argon needs in CCVD stage			
	Time (min)	Flow (cm ³ /min)	Vol. Ar (Nliter/batch)
Fill up	65.1	375	22.902
Heating	31.6	375	11.117
Post-cleaning	9.4	375	3.307
Cooling-down	840	30	23.641
Tot. Vol. Ar (Nliter/batch)			60.968

TABLE 17: Argon needs per batch in CCVD stage.

Needs of synthesis gases in CCVD stage			
Time batch (min)	Mass of CNF (g)	Vol. H ₂ (Nliter/g sup.)	Vol. C ₂ H ₆ (Nliter/g CNF.)
120	3.07	27.530	9.177
240	3.73	45.248	15.083
360	5.36	47.291	15.764
600	5.10	82.789	27.596

TABLE 18: synthesis gases needs during CCVD reaction per CNF deposited. For a total flow of 1000ml/min (75% H₂/25% C₂H₆).

Gas needs in reduction stage	
Time of reduction (min)	120
Flow of H ₂ (cm ³ H ₂ /min)	100
Flow of Ar (cm ³ Ar/min)	300
Tot. Vol. H₂ (Nliter/batch)	11.258
Vol. Ar in red (NliterAr/batch)	33.773
Fill up (NliterAr/batch)	22.902
time of fill up (min)	65.1
Heating (NliterAr/batch)	11.117
time of heating (min)	31.6
Cooling-down (NliterAr/batch)	23.641
time of cooling-down (min)	840.0
Tot. Vol. Ar (Nliter/batch)	91.434

TABLE 19: Gas needs per batch in reduction stage.

Referring to gas flows, they were measured at 18°C and 1 atm. However, the data of requirements of gases are given at normal-litter unit. (Normal conditions: 273K and 1 atm) As all gases are considered as perfect gases, each flow has had to be multiplied by (273/291) factor to convert the laboratory conditions into normal conditions.

4.8. Testing of catalysts obtained

The catalyst synthesized that had the best quality and characteristics was sent to Chemical Technology Institute (ITQ) in Valencia (Spain). Its purpose was to test its catalytic capacity to reduce bromates in aqueous medium employing H₂ as reducer gas. Two different experiments were accomplished: in a batch reactor and in a continuous plug flow reactor.

Due to the good quality of its fibbers, high Y-CNF and low t_{batch} , “*large scale test 3*” catalyst (reaction time of 4 hours) was chosen. A sample of around 1g was also exchanged with Palladium until 0.3%w and finally sent.

The ITQ tests were carried out by the professor Eduardo Palomares and the researcher Cristina Franch. The data received from them are shown in *Appendix B*.

In Fig. 22 the tendency of BrO₃⁻ conversion is plotted versus time of reaction, in a batch process. The aim of that test was to determinate the kinetic of reaction to remove BrO₃⁻, determining the time of total BrO₃⁻ elimination in addition to checking its repeatability and success. These were reaction conditions:

- Initial concentration: 50 ppm of bromates.
- Mass of catalyst (CF-CNF): 0.5 g.
- Flow of H₂ (reducer gas): 250 mL/min H₂.
- Stir velocity: 900 rpm.

2 repetitions were carried out to minimize the error, between which there is no significant different. This reaction had a good repeatability which would be necessary for future optimizations. Thus CF-CNFs have a high activity since it is possible to reach 100% in conversion. As it can be seen from Fig. 22 the final time of reaction is around **0.8 hours** (48min)

In Fig. 23 the tendency of BrO₃⁻ conversion is plotted versus time of reaction, in a continuous process. The aim of that test was to determinate the deactivation of catalyst in work conditions, determining the time of deactivation according to a low value of BrO₃⁻ conversion. These were reaction conditions:

- Initial concentration: 50 ppm of bromates.
- Mass of catalyst (CF-CNF): 0.22 g.
- Water flow to treat: 5 mL/min.

- Flow of H₂ (reducer gas): 250 mL/min H₂.

At the beginning of reaction the conversion decayed dramatically until 70% of conversion where it declined lineally. This provides information to adjust, in work conditions, the time of bed replacement. As the inlet water flow was constant, the area bellow curve divided into reaction time would give the mean conversion of outlet flow.

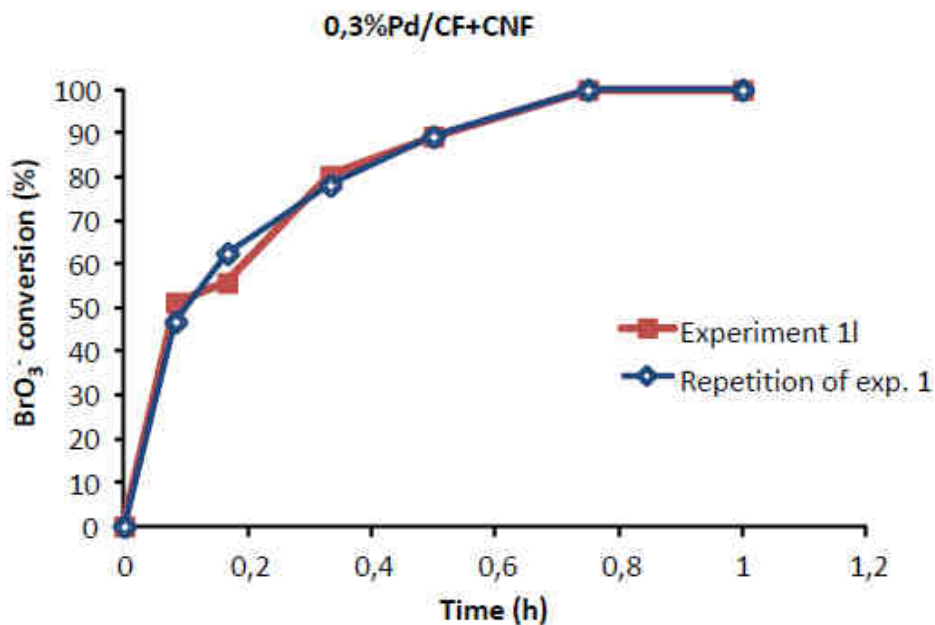


FIGURE 22: Results from ITQ experiments carried out in batch reactor.

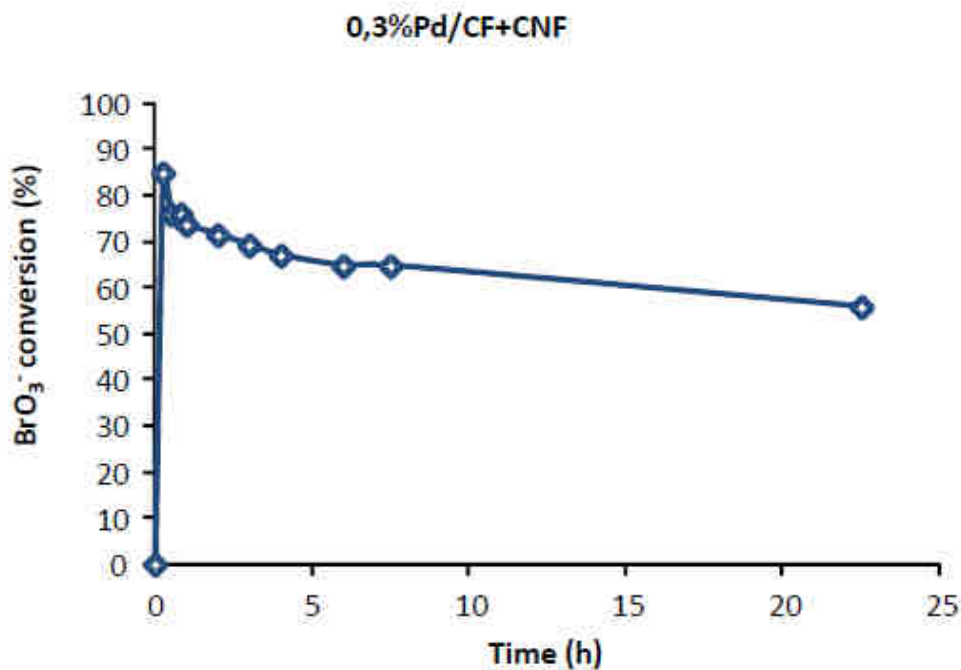


FIGURE 23: Results from ITQ experiments carried out in continuous plug flow reactor.

5. Conclusions

Similitude model has been a useful tool to establish previous conditions besides giving information to compare differences between small and large scale throughout this project. Moreover literature review has given initial data to begin the process of scaling up, which provided good results in CF-CNF synthesis.

CNF deposition on CF has been high despite the short times of reaction employed, compared to previous laboratory works. The most likely cause seems the high time of residence which has been longer than small scale. This deposition has been increasing in accordance with time of reaction up to reaching a point of saturation. Such yields can involve high head loss inside reactors; however pore distribution analysis concludes that the porosity is not so high in catalysts obtained. To optimize the plant according to Y-CNF results, the time of reaction may be reduced or the load of fixed bed increased. As a result, Y-CNF would be compromised; however Y-CNF is not a critical parameter.

SEM analysis has given interesting results. The mixture of gases inside catalytic support was quite homogeneous; since the distribution, size and shape of CNF were similar in whole CF-CNF synthesized, i.e. CNF deposition has not depended on the position in support. Up to 4 hours of t_{batch} the crystallinity, size, shape and distribution of fibbers have been satisfactory. But as from 6 hours encapsulation phenomenon is present, in which the structure turns to amorphous increasing its volume and reducing its quality.

Researching works to determine the origin of this encapsulation should be carried out, for instance: the installation of a gas analyzer in outlet position could control H_2 concentration, which is directly related to encapsulation. In affirmative case, a recirculation of outlet gases might be a good way to optimize reactants as well as it would prevent encapsulation by H_2 increment. If recirculation were not possible, increasing H_2 concentration in inlet current and the removal of synthesis gases before cooling the reactor could be good solutions.

TGA has provided values of oxidation temperature similar to small scale works, therefore thermal stability is not modified in scaling up. CF resistance has been reduced according to the time of reaction. Besides, when encapsulation has been present there has been no

difference between CF and CNF obtaining one oxidation temperature, the structure of CF might have formed a phase with the amorphous carbon compound.

BET surface analysis has concluded that specific surface increases according to CNF deposition, even in presence of encapsulation. Thus CNF already formed may not have been destroyed after 6 hours of reaction and the amorphous structure can have grown surrounding these CNF.

ITQ tests of CF-CNF synthesized at 4 in t_{batch} have given great results for BrO_3^- removal. The activity of catalysts has been high, because the yield of BrO_3^- elimination has reached 100%. Hence, it is supposed that fish-bone structure has been finally achieved, thanks operational conditions employed.

Summarising, “large scale 3” (t_{batch} of 4 hours) test is the catalyst obtained purposed to be sent to Veolia’s reactor; due to:

- The great quality of CNF.
- High Y-CNF.
- Small time of reaction.
- High catalytic activity.
- Satisfactory thermal properties.

References

- [1] H.W. Kroto, J.R. Heath, S.C. O'Brien, R.F. Curl, R.E. Smalley, *Nature* 318 (1985) 162–163.
- [2] S. Iijima, *Nature* 354 (1991) 56–58. [3] S. Iijima, T. Ichihashi, *Nature* 363 (1993) 603–605.
- [3] S. Iijima, T. Ichihashi, *Nature* 363 (1993) 603–605.
- [4] D.D.L. Chung, in: L.P. Biro, C.A. Bernardocca, G.G. Tibbetts, Ph. Lambin (Eds.), *Carbon Filaments and Nanotubes: Common Origins, Differing Applications*, Kluwer Academic Publishers, Dordrecht, 2001, pp. 275–288.
- [5] M.L. Lake, in: L.P. Biro, C.A. Bernardocca, G.G. Tibbetts, Ph. Lambin (Eds.), *Carbon Filaments and Nanotubes: Common Origins, Differing Applications*, Kluwer Academic Publishers, Dordrecht, 2001, pp. 331–342.
- [6] D.A.Bochvar and E.G.Gal'pern, *Dokl.Akad.Nauk.USSR*, 209, (610), 1973
- [7] I.V.Stankevich, M.V.Nikerov, and D.A.Bochvar, *Russ.Chem.Rev.*, 53, (640), 1984
- [8] H.W.Kroto, J.R.Heath, S.C.O'Brien, R.F.Curl, and R.E.Smalley, *Nature*, 318, (162), 1985)
- [9] Iijima, Sumio, *Nature (London, United Kingdom)*, 354, (6348), 1991
- [10] Serp, P.; Corrias, M.; Kalck, P. *Appl. Catal., A* 2003, 253, 337–358.
- [11] De Jong, K. P.; Geus, J. W. *Catal. Rev.sSci. Eng.* 2000, 42, 481–510.
- [12] Pham-Huu, C.; Ledoux, M. J. *Top. Catal.* 2006, 40, 49–63.
- [13] Downs, W. B.; Baker, R. T. K. *Carbon* 1991, 29, 1173–1179.
- [14] Downs, W. B.; Baker, R. T. K. *J. Mater. Res.* 1995, 10, 625–633.
- [15] Cybulski, Andrzej; Moulijn, Jacob A., eds (2005). *Structured Catalysts and Reactors (Second ed.)*. CRC Press. ISBN 978 0824723439. Chapter 1-3.
- [16] T.V. Reshetenko, L.B. Avdeeva, Z.R. Ismagilov, A.L. Chuvilin, V.A. Ushakov, *Appl. Catal. A* 247 (2003) 51–63.
- [17] Y.D. Li, J.L. Chen, L. Chang, Y.N. Qin, *J. Catal.* 178 (1998) 76–83.
- [18] Y.D. Li, J.L. Chen, Y.M. Ma, J.B. Zhao, Y.N. Qin, L. Chang, *Chem. Commun.* (1999) 1141–1142.
- [19] L. Dussault, J.C. Dupin, C. Guimon, M. Monthieux, N. Latorre, T. Ubieto, E. Romeo, C. Royo, A. Monzon, *J. Catal.* 251 (2007) 223-232.
- [20] F. Li, Q. Tan, D.G. Evans, X. Duan, *Catal. Lett.* 99 (2005) 151–156.
- [21] Zhixin Yu, De Chen, Magnus Rønning, Bård Tøtdal, Torbjørn Vrålstad, Esther Ochoa-Fernández, Anders Holmen. *Applied Catalysis A: General* 338 (2008) 147-158
- [22] I. Kvande, Z. Yu, T. Zhao, M. Rønning, A. Holmen and D. Chen. *Chemistry for Sustainable Development* 14 (2006) 583-589
- [23] C. Park and R. T. K. Baker, *J. Phys. Chem. B*, 1999, 103, 2453.
- [24] K. P. de Jong and J. W. Geus, *Catal. Rev.-Sci. Eng.*, 2000, 42, 481.
- [25] C. Pham-Huu, N. Keller, L. J. Charbonnière, R. Ziessel and M. J. Ledoux, *Chem. Commun.*, 2000, 19, 1871.
- [26] Pham-Huu, C.; Ledoux, M. J. *Top. Catal.* 2006, 40, 49–63.
- [27] Van der Lee, M. K.; van Dillen, A. J.; Geus, J. W.; de Jong, K. P.; Bitter, J. H. *Carbon* 2006, 44, 629–637.

- [28] Pham-Huu, C.; Vieira, R.; Louis, B.; Carvalho, A.; Amadou, J.; Dintzer, T.; Ledoux, M. J. J. *Catal.* 2006, 240, 194–202.
- [29] Stroom, P.D., Merry, R.P., and Gulati, S.T., *Systems Approach to Packaging Design for Automotive Catalytic Converters*, SAE paper 900500, 1990.
- [30] Yasuda, Ayumu, Kawase, Noboru, and Mizutani, Wataru, *Journal of Physical Chemistry B*, 106, (51), 2002.
- [31] Sinnott, S. B., Andrews, R., Qian, D., Rao, A. M., Mao, Z., Dickey, E. C., and Derbyshire, F., *Chem.Phys.Lett.*, 315, (25-30), 1999.
- [32] K.P. De Jong, J.W. Geus: *Carbon Nanofibers: Catalytic Synthesis and Applications*, *Catal. Rev.-Sci.Eng.*, 42(4), 481-510, 2000.
- [33] Jung, S. H., Kim, M. R., Jeong, S. H., Kim, S. U., Lee, O. J., Lee, K. H., Suh, J. H., and Park, C. K., *Applied Physics A Materials Science & Processing*, 76, (2), 285-286, 2003
- [34] Ebbesen, T. W. and Ajayan, P. M., *Nature*, 358, (220-222), 1992
- [35] Guo, T., Nikolaev, P., Thess, A., Colbert, D. T., and Smalley, R. E., *Chemical Physics Letters*, 243, (1,2), 1995
- [36] Yudasaka, M., Yamada, R., Sensui, N., Wilkins, T., Ichihashi, T., and Iijima, S., *Journal of Physical Chemistry B*, 103, (30), 1999
- [37] Eklund, P. C., Pradhan, B. K., Kim, U. J., Xiong, Q., Fischer, J. E., Friedman, A. D., Holloway, B. C., Jordan, K., and Smith, M. W., *Nano Letters*, 2, (6), 2002
- [38] Maser, W. K., Munoz, E., Benito, A. M., Martinez, M. T., de la Fuente, G. F., Maniette, Y., Anglaret, E., and Sauvajol, J. L., *Chemical Physics Letters*, 292, (4,5,6), 1998
- [39] Bolshakov, A. P., Uglov, S. A., Saveliev, A. V., Konov, V. I., Gorbunov, A. A., Pompe, W., and Graff, A., *Diamond and Related Materials*, 11, (3-6), 2002
- [40] Scott, C. D., Arepalli, S., Nikolaev, P., and Smalley, R. E., *Applied Physics A: Materials Science & Processing*, 72, (5), 2001
- [41] Ren, Z. F., Huang, Z. P., Xu, J. W., Wang, J. H., Bush, P., Siegel, M. P., and Provencio, P. N., *Science (Washington, D.C.)*, 282, (5391), 1998
- [42] Ren, Z. F., Huang, Z. P., Wang, D. Z., Wen, J. G., Xu, J. W., Wang, J. H., Calvet, L. E., Chen, J., Klemic, J. F., and Reed, M. A., *Applied Physics Letters*, 75, (8), 199
- [43] Yudasaka, Masako, Kikuchi, Rie, Matsui, Takeo, Ohki, Yoshimasa, Yoshimura, Susumu, and Ota, Etsuro, *Applied Physics Letters*, 67, (17), 1995
- [44] Yudasaka, Masako, Kikuchi, Rie, Ohki, Yoshimasa, Ota, Etsuro, and Yoshimura, Susumu, *Applied Physics Letters*, 70, (14), 1997
- [45] A. Huczko, *Appl. Phys. A* 74 (2002) 617–638.
- [46] H. Wiesmann, A.K. Ghosh, T. McMahon and M. Strongin // *J. Appl. Phys.* 50 (1979) 3752; H.J. Wiesmann: US patent 4,237,150; Dec. 2, 1980
- [47] R. Andrews, D. Jacques, D.L. Qian, T. Rantell, *Acc. Chem. Res.* 35 (2002) 1008–1017.
- [48] H.J. Dai, *Surf. Sci.* 500 (2002) 218–241.
- [49] J. Doyle, R. Robertson, G.H. Lin, M.Z. He and A. Gallagher // *J. Appl. Phys.* 64 (1988) 3215
- [50] H. Matsumura // *Materials Research Society Symp. Proc.* 118 (1988) 43.
- [51] H. Matsumura // *J. Appl. Phys.* 65 (1989) 439
- [52] J.A.Isaacs, A.Tanwani, M.L.Healy, L.J.Dahlben; *J Nanopart Res*, 12:551-562 (2010)

- [53] T.V. Reshetenko, L.B. Avdeeva, Z.R. Ismagilov, V.V. Pushkarev, S.V. Cherepanova, A.L. Chuvilin, V.A. Likhobolov, *Carbon* 41 (2003) 1605–1615.
- [54] T.V. Reshetenko, L.B. Avdeeva, V.A. Ushakov, E.M. Moroz, A.N. Shmakov, V.V. Krivenstov, D.I. Kochubey, Yu.T. Pavlyukhin, A.L. Chuvilin, Z.R. Ismagilov, *Appl. Catal. A* 270 (2004) 87–99.
- [55] M.S. Kim, N.M. Rodriguez, R.T.K. Baker, *J. Catal.* 131 (1991) 60–73.
- [56] N.M. Rodriguez, M.S. Kim, R.T.K. Baker, *J. Catal.* 144 (1993) 93–108.
- [57] N. Krishnankutty, N.M. Rodriguez, R.T.K. Baker, *J. Catal.* 158 (1996) 217–227.
- [58] C. Park, N.M. Rodriguez, R.T.K. Baker, *J. Catal.* 169 (1997) 212–227.
- [59] C. Park, R.T.K. Baker, *J. Catal.* 179 (1998) 361–37.
- [60] C. Park, R.T.K. Baker, *J. Catal.* 190 (2000) 104–117.
- [61] S. Amelinckx, X.B. Zhang, D. Bernaerts, X.F. Zhang, V. Ivanov, J. B.Nagy, *Science* 265 (1994) 635–639.
- [62] J. B.Nagy, G. Bister, A. Fonseca, D. Mehn, Z. Konya, I. Kirisci, Z.E. Horvath, *J. Nanosci. Nanotechnol.* 4 (2004) 326–345.
- [63] M.J. Ledoux, C. Pham-Huu, *Catal. Today* 102–103 (2005) 2–14.
- [64] G. Gulino, R. Vieira, J. Amadou, P. Nguyen, M.J. Ledoux, S. Galvagno, G. Centi, C. Pham-Huu, *Appl. Catal. A* 279 (2005) 89–97.
- [65] C. Pham-Huu, N. Keller, V.V. Roddatis, G. Mestl, R. Schlogl, M.J. Ledoux, *Phys. Chem. Chem. Phys.* 4 (2002) 514–521.
- [66] M.K. van der Lee, A.J. van Dillen, J.W. Geus, K.P. de Jong, J.H. Bitter, *Carbon* 44 (2006) 629–637.
- [67] M.L. Toebes, J.H. Bitter, A.J. van Dillen, K.P. de Jong, *Catal. Today* 76 (2002) 33–42.
- [68] Gianni Donati, Renato Paludetto. *Catalysis Today* 34 (1997) 483-533, chapter 17. *Scale-up of chemical reactors*.
- [69] Zhu, Ye. *Synthesis of CNF_CF composite with controlled nanostructures. Specialisation topic autumn 2007. TKP 4510 Catalysis and Petro-chemistry*
- [70] I. Kvande, D. Chen, Z. Yu, M. Rønning, A. Holmen. *Journal of Catalysis* 256 (2008) 204-214
- [71] Tiejun Zhao ,Ingvar Kvande, Yingda Yu, Magnus Ronning, Anders Holmen, and De Chen. *J. Phys. Chem. C* 2011, 115, 1123-1133
- [72] P.E. Anderson, N.M. Rodriguez, *J. Mater. Res.* 14 (1999) 2912–2921.
- [73] C. Park, M.A. Keane, *Langmuir* 17 (2001) 8386–8396
- [74] J. Chinthaginjala et al., "Preparation and application of carbon-nanofiber based microstructured materials as catalyst support", *Industrial & Engineering Chemistry Research* 2007, 46, 3968-3978
- [75] V.N. Parmon, G.G. Kuvshinov, V.A. Sadykov, V.A. Sobyenin, *Stud. Surf. Sci. Catal.* 119 (1998) 677–684.
- [76] A.M. Dunker, S. Kumar, P.A. Mulawa, *Int. J. Hydrogen Energy* 31 (2006) 473–484.
- [77] Y. Li, J. Chen, Y. Qin, L. Chang, *Energy Fuels* 14 (2000) 1188–1194.
- [78] N.Z. Muradov, *Energy Fuels* 12 (1998) 41–48.
- [79] E. Ochoa-Fernandez, C. Lacalle-Vila, K.O. Christensen, J.C. Walmsley, M. Ronning, A. Holmen, D. Chen, *Top. Catal.* 45 (2007) 3–8.
- [80] E. Ochoa-Fernandez, D. Chen, Z. Yu, B. Totdal, M. Ronning, A. Holmen, *Surf. Sci.* 554 (2004) L107–L112.

- [81] C.A. Bessel, K. Laubernds, N.M. Rodriguez, R.T.K. Baker, *J. Phys. Chem. B* 105 (2001) 1115–1118.
- [82] V.V. Chesnokov, I.P. Prosvirin, N.A. Zaitseva, V.I. Zaikovskii, V.V. Molchanov, *Kinet. Catal.* 43 (2002) 838–846.
- [83] P. E. Nolan, M. J. Schabel and D. C., *Carbon*, 33 (1995) 79.
- [84] N. Hammer, S. Sarkova, I. Kvande, D. Chen, M. Rønning: A novel internally heated Au/TiO₂ carbon-carbon composite structured reactor for low-temperature CO oxidation, Department of Chemical Engineering, NTNU Trondheim, Norway.
- [85] J.W. Snoeck, G.F. Froment, M. Fowles, *J. Catal.* 169 (1997) 250–262.
- [86] I. Alstrup, T. Tavares, *J. Catal.* 139 (1993) 513–524.
- [87] V.V. Chesnokov, R.A. Buyanov, *Russ. Chem. Rev.* 69 (2000) 623–638.
- [88] G.G. Kuvshinov, Y.I. Mogilnykh, D.G. Kuvshinov, *Catal. Today* 42 (1998) 357–360.
- [89] D. Chen, K.O. Christensen, E. Ochoa-Fernandez, Z. Yu, B. Toidal, N. Latorre, A. Monzon, A. Holmen, *J. Catal.* 229 (2005) 82–96.
- [90] Y. Nagayasu, A. Nakayama, S. Kurasawa, S. Iwamoto, E. Yagasaki, M. Inoue, *J. Jpn. Pet. Inst.* 48 (2005) 301–307.
- [91] C. Singh, M.S.P. Shaffer, A.H. Windle, *Carbon* 41 (2003) 359–368.
- [92] K. Bladh, L.K.L. Falk, F. Rohmund, *Appl. Phys. A Mater.* 70 (2000) 317–322.
- [93] H. Neumayer, R. Haubner, *Diam. Rel. Mater.* 13 (2004) 1191–1197.
- [94] P. Pinheiro, M.C. Schouler, P. Gadelle, M. Mermoux, E. Dooryhee, *Carbon* 38 (2000) 1469–1479.
- [95] I. Suelves, M.J. Lazaro, R. Moliner, B.M. Corbella, J.M. Palacios, *Int. J. Hydrogen Energy* 30 (2005) 1555–1567.
- [96] D. Venegoni, P. Serp, R. Feurer, Y. Kihn, C. Vahlas, P. Kalck, *Carbon* 40 (2002) 1799–1807.
- [97] L. Dong, J. Jiao, S. Foxley et al., *J. Nanoscience and Nanotechnol.*, 2 (2002) 155.
- [98] P. E. Nolan, M. J. Schabel and D. C. Lynch, *Carbon*, 33 (1995) 79.
- [99] Kline, Stephen J., "Similitude and Approximation Theory", Springer-Verlag, New York, 1986. ISBN 0-387-16518-5
- [100] Chanson, Hubert "Turbulent Air-water Flows in Hydraulic Structures: Dynamic Similarity and Scale Effects, *Environmental Fluid Mechanics*, 2009, Vol. 9, No. 2, pp. 125–142 (DOI: 10.1007/s10652-008-9078-3)
- [101] C.H. Bartholomew et al., "Fundamentals of industrial catalytic processes", 2nd edition, Wiley Interscience, New Jersey, 2006
- [102] Mansfield, E.; Kar, A.; Quinn, T. P.; Hooker, S. A. (2010). "Quartz Crystal Microbalances for Microscale Thermogravimetric Analysis". *Analytical Chemistry* 82 (24)
- [103] C.H. Bartholomew et al."Fundamentals of industrial catalytic processes", 2nd edition, Wiley Interscience, New Jersey, 2006
- [104] S. Brunauer, P. H. Emmett and E. Teller, *J. Am. Chem. Soc.*, 1938, 60, 309.
- [105] <http://mse.korea.ac.kr/~efml/aem-lect6.pdf>
- [106] <http://sorption.org/awm/ads/meso/BJH.htm>
- [107] <http://www.bronkhorst.com>
- [108] <http://carbolite.thomasnet.com/viewitems/furnaces-tube-furnaces/176c-1-3-zone-horizontal-split-hinge-tube-furnaces?&forward=1>
- [109] <http://www.speciation.net/Database/Instruments/Carl-Zeiss-AG/SUPRA-55VP-;i669>
- [110] <http://www.netzsch-thermal-analysis.com/en/products/simultaneous-thermal-analysis/>
- [111] Diploma thesis of Marco Schubert, NTNU, January 2008.

Appendixes

Appendix A: Veolia`s pilot plant

Appendix B: Tests from ITQ of catalysts synthesized

Appendix C: Standard synthesis of CNF_CF

Appendix D: Application of similitude model

Appendix E: Mass of Nickel Nitrate necessary to Ni deposition on CF

Appendix F: Calibration curves from volume flow controllers

Appendix G: Times of fill up and cleaning of large scale reactor

Appendix H: Ashrae 1997 Handbook Graphics

Appendix I: Risk assessment (Fan Huang)

Appendix J: Mass of Palladium II Nitrate necessary to Ni deposition on CF

Appendix K: Calculation of CNF deposition yield and fraction of CNF in CF

Appendix L: SEM pictures

Appendix M: Estimation of CNF diameter

Appendix N: TPO data

Appendix O: Pore size distribution data

Appendix P: Needs of electrical power

Appendix A: Veolia's pilot plant.

Reference: Salim Derrouiche, VEOLIA, Internal MONACAT presentation: Monolithic reactors structured at the nano and micro levels for catalytic water purification, Lausanne, May 2011.

A1. Veolia interview:

I have a few questions I hope you can help me with: In your presentation at the MONACAT Lausanne meeting in May you showed us the test reactor in your lab where you can put 6 monoliths (25x60mm) fitted in a teflon cylinder. What is the diameter of the cylinder?

ANSWER: inner diameter of our reactor = 99.9 mm (which is equal to the diameter of the Teflon block unit). Reactor high = 60 mm

We are currently setting up our large-scale synthesis reactor. In this tubular reactor we may also fit a 10 cm diameter large monolith. Would 1 large monolith be able to replace the 6 small monoliths in your reactor?

ANSWER: we already did the first experiment consisting on 100h of run using a light water matrix and using the 6 monoliths provided by Enrique. We are planning to perform a second experiment using a more concentrated water matrix. For this second experiment, we are going to use the same 6 monoliths as for the first experiment. I do not understand your point: are you proposing to send us a big monolith and ask us to perform our second experiment using your big monolith? I think it is better to perform experiments using the same conditions as before but if you want us to perform experiments using the big monolith, it is up to you. Please, check this with Enrique and let me know. Just so you know, if we use the big monolith in the second experiment, it would be then difficult to compare the results with the first experiment. Again, if the European commission agrees with this, it would be ok for us I think.

If **yes**, what would be the most convenient size?

ANSWER: inner diameter of our reactor = 99.9 mm. reactor high = 60 mm

A2. Presentation of Veolia's pilot plant:

Reference: The MONACAT project: EU-FP7 (FP7/2007-2013), Grant Agreement No. 226347, www.monacat.eu

MONACAT – meeting May 19th, 2011 Lausanne

Monolithic reactors structured
at the nano and micro levels
for catalytic water purification

M24



23/05/2011) Veolia Environnement Recherche & Innovation

Table of Content

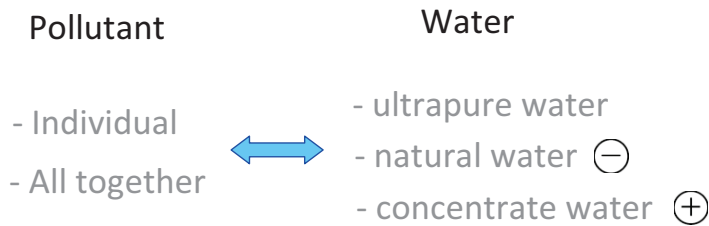
1. Performed activities

- Solutions : preparation and analysis
- Send samples to UPORTO
 - November 2010 —→ Atrazine / natural water
 - January 2011 —→ Σ pollutants / natural water
 - February 2011 —→ Σ pollutants / concentrate water
- Send samples to WU (January 2011) —→ pollutants / natural water
- Preliminary lab test (VERI) (February 2011)
- Design and building of the lab scale setup (June 2011)

2. Next steps and expectation

Performed activities

Solutions : preparation and analysis



Target pollutants selected :

Category / class	Substances	concentration (µg/L)		⊖	⊕
Antibiotic	erythromycin	0.4			
Pharmaceuticals	bezafibrate	0.5			
Pesticides	atrazine	1			
	metolachlor	1			
Endocrine disruptors	nonylphenol	0.5			

	⊖	⊕
TOC (mg/L)	0.5	40
pH	7.8	7.5
HCO ₃ ⁻ (mg/L)	180	1300

23/05/2011

Veolia Environnement Recherche & Innovation

3

Performed activities

- Send samples to WU (January 2011)
- Send samples to UPORTO (November 2010)

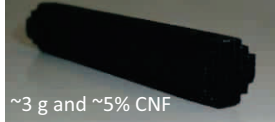
→ **Atrazine / natural water** ⊖

[Atr] = 1 µg/ L

→ Semi-batch and continuous experiments (UPORTO)

- Catalyst
- O₃
- O₃ + Catalyst

Catalyst (CSIC) :
N-doped CNF grown on ceramic monoliths



~3 g and ~5% CNF

Semi-Batch Experiments:

Gas flow rate: 100 cm³/min
Ozone in gas phase: 50 g/m³
Loop flow rate: 100 ml/min

Continuous Experiments:

Gas flow rate: 100 cm³/min
Ozone in gas phase: 50 g/m³
Loop flow rate: 100 ml/min
Feed flow rate: 10 ml/min

After 5h of reaction

		molecules : atrazine and by-products (µg/L)						
sample		Atrazine	DEA	DEDIA	DIA	Hydroxyatrazine	Simazine	matrix
Reference sample		0.99	ε	ε	ε	ε	ε	natural water
Semi-batch	Catalyst	0.93	ε	0.07	ε	ε	ε	natural water
	O ₃	ε	ε	1.1	ε	ε	ε	natural water
	O ₃ + Catalyst	ε	ε	0.43	ε	ε	ε	natural water
Continuous	Catalyst	0.81	ε	ε	ε	ε	ε	natural water
	O ₃	ε	ε	0.24	ε	ε	ε	natural water
	O ₃ + Catalyst	ε	ε	0.29	ε	ε	ε	natural water

ε : "<0.02 µg/L"

4

Performed activities ● Sending samples to UPORTO : Experimental plan

- Σ pollutants / natural water \ominus
- Σ pollutants / concentrate water \oplus

	SAMPLING TIME	FLASK AND VOLUMES	ANALYSES in OUR LABORATORY
O3 alone	t = 0	2 flasks of 1L + 1 flask of 500 ml	Atrazine, Erythromycin, Bezafibrate, Nonylphenol Metolachlore
	t = 2h-3h40	1 flask of 500 ml + 1 flask of 500 ml	Metolachlore Bezafibrate
	t = 3h40-6h10	1 flask of 500 ml + 1 flask of 1L	Atrazine, Erythromycin, Nonylphenol
	t = 6h10-7h50	1 flask of 500 ml + 1 flask of 500 ml	Metolachlore Bezafibrate
O3 + catalyst	t = 0	2 flasks of 1L + 1 flask of 500 ml	Atrazine, Erythromycin, Bezafibrate, Nonylphenol Metolachlore
	t = 2h-3h40	1 flask of 500 ml + 1 flask of 500 ml	Metolachlore Bezafibrate
	t = 3h40-6h10	1 flask of 500 ml + 1 flask of 1L	Atrazine, Erythromycin, Nonylphenol
	t = 6h10-7h50	1 flask of 500 ml + 1 flask of 500 ml	Metolachlore Bezafibrate
Catalyst alone	t = 0	2 flasks of 1L + 1 flask of 500 ml	Atrazine, Erythromycin, Bezafibrate, Nonylphenol Metolachlore
	t = 2h-3h40	1 flask of 500 ml + 1 flask of 500 ml	Metolachlore Bezafibrate
	t = 3h40-6h10	1 flask of 500 ml + 1 flask of 1L	Atrazine, Erythromycin, Nonylphenol
	t = 6h10-7h50	1 flask of 500 ml + 1 flask of 500 ml	Metolachlore Bezafibrate

23/05/2011

Veolia Envi

5

Performed activities

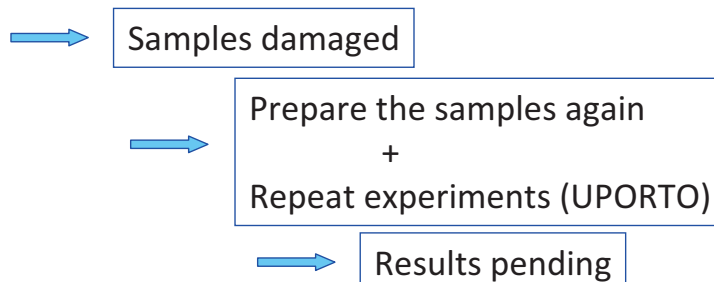
● Send samples to UPORTO (January 2011)

→ Σ pollutants / natural water \ominus

- [Atr] = 1 $\mu\text{g/L}$
- [Bez] = 0.27 $\mu\text{g/L}$
- [Ery] = 0.19 $\mu\text{g/L}$
- [Met] = 0.88 $\mu\text{g/L}$
- [Non] = 0.3 $\mu\text{g/L}$
- TOC = 0.5 mg/L

→ Semi-batch and continuous experiments (UPORTO)

- Catalyst
- O3
- O3 + Catalyst



23/05/2011

Veolia Environnement Recherche & Innovation

6

Performed activities

Send samples to UPORTO (February 2011)

→ Σ pollutants / concentrate water (+)

- [Atr] = 1.3 $\mu\text{g/L}$
- [Bez] = 1.1 $\mu\text{g/L}$
- [Ery] = 0.23 $\mu\text{g/L}$
- [Met] = 0.96 $\mu\text{g/L}$
- [Non] = 0.7 $\mu\text{g/L}$
- TOC = 21 mg/L

→ Semi-batch and continuous experiments (UPORTO)

- Catalyst
- O₃
- O₃ + Catalyst

→ Results pending

23/05/2011

Veolia Environnement Recherche & Innovation

7

Performed activities

Preliminary lab test (VERI) (February 2011)

→ **Atrazine / ultrapure water**

- [Atr] = 1 $\mu\text{g/L}$

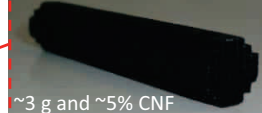
→ Continuous experiments

- Catalyst
- O₃
- O₃ + Catalyst

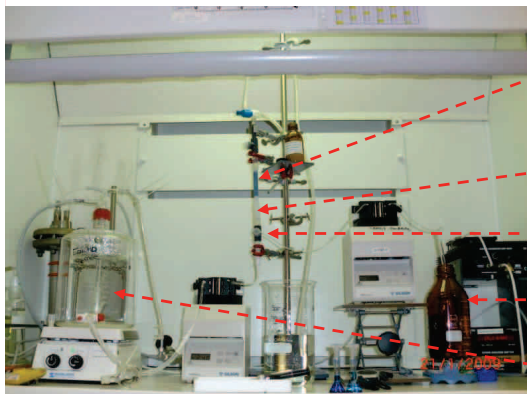
Exp. conditions :

- T°C = 20°C
- [O₃]_g = 100g/ Nm³
- [O₃]_{diss} = 4 mg/L
- Pressure drop (1 monolith) :
0.3 mBar with Q=2 L/h
- Contact time = 3 min

Catalyst (CSIC) :
N-doped CNF grown on
ceramic monoliths



~3 g and ~5% CNF



static mixer

sampling

contact column



Introduction of atrazine

23/05/2011

Veolia Environnement Recherche & Innovation

8

Performed activities

• Preliminary lab test (VERI) (February 2011)

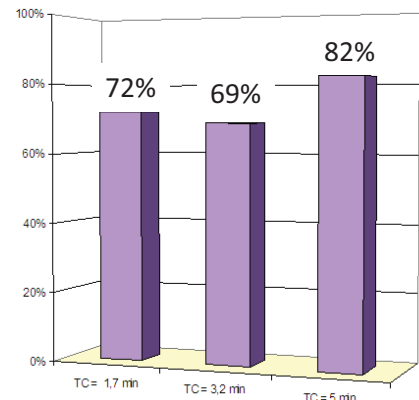
→ Atrazine / ultrapure water

- Different contact time (min) : $T_c = 1.7 ; 3.2 ; 5$
- Different configurations : 1 or 2 monoliths in series

% of atrazine removed ($T_c = 3.2\text{min}$ & 2 monoliths) :
(steady state after 2h of reaction)

	Xatrazine
O3	50%
Cata	69%
O3 + Cata	69%

Atrazine removal (%)
VS
Contact time (min)



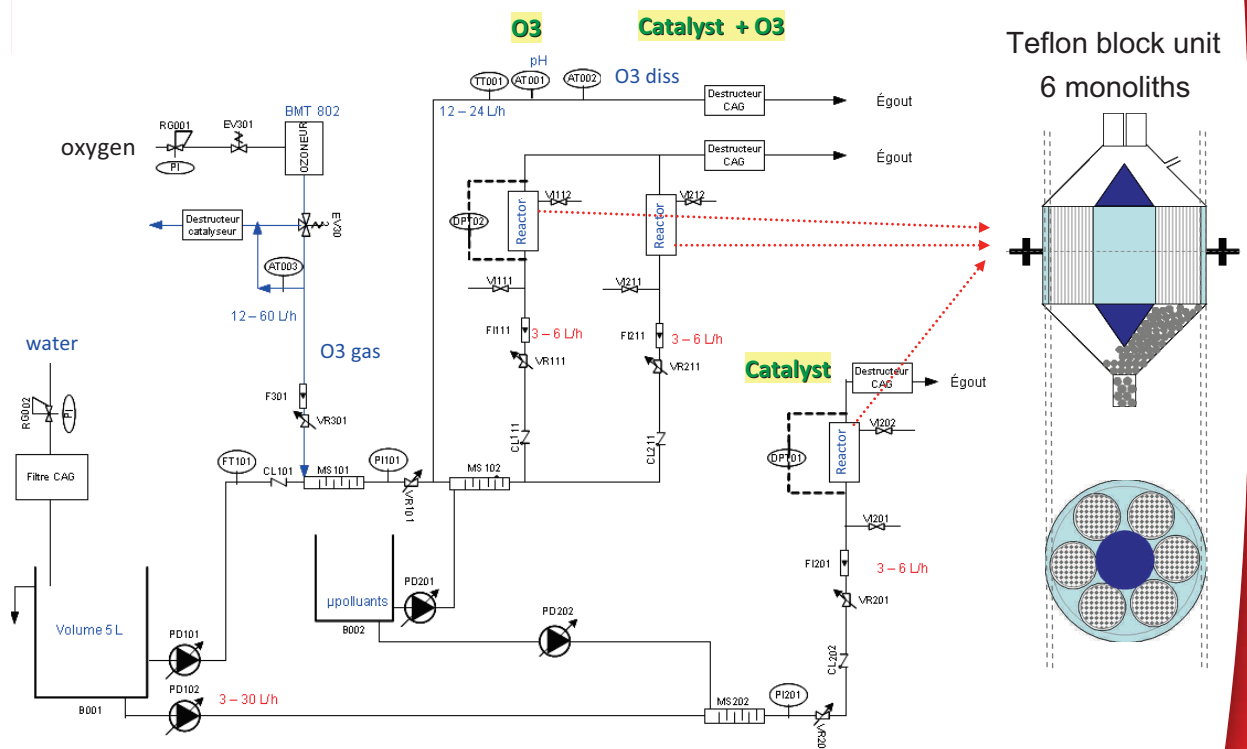
23/05/2011

Veolia Environnement Recherche & Innovation

9

Performed activities

• Design and building of the lab scale pilot (June 2011)



10

Next steps & expectations

• Catalytic ozonation

- ◆ Experiments using only 1 type of catalyst → monolith (CSIC)
- ◆ Deliverable D9.2. (August 2011) :
 - will contain only results on experiments Σ pollutant/ natural water ⊖
 - Experiments Σ pollutant/ concentrate water ⊕ → Nov. 2011

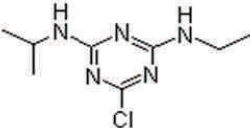
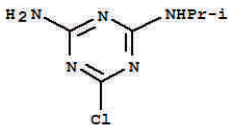
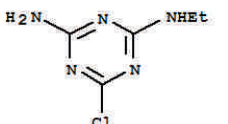
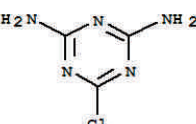
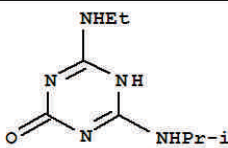
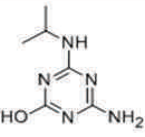
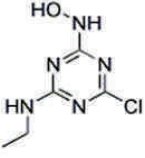
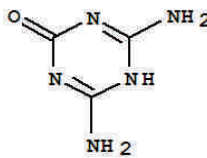
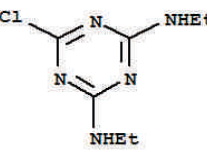
• Catalytic reduction

- ◆ What exactly VERI is expected to do ?
 - bromate most important : which catalyst ?
- ◆ Tentative & realistic schedule :
 - Lab scale pilot → January 2012
 - Deliverable → March 2012

• Catalyst stability & comparison

Activity : ok but stability ?

- ◆ Criteria that validate the chemical and physical stability of the catalyst ?
 - leaching of nanostructured material (metals, CNF, ACF, ...) ?
 - structure collapse ?
- ◆ Criteria for catalyst comparison : TOF ? (kinetic regime ?)

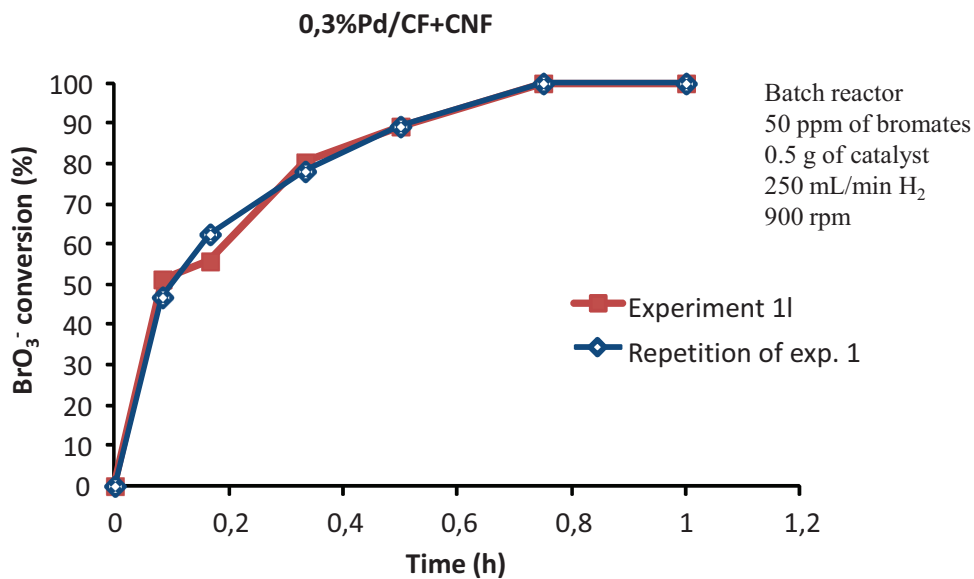
Abbreviation	Chemical name	Formulae
A	Atrazine	
DEA	Deethylatrazine	
DIA	Deisopropylatrazine	
DDA or DEDIA	Didealkylatrazine or Deethyldeisopropylatrazine	
HA	Hydroxyatrazine	
HDEA	Hydroxydeethylatrazine	
HDIA	Hydroxydeisopropylatrazine	
HDEDIA or DEDIHA	Ammeline	
SIM	Simazine	

- Total alkalinity
- pH
- Water hardness
- Bromide
- Calcium
- Magnesium
- TOC

Appendix B: Tests from ITQ of catalysts synthesized

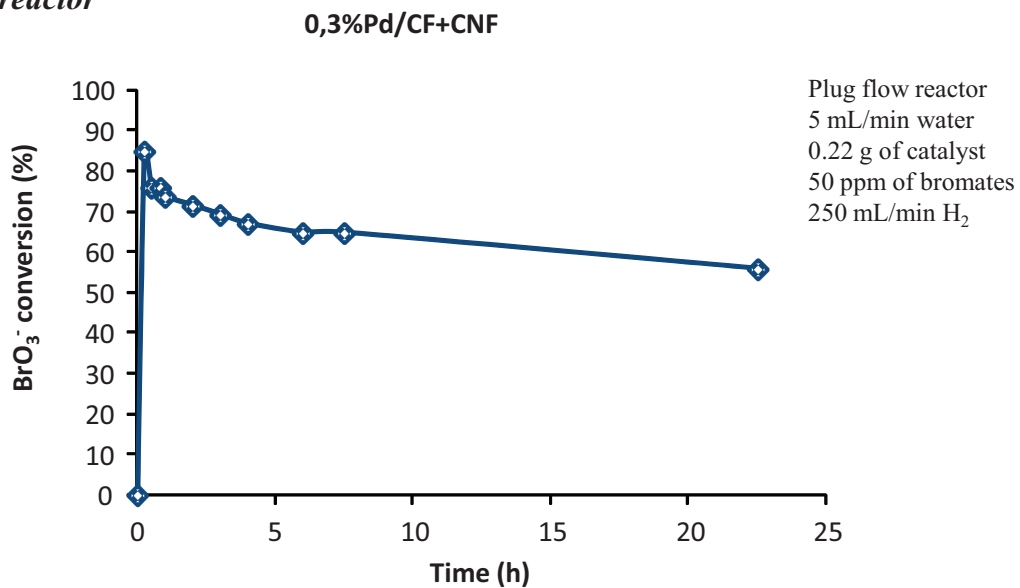
Discontinuous reactions

Repeatability reactions



Continuous reaction

Plug flow reactor



Appendix C: Standard synthesis of CNF_CF

Fishbone CNF:

Carbon felt (CF) from the Carbon Lorraine Company with a surface area of approximately 1 m²/g was used as a host material (22 mm diameter, 6 mm thickness). The CF has was refluxed in concentrated HNO₃ for 1 hour followed by filtration, washing in distilled water until stable pH (close to 6) and dried in an furnace at 100°C for 12 hours.

Nickel was used as a catalyst for the CCVD process and the amount corresponded to 2 wt.% of the CF. The catalyst was prepared by incipient wetness impregnation using ethanol as the solvent. Pore volume measurements were conducted to determine the amount of ethanol necessary to fill the pores. After impregnation the material was dried at room temperature for 3 hours before drying in an oven at 100°C for 12 hours. The impregnated CF was calcined at 300°C for 2 hours in static air to obtain the NiO phase.

The reduction of NiO was performed in situ at 600°C or 650°C for 2 hours in 25 ml/min H₂ and 75 ml/min N₂. CNF synthesis was performed at 650°C for 5 hours, using a reaction mixture of ethane and H₂ (25/75 ml/min). The reactor was cooled down to room temperature in N₂.

Platelet CNF:

Two weight percent Ni–Cu (1:1)/CF catalysts were prepared by incipient wetness impregnation. An ethanol solution containing Ni(NO₃)₂·6H₂O and Cu(NO₃)₂·3H₂O was impregnated onto a macroscopic CF (Carbone Lorraine Co) disk (22 mm diameter, 6 mm thickness) and subsequently dried overnight at room temperature. No pre-treatment of the CF in concentrated nitric acid was performed. The as-impregnated solid was dried overnight at room temperature.

The catalytic synthesis of the CNF/CF composite was carried out in a vertical quartz reactor. Five pieces of dried Ni–Cu/CF catalysts were directly reduced by a H₂/N₂ mixture (40/160 mL/min) at 923 K (temperature ramp rate 5 K/min) for 2 h. This procedure is expected to fully reduce the impregnated metal precursors to the corresponding metallic phase. After reduction, CNF growth was performed by using a C₂H₆/H₂ mixture (90/150 mL/min) for 2 h.

Reference: Carbon Lorraine Co.

Appendix D: Similitude model application

Defining 1 as small-scale reactor and 2 as up-scaled reactor

D = inner diameter of reactor (m)

v = mean velocity throughout reactor (m/sec)

A = inner area of reactor (m²)

Q = total flow of gaseous current (m³/sec)

τ_{CF} = spatial time of gaseous current inside carbon felt bed (sec)

V_{free} = free volume in carbon felt (m³)

V_T = total volume occupied by reactor bed (m³)

ε = porosity of carbon felt (m³/m³)

L_{CF} = bed length (m)

ρ = density of fluid (kg/m³)

μ = dynamic viscosity (kg/m·sec)

$$v = Q/A = (Q \cdot 4)/(D^2 \cdot \pi)$$

$$\tau_{CF} = V_{free}/Q$$

$$V_{free} = V_T \cdot \varepsilon$$

$$V_T = A \cdot L_{CF}$$

D1 Dimensional similitude: $(D_1/D_2) = (L_{CF1}/L_{CF2}) = \text{constant}$

$$(D_1/D_2) = (L_{CF1}/L_{CF2})$$

D2 Kinematic similitude: $\tau_{CF} = \text{constant}$

Assuming: total mixed flow inside reactor (homogeneous physical-chemical properties)

$$\tau_{CF1} = \tau_{CF2} \quad (V_{T1} \cdot \varepsilon)/Q_1 = (V_{T1} \cdot \varepsilon)/Q_2$$

$$(V_{T1})/Q_1 = (V_{T1})/Q_2$$

$$(D_1^2 \cdot \pi \cdot L_{CF1})/(Q_1 \cdot 4) = (D_2^2 \cdot \pi \cdot L_{CF2})/(Q_2 \cdot 4)$$

$$(D_1^2 \cdot L_{CF1})/(Q_1) = (D_2^2 \cdot L_{CF2})/(Q_2)$$

D1 Dynamic similitude: $Re_i = \text{constant}$

For tubular reactors, Reynolds number is defined as: $Re = (D \cdot v \cdot \rho)/\mu$

$$Re_1 = Re_2 \quad (D_1 \cdot v_1 \cdot \rho_1)/\mu_1 = (D_2 \cdot v_2 \cdot \rho_2)/\mu_2$$

The fluid is the same mixture of gases, at the same temperature and total pressure:

$$\rho_1 = \rho_2; \mu_1 = \mu_2$$

$$\rightarrow D_1 \cdot v_1 = D_2 \cdot v_2;$$

$$(D_1 \cdot Q_1 \cdot 4)/(D_1^2 \cdot \pi) = (D_2 \cdot Q_2 \cdot 4)/(D_2^2 \cdot \pi)$$

$$\rightarrow (Q_1/D_1) = (Q_2/D_2);$$

$$(Q_1/Q_2) = (D_1/D_2)$$

The up-scaling model is defined for three different variables, which are D_2 , L_{CF2} and Q_2 ; and they are related by 3 equations to small-scale variables. Thus, in order to achieve total similitude only one solution will exist, limiting our range of scaling and making it impossible to accomplish. A compromising solution will have to be found.

Appendix E: Mass of Nickel Nitrate necessary to Ni deposition on CF

It is aimed to deposit 2% in weight of Ni on CF supports.

For this task a salt of Nickel is employed: $\text{Ni}(\text{NO}_3)_2 \cdot 6\text{H}_2\text{O}$. From the salt bottle, the following data are obtained:

$$M_{\text{W}_{\text{salt}}} = 290.8 \text{ g/mol}; \quad \text{Purity} = 97\% \text{ in weight}; \quad M_{\text{W}_{\text{Ni}}} = 58.69 \text{ g/mol}$$

They have been defined: m_{CF} = mass of CF

m_{Ni} = mass of Nickel

m_{salt} = mass of $\text{Ni}(\text{NO}_3)_2 \cdot 6\text{H}_2\text{O}$

m_1 = mass Ni plus mass of CF

Proportion of Nickel in the salt (A)

$$\text{Prop}_{\text{Ni}} (\text{gNi/gSalt}) = 58.69 \text{ gNi/molNi} \cdot 1 \text{ molNi/1 molPureSalt} \cdot 1 \text{ molSaltPute/290.8 gPureSalt} \cdot 0.97 \text{ gPureSalt/gSalt};$$

$$\text{Prop}_{\text{Ni}} (\text{gNi/gSalt}) = 0.1958 \text{ gNi/gSalt}$$

$$m_{\text{Salt}} = (m_{\text{Ni}})/0.1958 \text{ (A)}$$

Relation in weight between Nickel and CF (B)

$$m_1 = m_{\text{CF}} + m_{\text{Ni}}; [m_1 = m_{\text{Ni}}/0.02]; \quad m_{\text{Ni}}/0.02 = m_{\text{CF}} + m_{\text{Ni}}$$

$$m_{\text{Ni}} = ((m_{\text{CF}}) \cdot 0.02)/(1-0.02) \text{ (B)}$$

Mass of salt to be weighted: combining (B) and (A)

$$m_{\text{Salt}} = m_{\text{CF}} \cdot (0.02/(1-0.02))/0.1958$$

$$m_{\text{Salt}} = (m_{\text{CF}}) \cdot 0.1042$$

Check-up: $\%_{\text{Ni}} (\text{gNi/gSalt}) = (0.97 \text{ gPureSalt/gSalt} \cdot m_{\text{Salt}}) \cdot (M_{\text{W}_{\text{Ni}}}/M_{\text{W}_{\text{Salt}}})/m_{\text{CF}} = 0.0204\% \text{ (close to 2\%)}$

Appendix F: Calibration curves from volume flow controllers

Small-scale:

Obtained from laboratory:

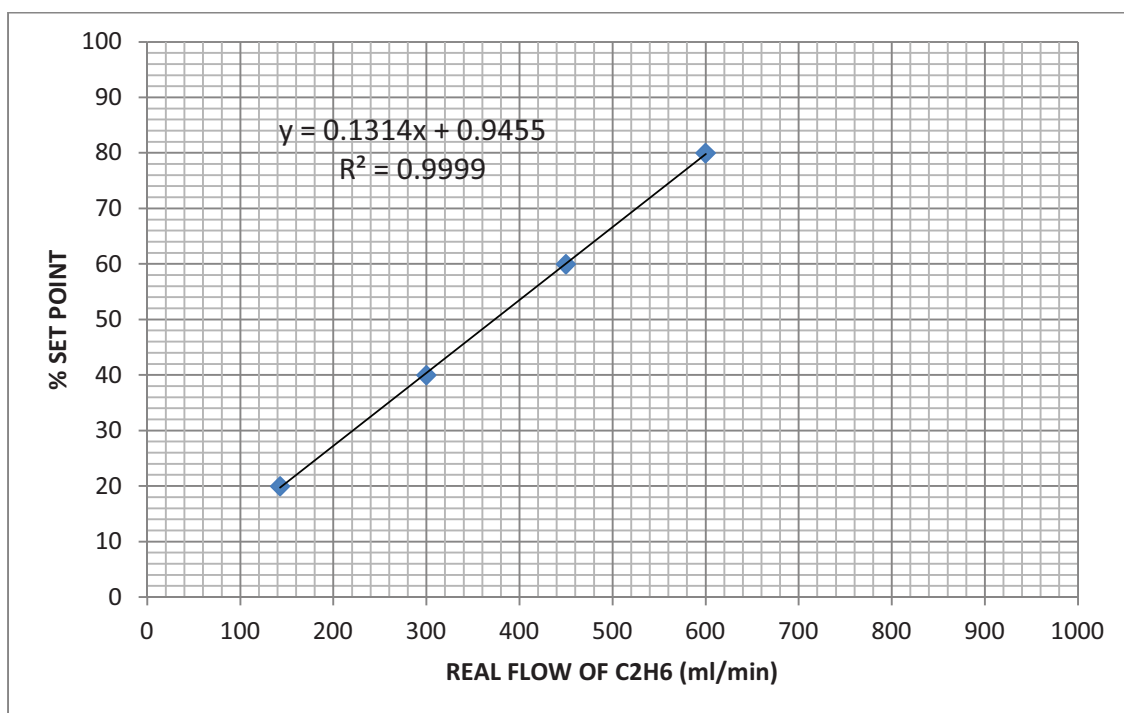
$$\text{C}_2\text{H}_4: Q_{\text{C}_2\text{H}_4} = 6.1096 \cdot \% \text{SET}_{\text{C}_2\text{H}_4} + 19.259$$

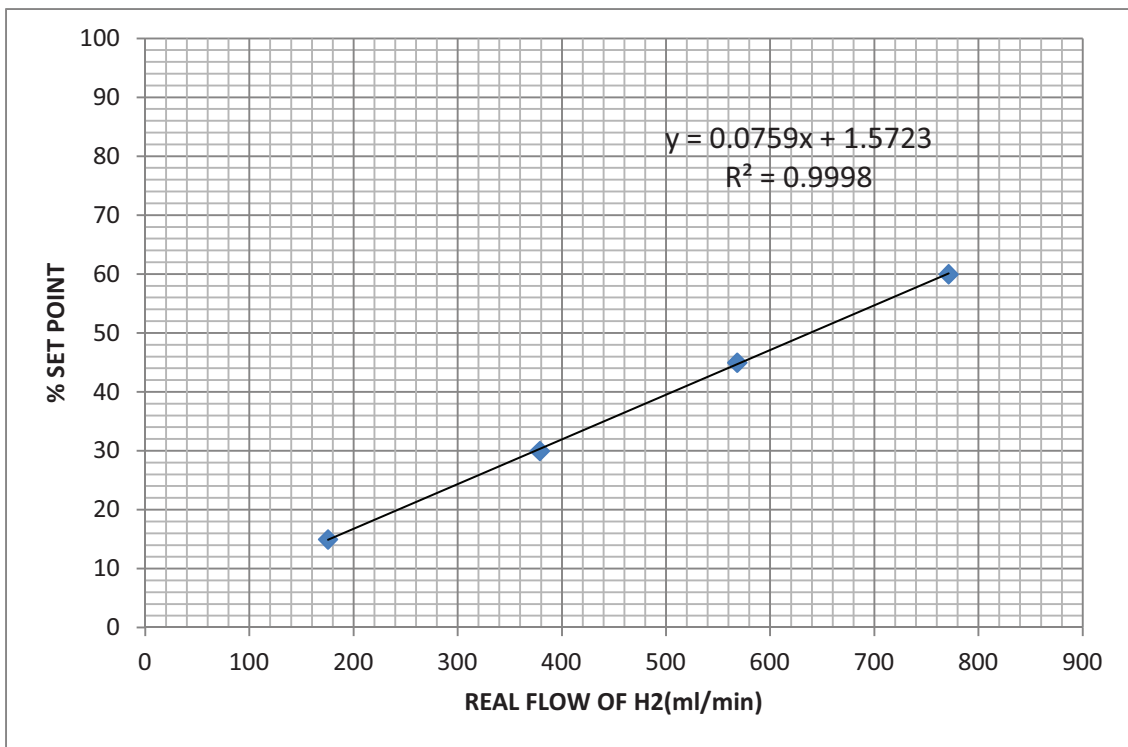
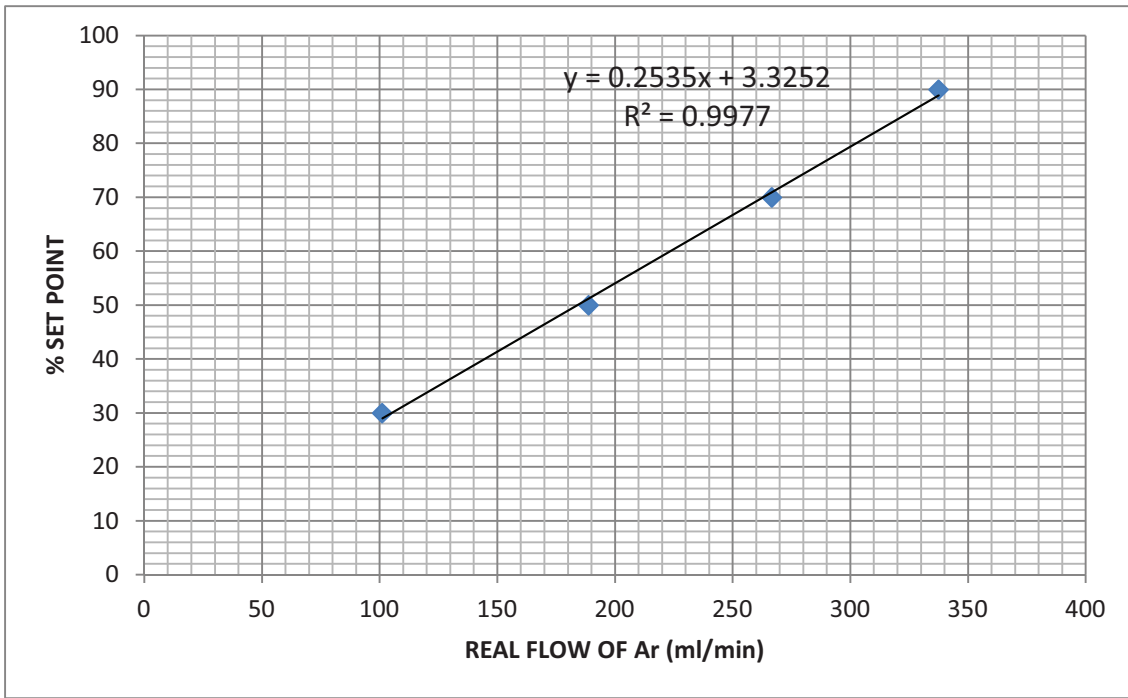
$$\text{Ar}: Q_{\text{Ar}} = 7.3879 \cdot \% \text{SET}_{\text{Ar}} + 28.171$$

$$\text{H}_2: Q_{\text{H}_2} = 2.3406 \cdot \% \text{SET}_{\text{H}_2} - 0.7947$$

Large-scale:

	Set flow (ml/min)	% Set point	Mean time for 90 ml (sec)	Real flow (ml/min)
C ₂ H ₆	200	20	37.8	142.857
	400	40	18	300
	600	60	12	450
	800	80	9	600
Ar	90	30	53.4	101.123
	150	50	28.6	188.811
	210	70	20.25	266.667
	270	90	16	337.5
H ₂	150	15	30.75	175.609
	300	30	14.25	378.947
	450	45	9.5	568.421
	600	60	7	771.428





Appendix G: Times of fill up and cleaning of large scale reactor

G1. Fill up of Argon:

$Q_{Ar} = \text{CONSTANT}$ (P and T are constant, besides Argon and Air are considered as perfect gases)
The volumes are aditives when are mixed.

$$V_{\text{reactor}} := 10602.9 \text{ cm}^3 \quad Q_{ArT} := 375 \frac{\text{cm}^3}{\text{min}} \quad T_{\text{room}} := (18 + 273.13) \text{ K}$$

$$P := 1 \text{ atm} \quad X_{Ar_in} := 1$$

$$MW_{Ar} := 0.039948 \frac{\text{kg}}{\text{mole}} \quad R_{GP} := 0.082 \frac{\text{atm} \cdot \text{L}}{\text{mole} \cdot \text{K}} \quad \rho_{Ar}(T) := \frac{MW_{Ar} \cdot P}{R_{GP} \cdot T}$$

$$\rho_{Ar}(T_{\text{room}}) = 1.673 \frac{\text{kg}}{\text{m}^3}$$

Boundary conditions: with a filling up around 90% in Argon, there will be enough.

$$\text{Initial state:} \quad X_{Ar0} := 0 \quad X_{Air0} := 1 \quad \text{time}_0 := 0$$

$$\text{Final state:} \quad X_{ArF} := 0.90 \quad X_{AirF} := 1 - X_{ArF}$$

Mass balances (reactor as control volume):

Total mass:

$$\frac{d}{dt} m_T = Q_{in} \cdot \rho_{in} - Q_{out} \cdot \rho_{out}(t) \quad \rho_{out}(t) = \rho_{VC}(t) = \rho_{Ar} \cdot X_{Ar}(t) + \rho_{Air} \cdot X_{Air}(t)$$

$$V_{\text{reactor}} \cdot \frac{d}{dt} \rho_{VC}(t) = Q_T \cdot (\rho_{in} - \rho_{out}(t)) \quad Q_T = Q_{in} = Q_{out} \quad \text{Perfect gases mixture at } T = \text{cte}$$

Argon mass:

$$\frac{d}{dt} m_{Ar} = Q_{Ar_in}(t) \cdot \rho_{Ar} - Q_{Ar_out}(t) \cdot \rho_{Ar} \quad Q_T := Q_{ArT}$$

$$V_{\text{reactor}} \cdot \rho_{Ar} \cdot \left(\frac{d}{dt} X_{Ar} \right) = (Q_{Ar_in} - Q_{Ar_out}) \cdot \rho_{Ar} \quad X_{Ar} = X_{Ar_out}$$

$$V_{\text{reactor}} \cdot \rho_{Ar} \cdot \left(\frac{d}{dt} X_{Ar} \right) = Q_T \cdot \rho_{Ar} \cdot (X_{Ar_in} - X_{Ar})$$

Variable initialization: $\text{time}_F := 1 \text{ min}$

$$\text{Dado}$$

$$\frac{V_{\text{reactor}}}{Q_T} \cdot \int_0^{X_{ArF}} \frac{1}{X_{Ar_in} - X_{Ar}} dX_{Ar} = \int_{\text{time}_0}^{\text{time}_F} 1 dt$$

$$\text{fill_up_time} := \text{Find}(\text{time}_F) \quad \text{fill_up_time} = 65.104 \cdot \text{min}$$

References: ASHRAE 1997 FUNDAMENTALS HANDBOOK

G2. Cleaning of reactor before synthesis:

$Q_{Ar} = \text{CONSTANT}$ (P and T are constant, besides Argon and synthesis gases are considered as perfect gases)
The volumes are additive when mixed.

$$T_{\text{reac}} := (650 + 273.15)\text{K} \quad \rho_{Ar}(T_{\text{reac}}) = 0.528 \frac{\text{kg}}{\text{m}^3} \quad \rho_{Ar_out} := \rho_{Ar}(T_{\text{reac}})$$

$$Q_T = Q_{Ar} = 375 \frac{\text{cm}^3}{\text{min}}$$

Boundary conditions: with a filling up around 90% in Argon, there will be enough.

Mass balances (reactor as control volume):

Argon mass:

$$\frac{d}{dt} m_{Ar} = Q_{Ar_in}(t) \cdot \rho_{Ar}(T_{\text{room}}) - Q_{Ar_out}(t) \cdot \rho_{Ar}(T_{\text{reac}}) \quad X_{Ar}(t) = X_{Ar_out}(t)$$

$$V_{\text{reactor}} \cdot \rho_{Ar}(T_{\text{reac}}) \cdot \left(\frac{d}{dt} X_{Ar} \right) = Q_T \cdot (\rho_{Ar}(T_{\text{room}}) \cdot 1 - \rho_{Ar_out} \cdot X_{Ar})$$

Variable initialization: $\text{time}_{F2} := 1 \text{ min}$

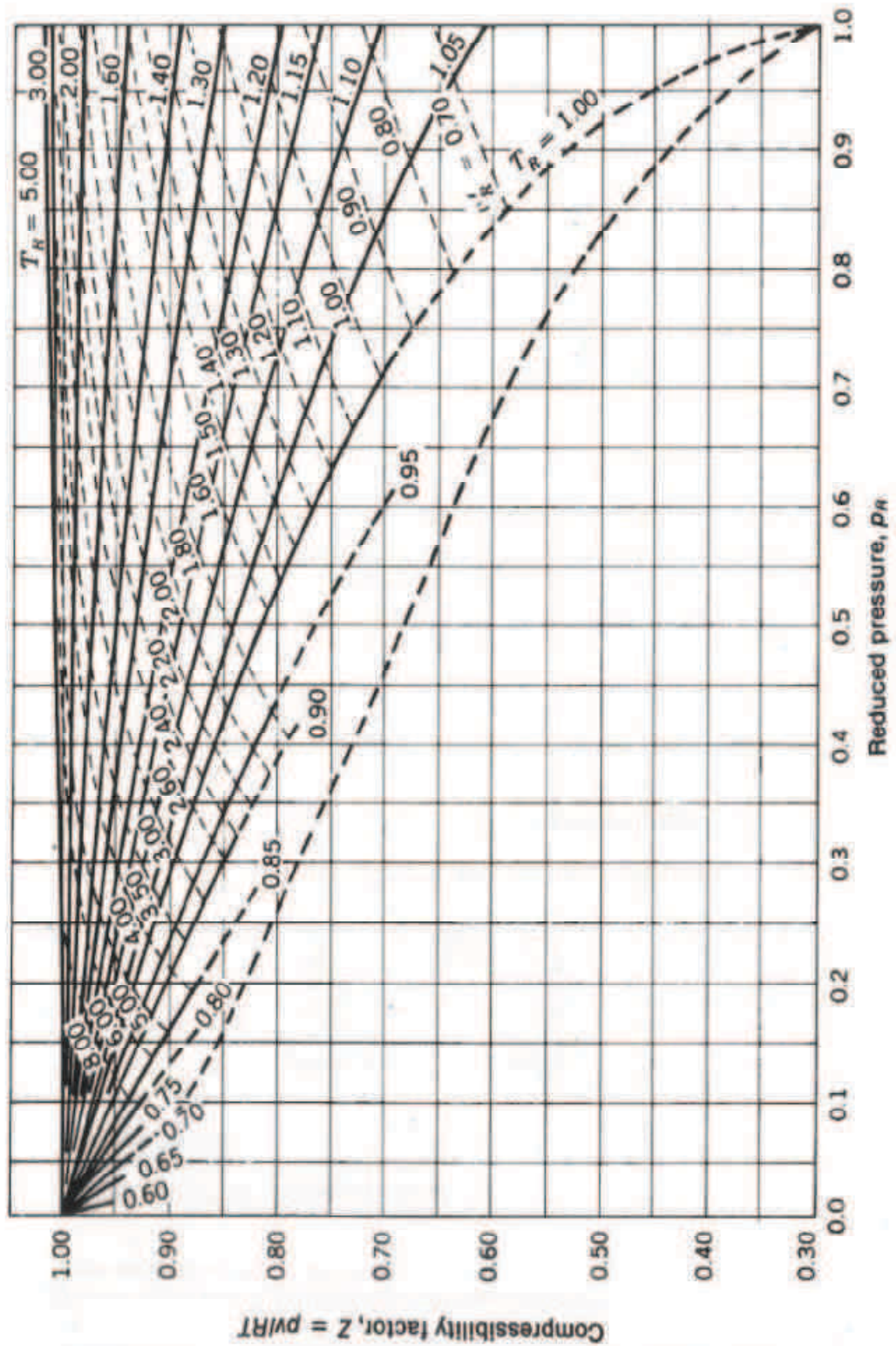
Dado

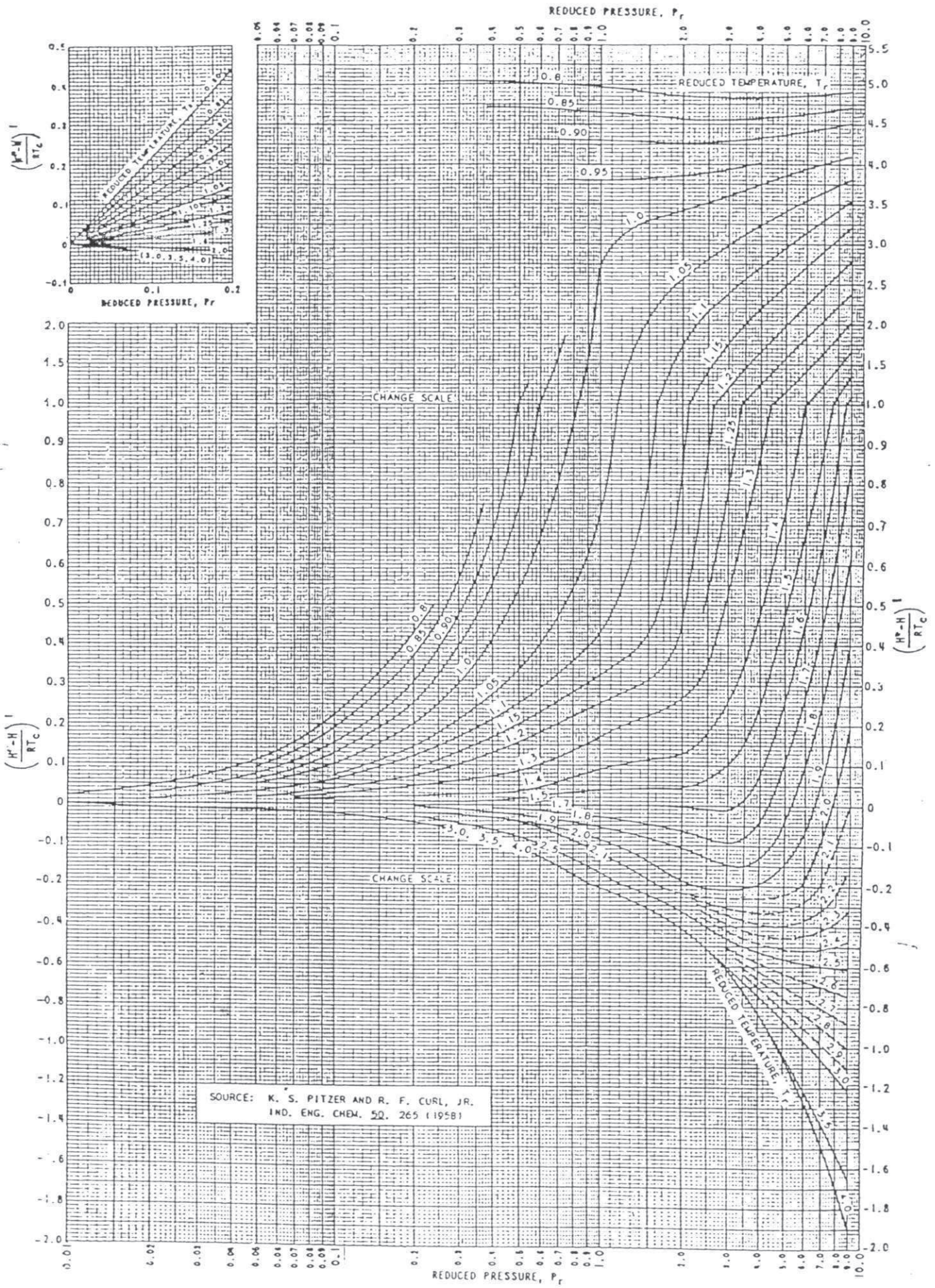
$$\frac{V_{\text{reactor}}}{Q_T} \int_0^{X_{ArF}} \frac{\rho_{Ar}(T_{\text{reac}})}{(\rho_{Ar}(T_{\text{room}}) \cdot X_{Ar_in} - \rho_{Ar_out} \cdot X_{Ar})} dX_{Ar} = \int_{\text{time}_0}^{\text{time}_{F2}} 1 dt$$

$$\text{fill_up_time2} := \text{Find}(\text{time}_{F2}) \quad \text{fill_up_time2} = 9.439 \cdot \text{min}$$

References: ASHRAE 1997 FUNDAMENTALS HANDBOOK

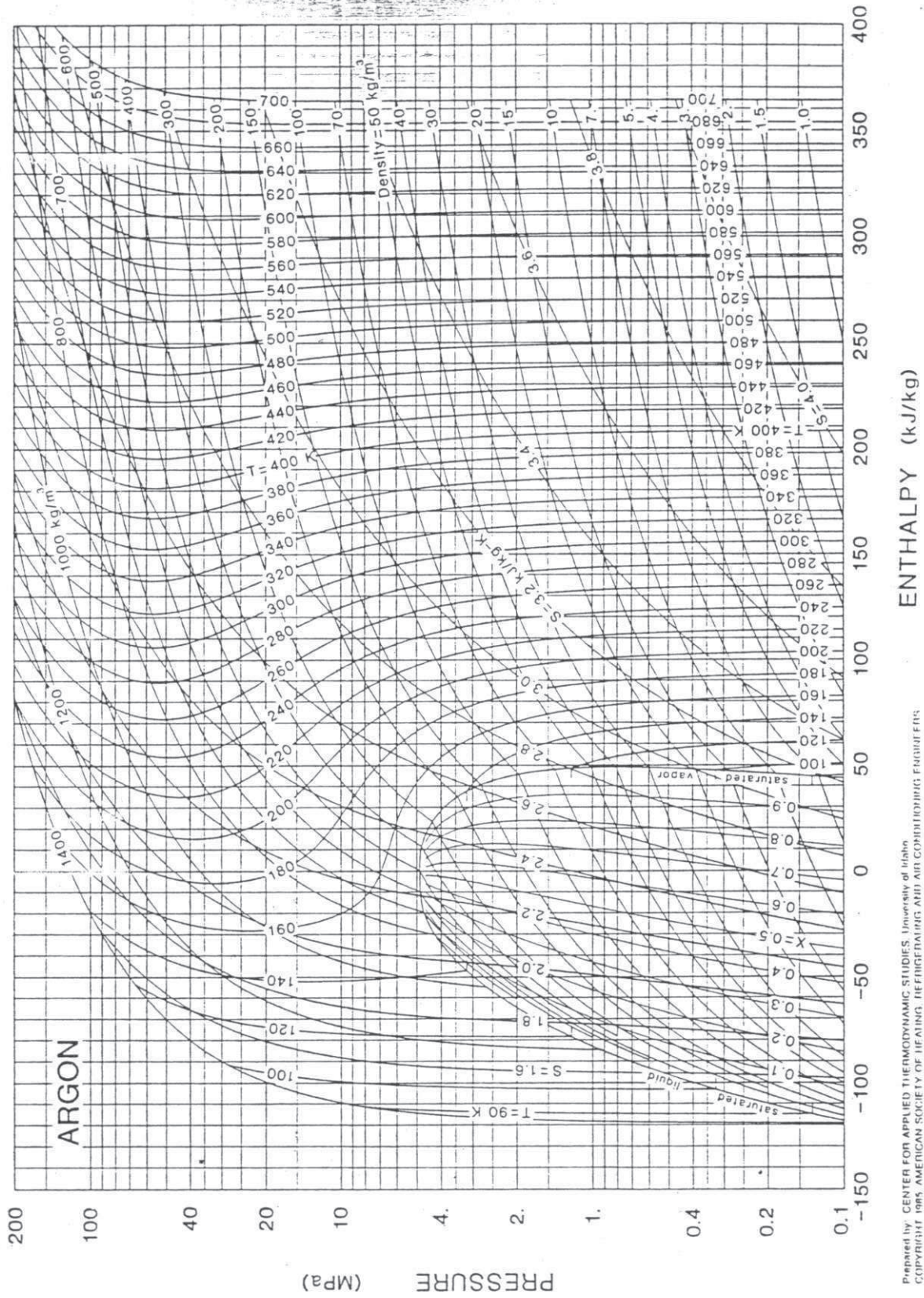
Appendix H: Ashrae 1997 Handbook Graphics





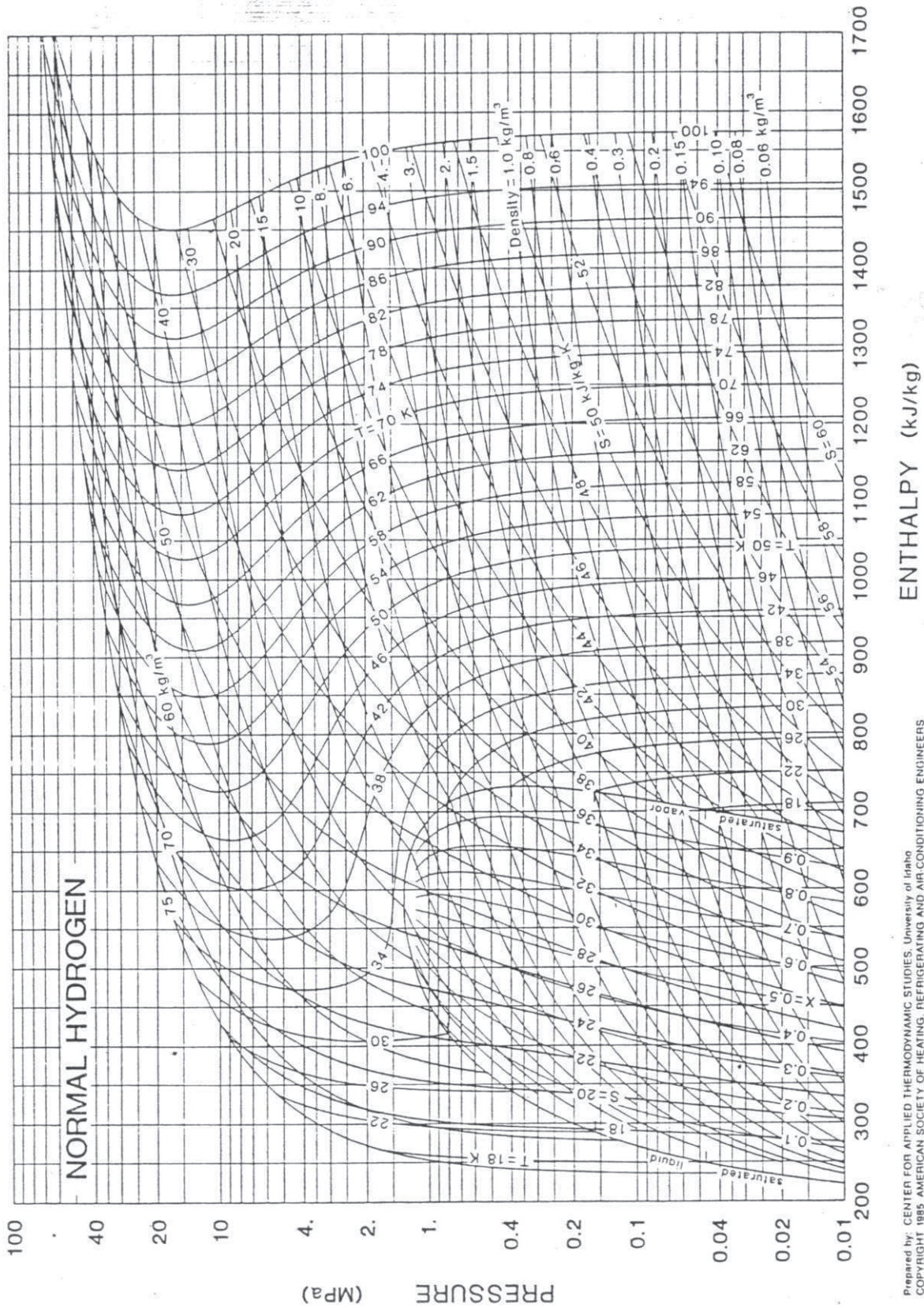
SOURCE: K. S. PITZER AND R. F. CURL, JR.
IND. ENG. CHEM. 50, 265 (1958)

Figura 5



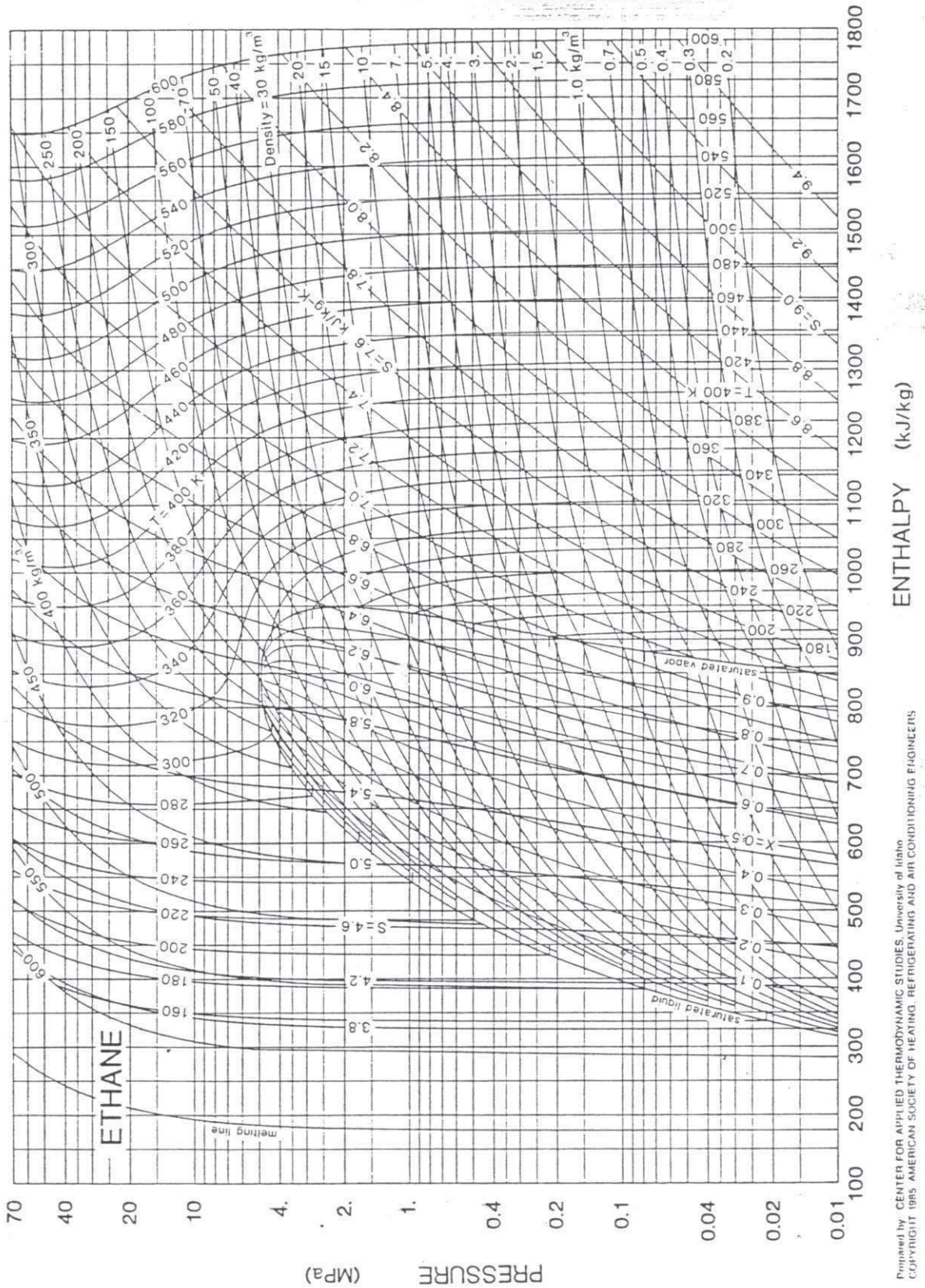
Prepared by: CENTER FOR APPLIED THERMODYNAMIC STUDIES, University of Idaho
 Copyright 1985, AMERICAN SOCIETY OF HEATING, REFRIGERATING AND AIR CONDITIONING ENGINEERS

Fig. 38 Pressure-Enthalpy Diagram for Refrigerant 740 (Argon)



Prepared by: CENTER FOR APPLIED THERMODYNAMIC STUDIES, University of Idaho
COPYRIGHT 1985 AMERICAN SOCIETY OF HEATING, REFRIGERATING AND AIR-CONDITIONING ENGINEERS

Fig. 31 Pressure-Enthalpy Diagram for Refrigerant 702 (Normal Hydrogen)



Prepared by CENTER FOR APPLIED THERMODYNAMIC STUDIES, University of Idaho
COPYRIGHT 1995 AMERICAN SOCIETY OF HEATING, REFRIGERATING AND AIR CONDITIONING ENGINEERS

Fig. 25 Pressure-Enthalpy Diagram for Refrigerant 170 (Ethane)

NTNU	 Hazardous activity identification process				Risikovurdering	Nummer	Dato
HMS					HMS-avd.	HMSRV2601	
		Godkjent av	Side	Erstatter			



Unit:

Kjemisk prosess teknologi

Date: 17,10,2011

Line manager:

Øyvind Gregersen

Participants in the identification process (including their function):

Fan Huang (researcher), Pablo Saz (master student)

Room 228

Short description of the main activity/main process:

ID no.	Activity/process	Responsible person	Laws, regulations etc.	Existing documentation	Existing safety measures	Comment
1	CVD synthesis of CNF/flamable gases (H ₂ , C ₂ H ₆) are used	Fan Huang		MSDS	Room detector, local detector, leak testing, gloves, goggles, lab	Leak testing with noble gases and room and local detectors
2	Oven	Fan Huang			Gloves, goggles, lab coat.	Leak testing before heating up. No activity by the instrument while temperature above 200 C.

Operating Instructions

Instrument/Apparatus:		
Serial Number:	Placement: K5-228	
Original Manual:		
Log book with signature for training & maintenance:	None	
Risk Evaluation		
Date: 17,10,2011		
Archived:		
Compulsory Protection Equipment:	Hazards:	
Safety Goggles	<input checked="" type="checkbox"/>	Fire <input checked="" type="checkbox"/>
Gloves	<input checked="" type="checkbox"/>	Chemicals/Gasses <input checked="" type="checkbox"/>
Hearing Protection	<input checked="" type="checkbox"/>	Electricity/Power <input checked="" type="checkbox"/>
Protective Clothing	<input checked="" type="checkbox"/>	Temperature/Pressure <input checked="" type="checkbox"/>
Breathing Protection	<input type="checkbox"/>	Cutting/Crushing <input type="checkbox"/>
Shielding	<input type="checkbox"/>	Rotating Equipment <input type="checkbox"/>
Other	<input type="checkbox"/>	Hazardous Waste <input type="checkbox"/>
None	<input type="checkbox"/>	Beyond regular working hours <input type="checkbox"/>
		Others <input type="checkbox"/>
		None <input type="checkbox"/>
Operating Instructions		
(Fill In or Attach Seperate Instructions)		
HSE - course; leak testing before every experiment.		
Emergency Procedure		
Shut down gas bottles and cut power, Then evacuate.		
Maintenance Routines		
Frequency: When needed		
Service Agreements:		
Maintenance Contact:		
Maintenance Described In Seperate Attachme None outside maintinence.		
Equipment Responsible:	Deputy:	
Name: De Chen	Name: Fan Huang	
Telephone: 73593149	Telephone: 73551128	
Mobile:	Mobile:	
Signature:	Signature:	
Controlled & Updated:		
Date:	Date:	Date:
Date:	Date:	Date:

Potential undesirable incident/strain

Identify possible incidents and conditions that may lead to situations that pose a hazard to people, the environment and any materiel/equipment involved.

Criteria for the assessment of likelihood and consequence in relation to fieldwork

Each activity is assessed according to a worst-case scenario. Likelihood and consequence are to be assessed separately for each potential undesirable incident. Before starting on the quantification, the participants should agree what they understand by the assessment criteria:

Minimal 1 Once every 50 years or less	Low 2 Once every 10 years or less	Medium 3 Once a year or less	High 4 Once a month or less	Very high 5 Once a week
Grading		Human	Environment	Financial/material
E Very critical	May produce fatality/ies	Very prolonged, non-reversible damage	Shutdown of work >1 year.	
D Critical	Permanent injury, may produce serious health damage/sickness	Prolonged damage. Long recovery time.	Shutdown of work 0.5-1 year.	
C Dangerous	Serious personal injury	Minor damage. Long recovery time	Shutdown of work < 1 month	
B Relatively safe	Injury that requires medical treatment	Minor damage. Short recovery time	Shutdown of work < 1week	
A Safe	Injury that requires first aid	Insignificant damage. Short recovery time	Shutdown of work < 1day	

Likelihood

Consequence

The unit makes its own decision as to whether opting to fill in or not consequences for economy/materiel, equipment.

It is up to the individual unit to choose the assessment criteria for this column.

Risk = Likelihood x Consequence

Please calculate the risk value for "Human", "Environment" and, if chosen, "Economy/materiel", separately.

About the column "Comments/status, suggested preventative and corrective measures": Measures can impact on both likelihood and consequences.

that can prevent the incident from occurring; in other words, likelihood-reducing measures are to be prioritised above greater emergency preparedness,

Appendix J: Mass of Palladium II Nitrate necessary to Ni deposition on CF

It is aimed to deposit 0.3% in weight of Pd on CF_CNF support from 6h and 4h of batch time.

For this task a salt of Palladium is employed: $\text{Pd}(\text{N}_2\text{O}_8)_2 \cdot 2\text{H}_2\text{O}$. From the salt bottle, the following data are obtained:

$$M_{w_{\text{salt}}} = 266.4.8 \text{ g/mol}; \quad M_{w_{\text{Pd}}} = 106.4 \text{ g/mol}$$

$$\text{Purity} = 100\% \text{ in weight}; \quad \% \text{Pd} = 40\% \text{ w}$$

They have been defined: $m_{\text{CF_CNF}}$ = mass of CF with CNF deposited

$$M_{\text{Pd}} = \text{mass of Nickel}$$

$$m_{\text{salt}} = \text{mass of } \text{Pd}(\text{N}_2\text{O}_8)_2 \cdot 2\text{H}_2\text{O}$$

$$m_1 = \text{mass Pd plus mass of CF}$$

Proportion of Pd in the salt (A): 40% (already indicated)

$$\text{Check-up: } M_{w_{\text{Pd}}}/M_{w_{\text{salt}}} = 106.4/266.4 = 0.3994 \text{ g/g (approximately 0.4)}$$

$$m_{\text{Ni}} = m_{\text{salt}} \cdot 0.4$$

Relation in weight between Palladium and CF_CNF (B)

$$m_1 = m_{\text{CF}} + m_{\text{Pd}}; [m_1 = m_{\text{Ni}}/0.003]; m_{\text{Pd}}/0.003 = m_{\text{Pd}} + m_{\text{Ni}}$$

$$m_{\text{Ni}} = ((m_{\text{CF}}) \cdot 0.003)/(1-0.003)$$

Combining A and B:

$$m_{\text{Salt}} = m_{\text{CF_CNF}} \cdot (0.003/(1-0.003))/0.4$$

$$m_{\text{Salt}} = (m_{\text{CF_CNF}}) \cdot 0.007523$$

Appendix K: Calculation of CNF deposition yield and fraction of CNF

K1. CNF deposition yield:

Definition of CNF growth yield: $\%Y\text{-CNF} = (100 \cdot m_{\text{CNF}}) / (m_{\text{CF}} + m_{\text{Ni}})$

That is: $\%Y\text{-CNF} = 100 \cdot (m_{\text{after}} - m_2) / m_2$

They have been defined: $m_{\text{after}} = m_{\text{CF}} + m_{\text{Ni}} + m_{\text{CNF}}$ mass of support after CCVD

$$m_2 = m_{\text{CF}} + m_{\text{Ni}}$$

$m_{\text{before}} =$ mass of support before CCVD

$m_{\text{CNF}} =$ mass of CNFs deposited on support

After CCVD: $m_{\text{after}} = m_{\text{CF}} + m_{\text{Ni}} + m_{\text{CNF}}$

Before CCVD (small scale): $m_{\text{before}} = m_{\text{CF}} + m_{\text{Salt}}$

Before CCVD (large scale): $m_{\text{before}} = m_{\text{CF}}$

For small scale: initial mass of CF is not available.

During the reaction the nitrates and water are removed from the catalyst.

Previous formulae (from *appendix E*)

$$m_{\text{Salt}} = (m_{\text{CF}}) \cdot 0.1042 \text{ (C)}$$

$$m_{\text{Ni}} = (0.02/0.98) \cdot (m_{\text{CF}}) \text{ (D)}$$

Relation aimed: $m_2 = f(m_{\text{before}})$

$$m_{\text{before}} = m_{\text{CF}} + m_{\text{Salt}} ; \quad m_{\text{CF}} = m_{\text{before}} - m_{\text{Salt}} ; \quad (\text{applying C}) \rightarrow m_{\text{CF}} = m_{\text{before}} - m_{\text{CF}} \cdot 0.1042$$

$$m_{\text{CF}} = (m_{\text{before}}) / (1 + 0.1042) \text{ (E)}$$

$$m_2 = m_{\text{CF}} + m_{\text{Ni}} ; \quad (\text{applying D}) \rightarrow m_2 = m_{\text{CF}} + (0.02/0.98) \cdot m_{\text{CF}} = (1 + (0.02/0.98)) \cdot m_{\text{CF}}$$

$$(\text{applying E}) \rightarrow m_2 = (1 + (0.02/0.98)) \cdot (m_{\text{before}} / (1 + 0.1042))$$

$$m_2 = 0.9241 \cdot (m_{\text{before}})$$

That is why:

$$\%Y\text{-CNF} = (100 \cdot (m_{\text{after}} - 0.9241 \cdot m_{\text{before}})) / (0.9241 \cdot m_{\text{before}}) \quad (\%g\text{CNF/g support})$$

For large scale: initial mass of CF is available, that is why previous formula is not applied.

$$\%Y\text{-CNF} = (100 \cdot (m_{\text{after}} - m_{\text{before}} - m_{\text{Ni}})) / (m_{\text{before}} + m_{\text{Ni}})$$

$$\%Y\text{-CNF} = (100 \cdot (m_{\text{after}} - 1.02 \cdot m_{\text{before}})) / (1.02 \cdot m_{\text{before}}) \quad (\%g\text{CNF/g support})$$

K2. Fraction of CNF in catalyst:

Fraction of CNF in catalyst: $X_{\text{CNF}} = (m_{\text{CNF}})/(m_{\text{CF}}+m_{\text{Ni}}+m_{\text{CNF}})$

They have been defined: $m_{\text{after}} = \text{mass of support after CCVD}$

$m_{\text{before}} = \text{mass of support before CCVD}$

$m_{\text{CNF}} = \text{mass of CNFs deposited on support}$

Deposition of Ni $m_{\text{CF}} + m_{\text{Ni}} = 1.02 \cdot m_{\text{CF}}$

After CCVD: $m_{\text{after}} = m_{\text{CF}} + m_{\text{Ni}} + m_{\text{CNF}}$

Before CCVD (large scale): $m_{\text{before}} = m_{\text{CF}}$

This property only has been calculated for large scale:

Initial mass of CF is available: $m_{\text{CF}} = m_{\text{before}}$

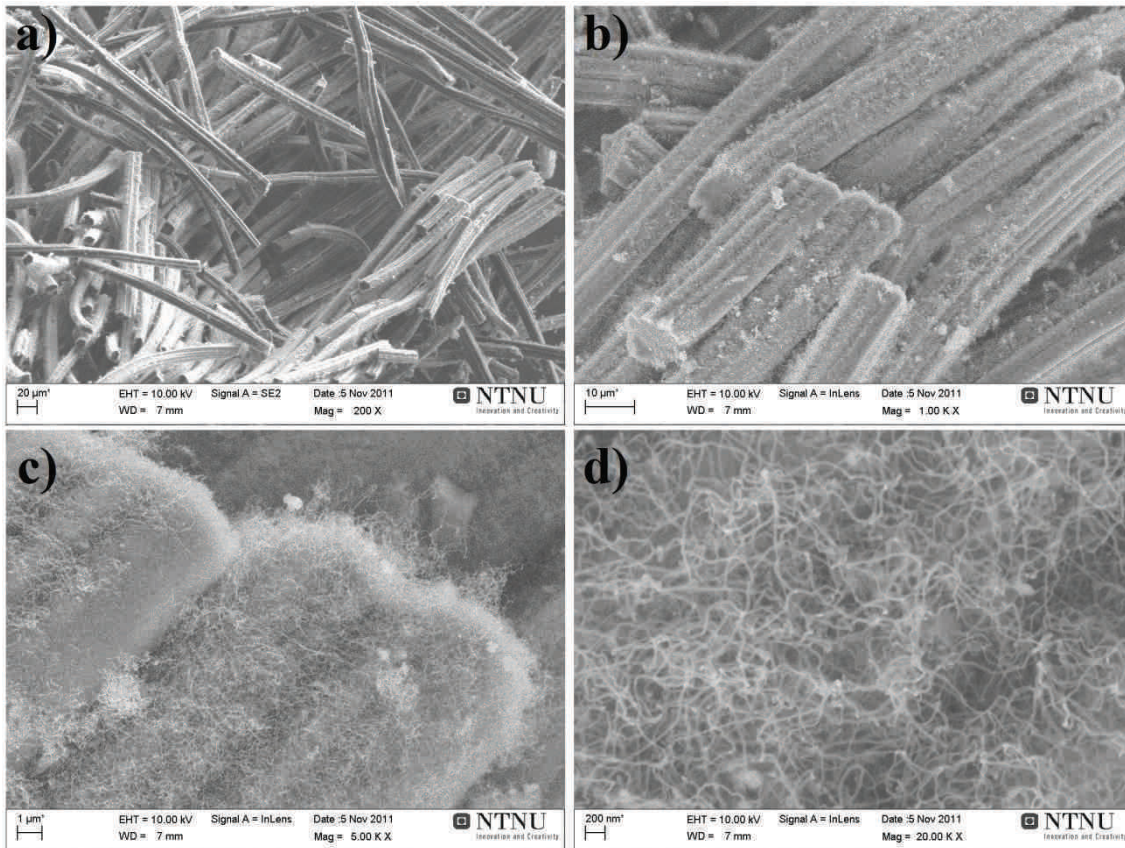
From point K1.: $m_{\text{CNF}} = m_{\text{after}} - 1.02 \cdot m_{\text{before}}$

Mass_CNF/total mass = $((m_{\text{after}} - m_{\text{before}} - m_{\text{Ni}}))/(m_{\text{after}})$

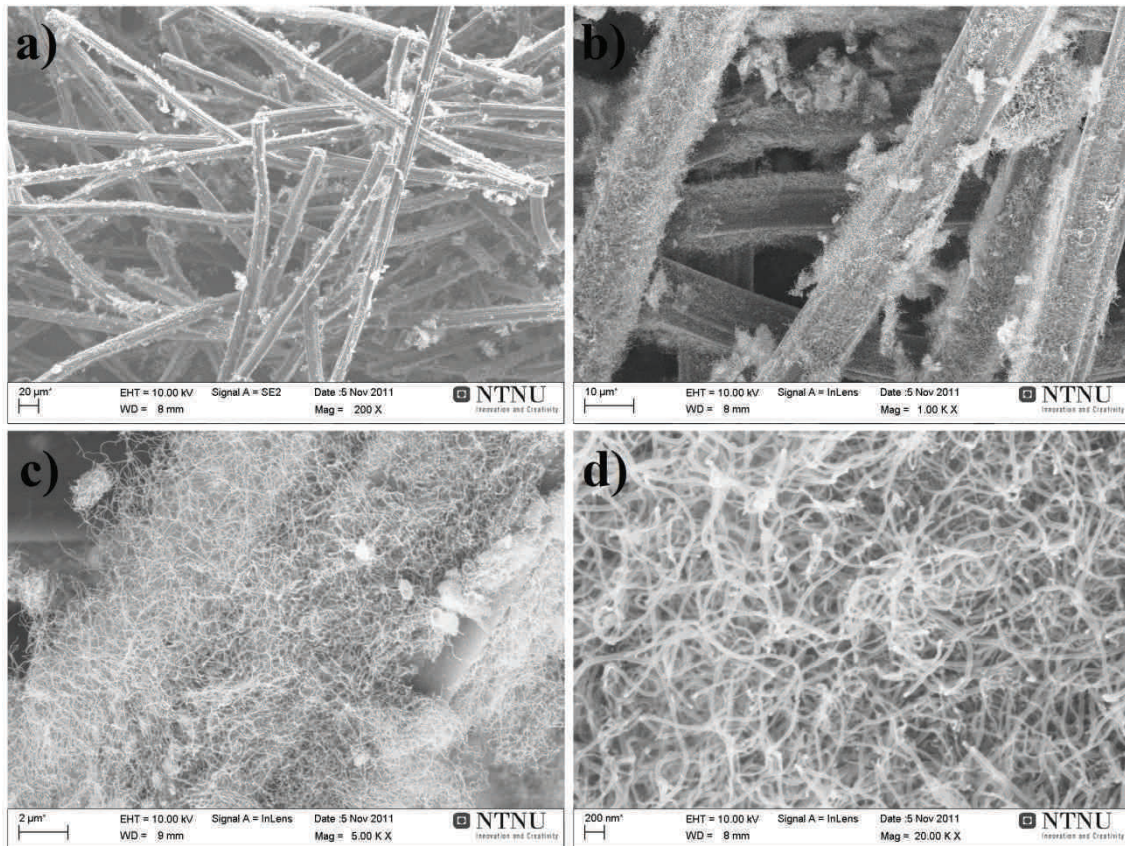
$X_{\text{CNF}} = (m_{\text{after}} - 1.02 \cdot m_{\text{before}})/(m_{\text{after}})$ (gCNF/total grams)

Appendix L: SEM pictures

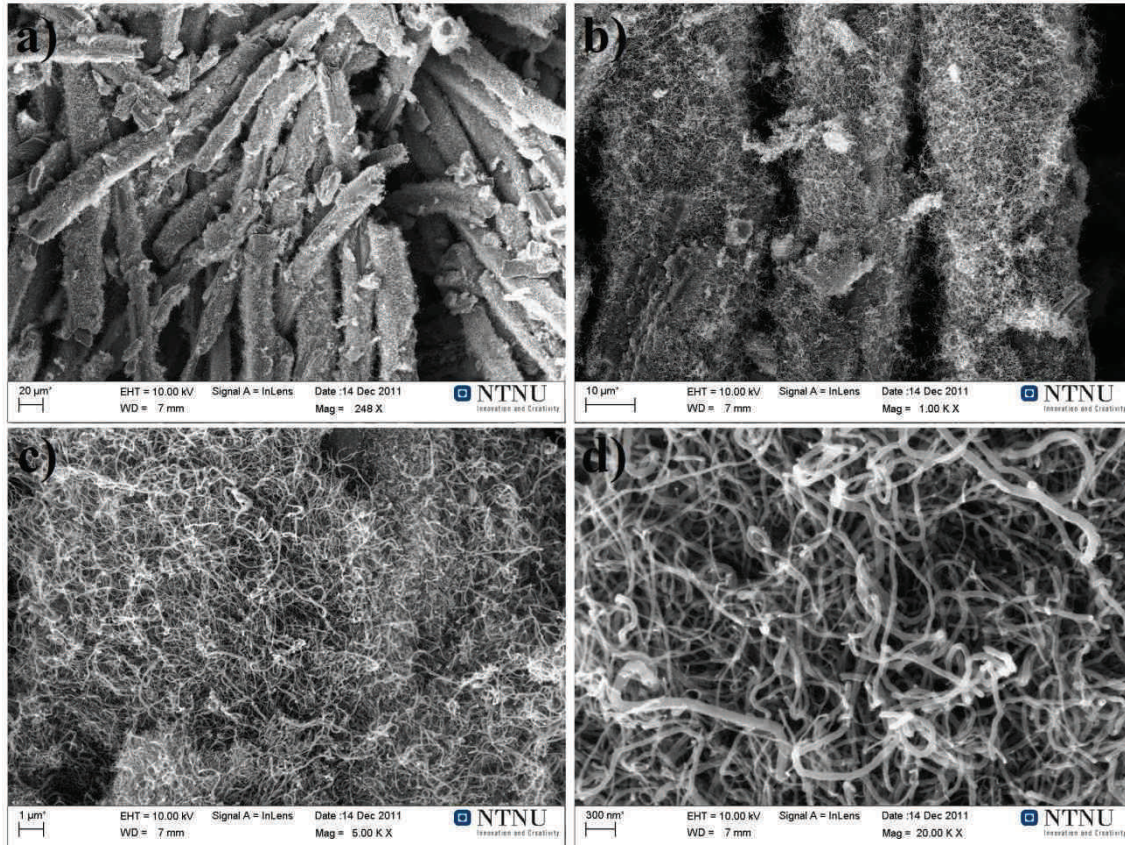
L1. Small scale test. Inside the sample.



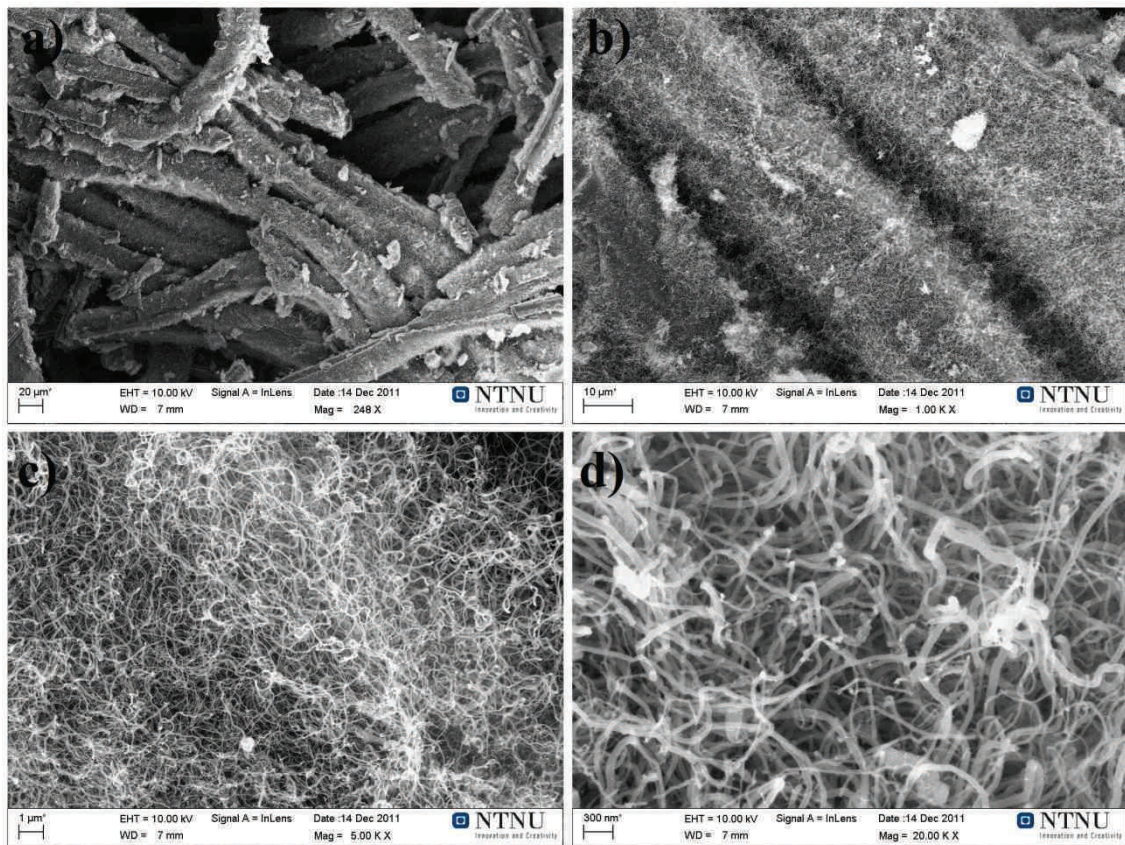
L2. Small scale test. Sample surface.



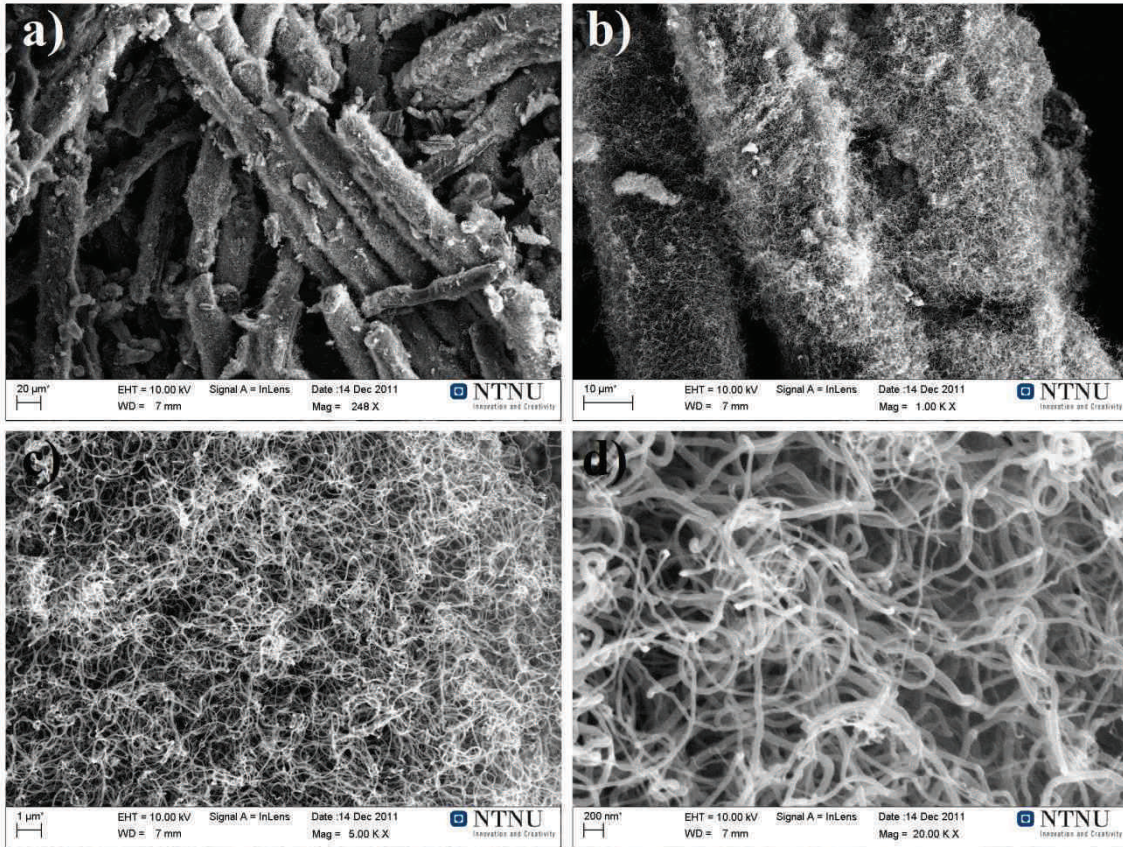
L3. Large scale test 4: 2 hours of t_{batch}



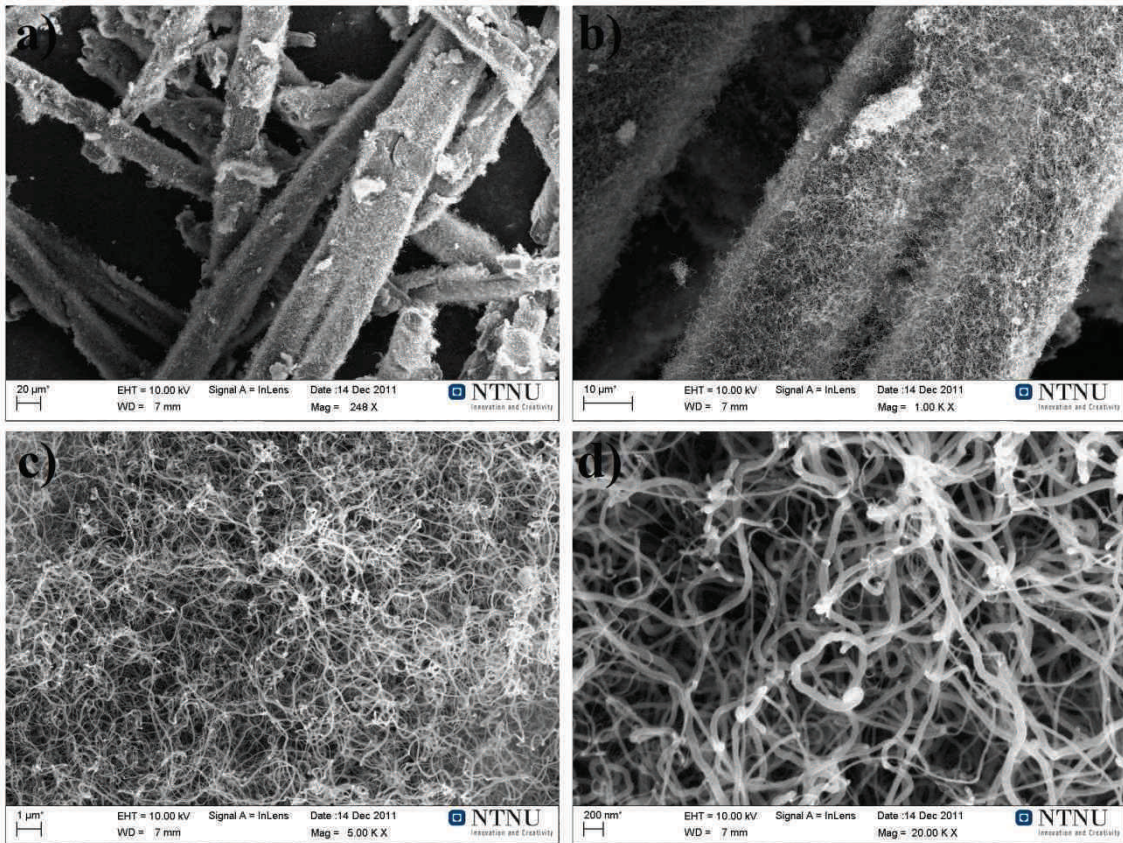
L4. Large scale test 3: 4 hours of t_{batch} (center)



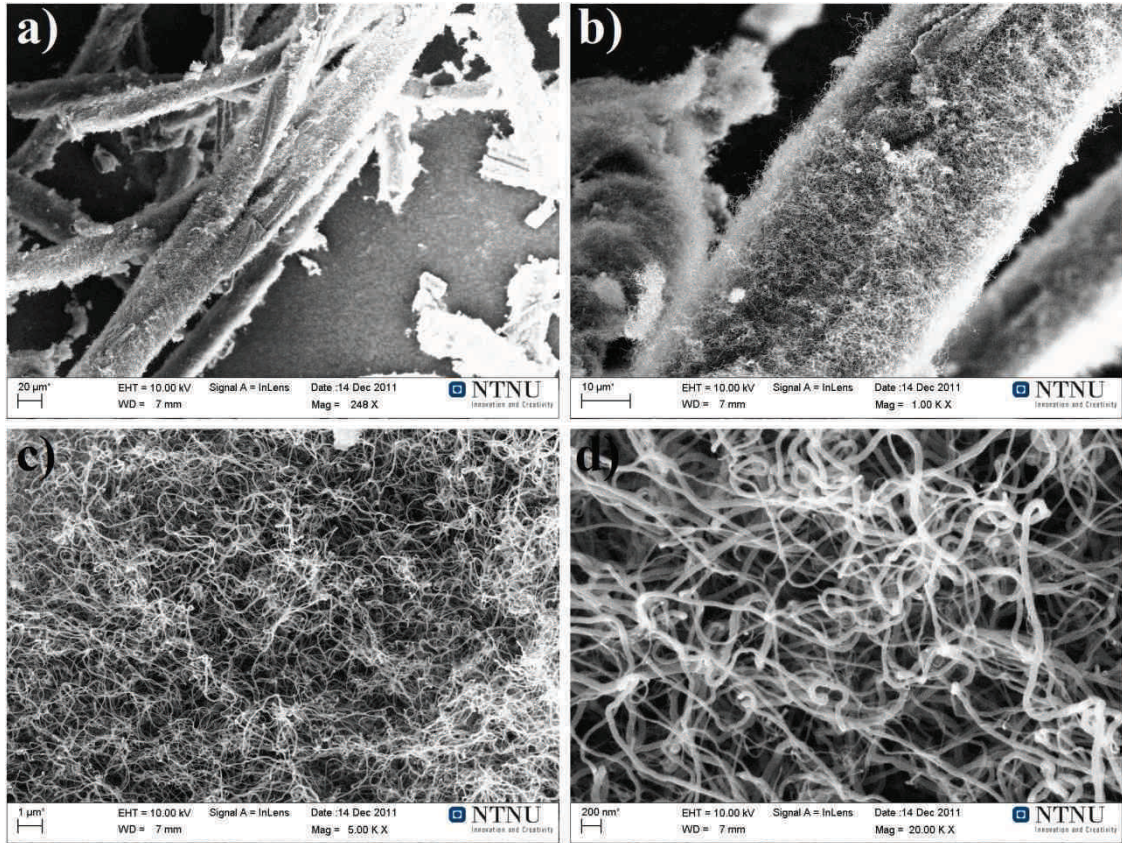
L5. Large scale test 3: 4 hours of t_{batch} (1.66cm from center)



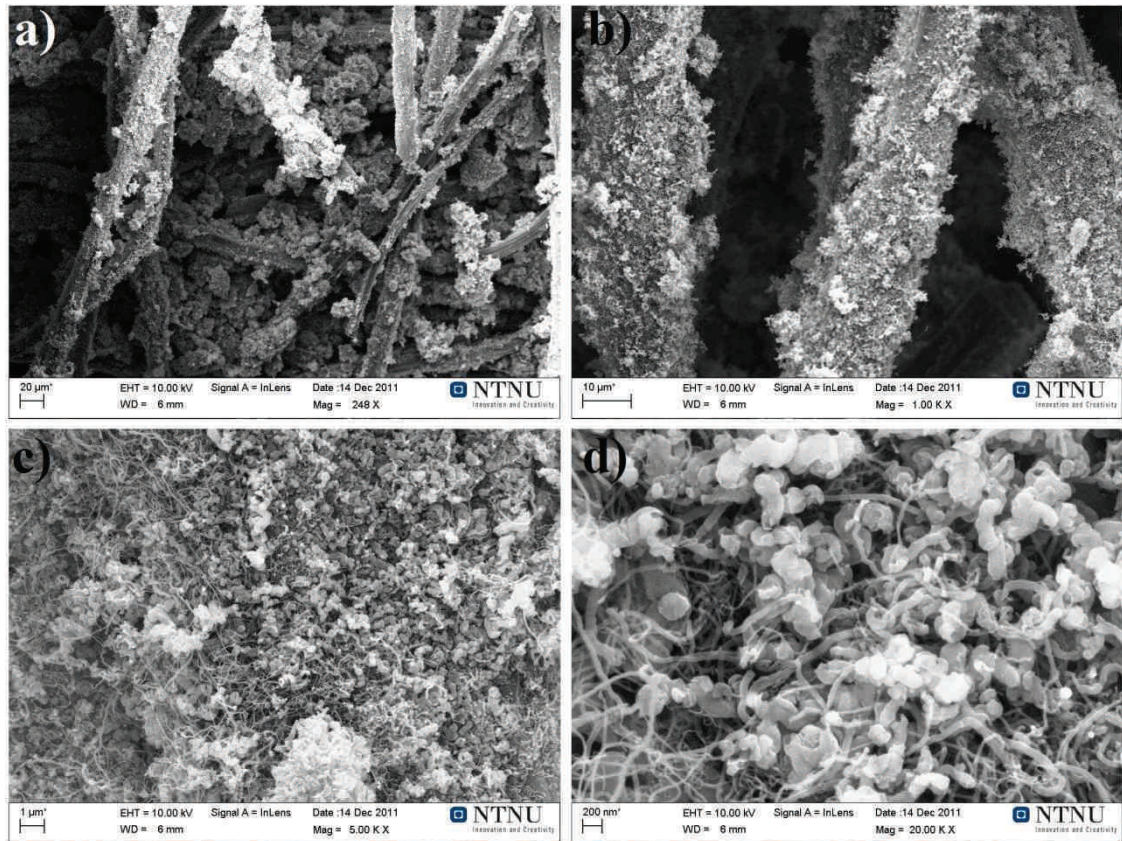
L6. Large scale test 3: 4 hours of t_{batch} (3.33cm from center)



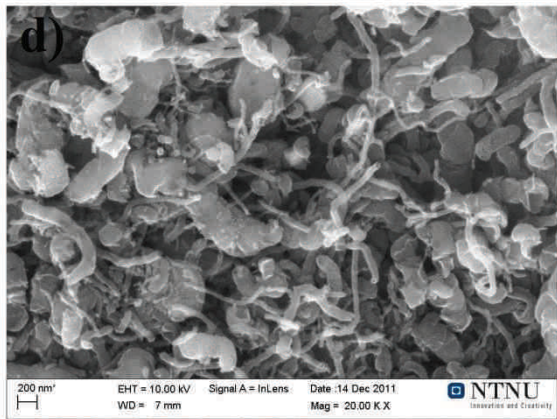
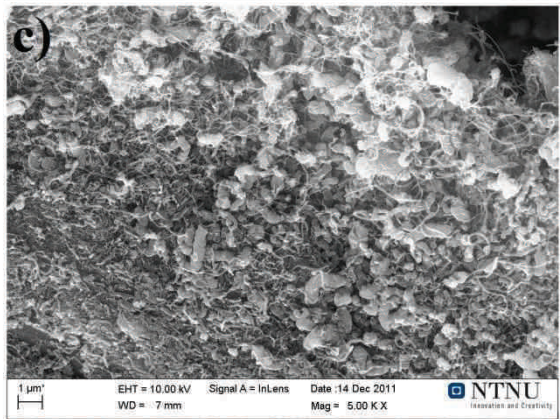
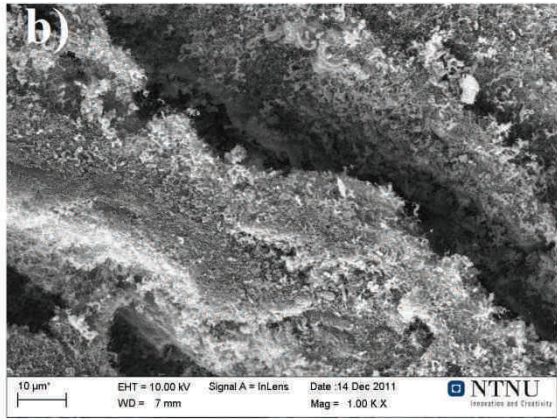
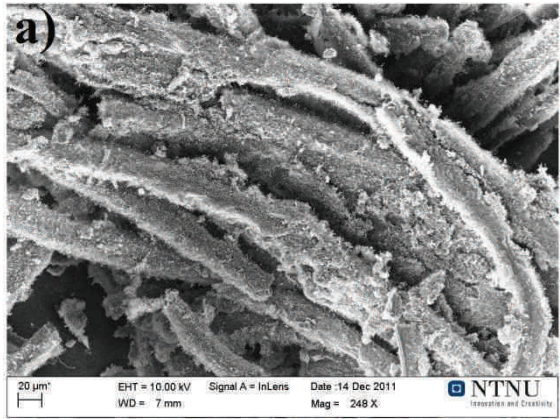
L7. Large scale test 3: 4 hours of t_{batch} (edge, 5cm from center)



L8. Large scale test 1: 6 hours of t_{batch}



L9. Large scale test 2: 10 hours of t_{batch}



Appendix M: Estimation of CNF diameter

M1. Large scale test 4: 2 hours of t_batch

Point n°	Real measure (mm)	Diameter (nm)	Point n°	Real measure (mm)	Diameter (nm)
1	5	37	51	8	59
2	7	51	52	5	37
3	7	51	53	5	37
4	12	88	54	4	29
5	8	59	55	5	37
6	5	37	56	3	22
7	4	29	57	8	59
8	4	29	58	5	37
9	11	80	59	9	66
10	4	29	60	4	29
11	8	59	61	4	29
12	10	73	62	3	22
13	3	22	63	4	29
14	12	88	64	5	37
15	2.5	18	65	11	80
16	8	59	66	6	44
17	6	44	67	4	29
18	6	44	68	4	29
19	6	44	69	15	110
20	9	66	70	19	139
21	4	29	71	4	29
22	13	95	72	3	22
23	2	15	73	4	29
24	10	73	74	2	15
25	7	51	75	7	51
26	6	44	76	15	110
27	9	66	77	9	66
28	3	22	78	5	37
29	5	37	79	4	29
30	3	22	80	9	66
31	4	29	81	4	29
32	8	59	82	3	22
33	1.5	11	83	4	29
34	3	22	84	5	37
35	8	59	85	2	15
36	4	29	86	12	88
37	4	29	87	3	22
38	6	44	88	3	22
39	5	37	89	4	29
40	15	110	90	5	37
41	3	22	91	6	44
42	4	29	92	11	80
43	4	29	93	7	51
44	11	80	94	5	37
45	5	37	95	5	37
46	5	37	96	6	44
47	5	37	97	6	44
48	6	44	98	1	7
49	3	22	99	7	51
50	9	66	100	3	22

M2. Large scale test 3: 4 hours of t_batch

Point n°	Real measure (mm)	Diameter (nm)	Point n°	Real measure (mm)	Diameter (nm)
1	12	88	51	8	59
2	8	59	52	4	30
3	5	37	53	11	81
4	4	29	54	4	30
5	8	59	55	3	22
6	5	37	56	6	44
7	7	51	57	10	74
8	7	51	58	8	59
9	4	29	59	5	37
10	3	22	60	5	37
11	4	29	61	12	89
12	6	44	62	5	37
13	8	59	63	2	15
14	5	37	64	7	52
15	13	95	65	8	59
16	7	51	66	12	89
17	2	15	67	9	67
18	3	22	68	3	22
19	5	37	69	8	59
20	8	59	70	11	81
21	5	37	71	6	44
22	6	44	72	10	74
23	11	80	73	5	37
24	2	15	74	2	15
25	5	37	75	6	44
26	8	59	76	7	52
27	7	52	77	8	59
28	6	44	78	4	30
29	8	59	79	9	67
30	5	37	80	4	30
31	11	81	81	8	59
32	9	67	82	4	30
33	8	59	83	6	44
34	3	22	84	11	81
35	6	44	85	5	37
36	3	22	86	10	74
37	5	37	87	9	67
38	9	67	88	5	37
39	8	59	89	2	15
40	4	30	90	8	59
41	6	44	91	4	30
42	5.5	41	92	10	74
43	10	74	93	4	30
44	5	37	94	9	67
45	11	81	95	2	15
46	7	52	96	6	44
47	6	44	97	8	59
48	13	96	98	9	67
49	4	30	99	7	52
50	10	74	100	8	59

Appendix N: TPO data

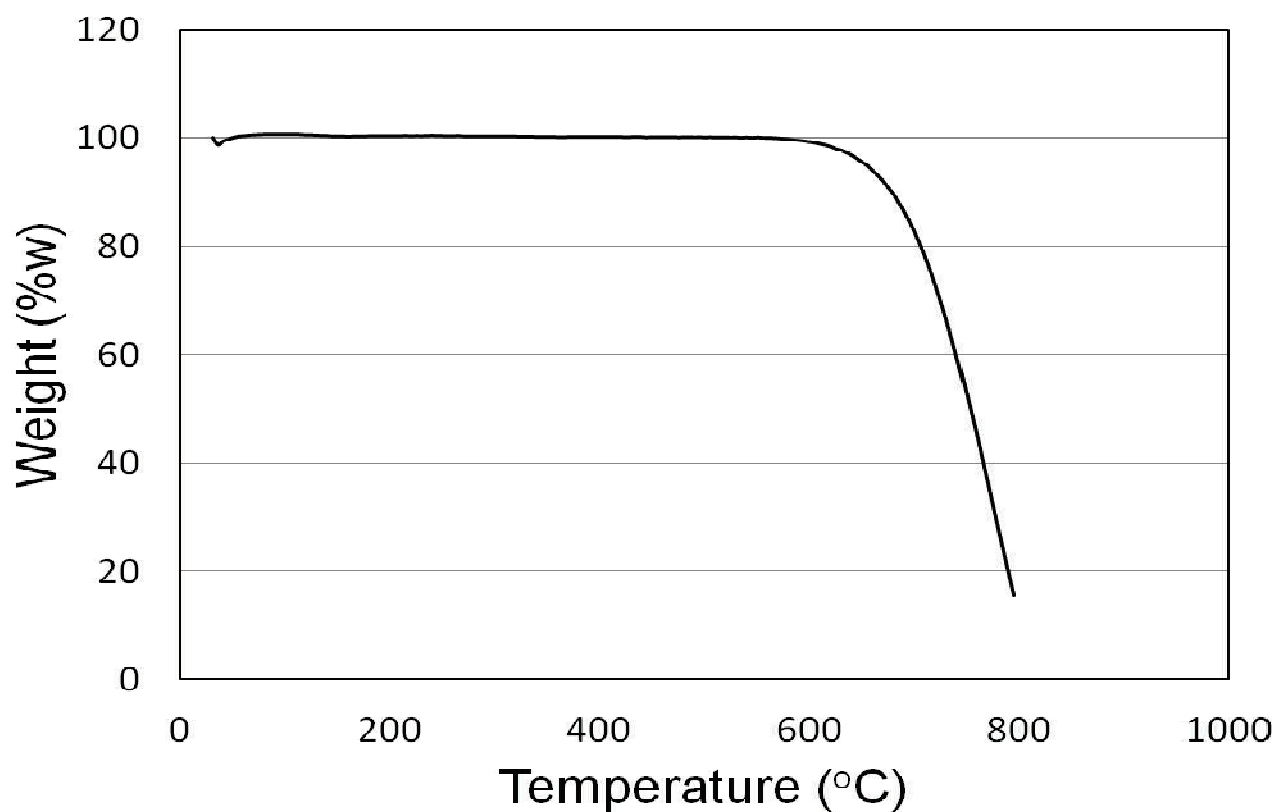
N1. Carbon felt analysis

Temp.°C	Mass/%	derivative (1/°C)	int temp
29.847	100	-0.261406	32.347
34.847	98.69297	0.141564	37.347
39.847	99.40079	0.068414	42.347
44.847	99.74286	0.061444	47.347
49.847	100.05008	0.046492	52.347
54.847	100.28254	0.015094	57.347
59.847	100.35801	0.020056	62.347
64.847	100.45829	0.011173	67.347
69.847	100.51694	0.008026	72.347
74.847	100.55707	0.00904	77.347
79.847	100.60227	0.003108	82.347
84.847	100.61781	0.00205	87.347
89.847	100.62806	-0.002644	92.347
94.847	100.61484	0.00148	97.347
99.847	100.62224	-0.000216	102.347
104.847	100.62116	-0.002296	107.347
109.847	100.60968	-0.00792	112.347
114.847	100.57008	-0.01333	117.347
119.847	100.50343	-0.003288	122.347
124.847	100.48699	-0.00666	127.347
129.847	100.45369	-0.010254	132.347
134.847	100.40242	-0.005784	137.347
139.847	100.3735	-0.013384	142.347
144.847	100.30658	-0.005684	147.347
149.847	100.27816	7.2E-05	152.347
154.847	100.27852	-0.004054	157.347
159.847	100.25825	0.003386	162.347
164.847	100.27518	0.005126	167.347
169.847	100.30081	0.002042	172.347
174.847	100.31102	0.003194	177.347
179.847	100.32699	0.00626	182.347
184.847	100.35829	-0.001056	187.347
189.847	100.35301	-0.002776	192.347
194.847	100.33913	0.005966	197.347
199.847	100.36896	-0.00417	202.347
204.847	100.34811	0.00197	207.347
209.847	100.35796	0.008032	212.347
214.847	100.39812	-0.01351	217.347
219.847	100.33057	0.012706	222.347
224.847	100.3941	-0.008292	227.347
229.847	100.35264	0.010298	232.347
234.847	100.40413	0.007334	237.347
239.847	100.4408	-0.01253	242.347
244.847	100.37815	-0.000588	247.347
249.847	100.37521	-0.007124	252.347
254.847	100.33959	0.004588	257.347
259.847	100.36253	0.005424	262.347
264.847	100.38965	-0.014852	267.347
269.847	100.31539	-0.007456	272.347
274.847	100.27811	-1.028902147	277.347

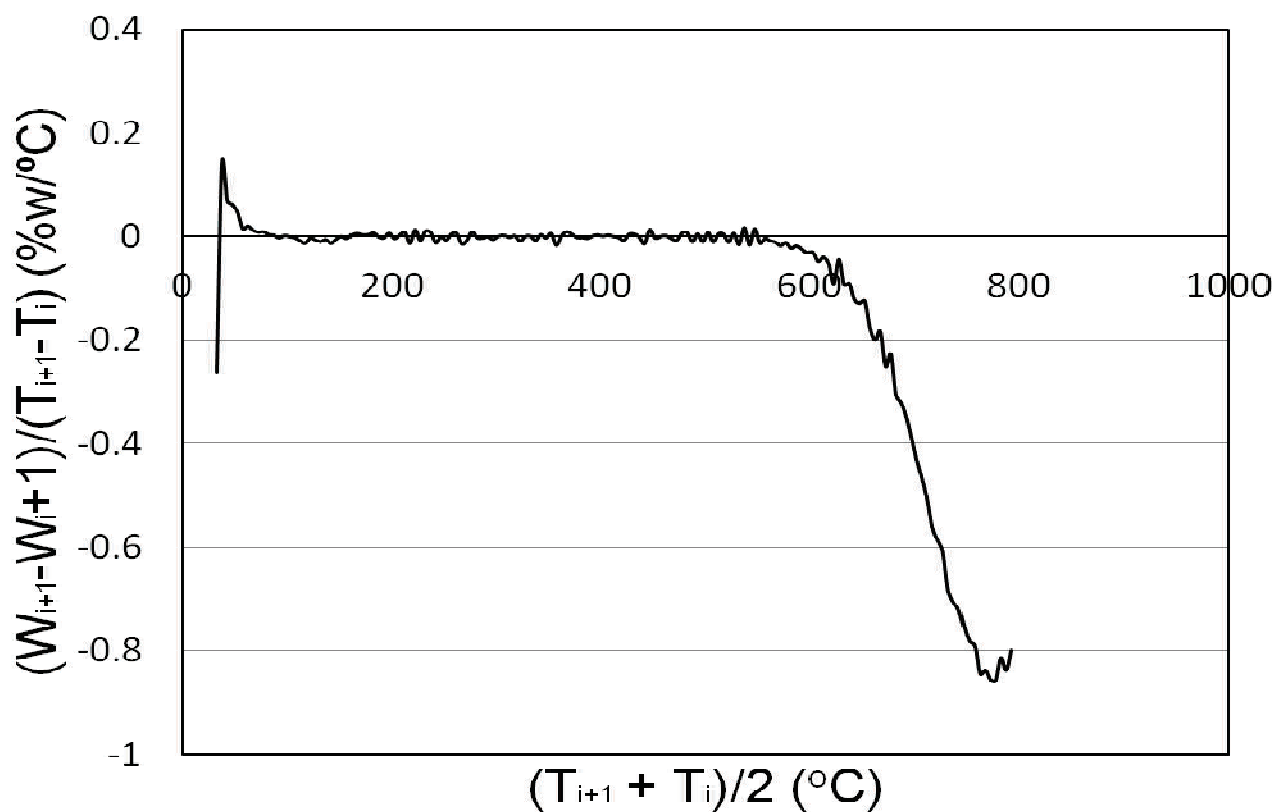
Temp.°C	Mass/%	derivative (1/°C)	int temp
279.847	100.32225	-0.002622	282.347
284.847	100.30914	-0.003234	287.347
289.847	100.29297	-0.000558	292.347
294.847	100.29018	-0.005932	297.347
299.847	100.26052	4.6E-05	302.347
304.847	100.26075	0.001658	307.347
309.847	100.26904	-0.001774	312.347
314.847	100.26017	0.001078	317.347
319.847	100.26556	-0.009132	322.347
324.847	100.2199	4.8E-05	327.347
329.847	100.22014	0.000618	332.347
334.847	100.22323	-0.007966	337.347
339.847	100.1834	0.00302	342.347
344.847	100.1985	-0.002924	347.347
349.847	100.18388	0.005394	352.347
354.847	100.21085	-0.017102	357.347
359.847	100.12534	0.001008	362.347
364.847	100.13038	0.009102	367.347
369.847	100.17589	0.003816	372.347
374.847	100.19497	-0.002258	377.347
379.847	100.18368	-0.00225	382.347
384.847	100.17243	-0.00371	387.347
389.847	100.15388	0.000916	392.347
394.847	100.15846	0.002512	397.347
399.847	100.17102	0.000582	402.347
404.847	100.17393	0.002296	407.347
409.847	100.18541	-8.2E-05	412.347
414.847	100.185	-0.001838	417.347
419.847	100.17581	-0.007762	422.347
424.847	100.137	0.003788	427.347
429.847	100.15594	0.004194	432.347
434.847	100.17691	-0.00131	437.347
439.847	100.17036	-0.014094	442.347
444.847	100.09989	0.012862	447.347
449.847	100.1642	-0.003	452.347
454.847	100.1492	0.000656	457.347
459.847	100.15248	0.001078	462.347
464.847	100.15787	-0.00464	467.347
469.847	100.13467	-0.007248	472.347
474.847	100.09843	0.006436	477.347
479.847	100.13061	0.0068	482.347
484.847	100.16461	-0.01055	487.347
489.847	100.11186	0.004534	492.347
494.847	100.13453	-0.010574	497.347
499.847	100.08166	0.007464	502.347
504.847	100.11898	-0.010756	507.347
509.847	100.0652	0.004492	512.347
514.847	100.08766	0.004048	517.347
519.847	100.1079	0.16822	522.347
524.847	100.949	-0.173696	527.347

529.847	100.08052	-0.015882	532.347
534.847	100.00111	0.016694	537.347
539.847	100.08458	-0.01686	542.347
544.847	100.00028	0.014458	547.347
549.847	100.07257	-0.012868	552.347
554.847	100.00823	-0.004048	557.347
559.847	99.98799	-0.008498	562.347
564.847	99.9455	-0.011204	567.347
569.847	99.88948	-0.017948	572.347
574.847	99.79974	-0.011982	577.347
579.847	99.73983	-0.022786	582.347
584.847	99.6259	-0.01821	587.347
589.847	99.53485	-0.023862	592.347
594.847	99.41554	-0.031508	597.347
599.847	99.258	-0.030768	602.347
604.847	99.10416	-0.047646	607.347
609.847	98.86593	-0.039946	612.347
614.847	98.6662	-0.05191	617.347
619.847	98.40665	-0.091146	622.347
624.847	97.95092	-0.044038	627.347
629.847	97.73073	-0.09353	632.347
634.847	97.26308	-0.0909	637.347
639.847	96.80858	-0.122022	642.347
644.847	96.19847	-0.129192	647.347
649.847	95.55251	-0.124838	652.347
654.847	94.92832	-0.17822	657.347
659.847	94.03722	-0.200166	662.347
664.847	93.03639	-0.183984	667.347
669.847	92.11647	-0.250912	672.347
674.847	90.86191	-0.226384	677.347
679.847	89.72999	-0.305646	682.347
684.847	88.20176	-0.32094	687.347
689.847	86.59706	-0.34872	692.347
694.847	84.85346	-0.38856	697.347
699.847	82.91066	-0.432176	702.347
704.847	80.74978	-0.466476	707.347
709.847	78.4174	-0.507638	712.347
714.847	75.87921	-0.561518	717.347
719.847	73.07162	-0.586056	722.347
724.847	70.14134	-0.607782	727.347
729.847	67.10243	-0.681828	732.347
734.847	63.69329	-0.705206	737.347
739.847	60.16726	-0.720174	742.347
744.847	56.56639	-0.753488	747.347
749.847	52.79895	-0.781084	752.347
754.847	48.89353	-0.789316	757.347
759.847	44.94695	-0.844308	762.347
764.847	40.72541	-0.836224	767.347
769.847	36.54429	-0.85483	772.347
774.847	32.27014	-0.856932	777.347
779.847	27.98548	-0.812852	782.347
784.847	23.92122	-0.83744	787.347
789.847	19.73402	-0.79903	792.347
794.847	15.73887		

TPO - Carbon felt



First derivative - Carbon felt



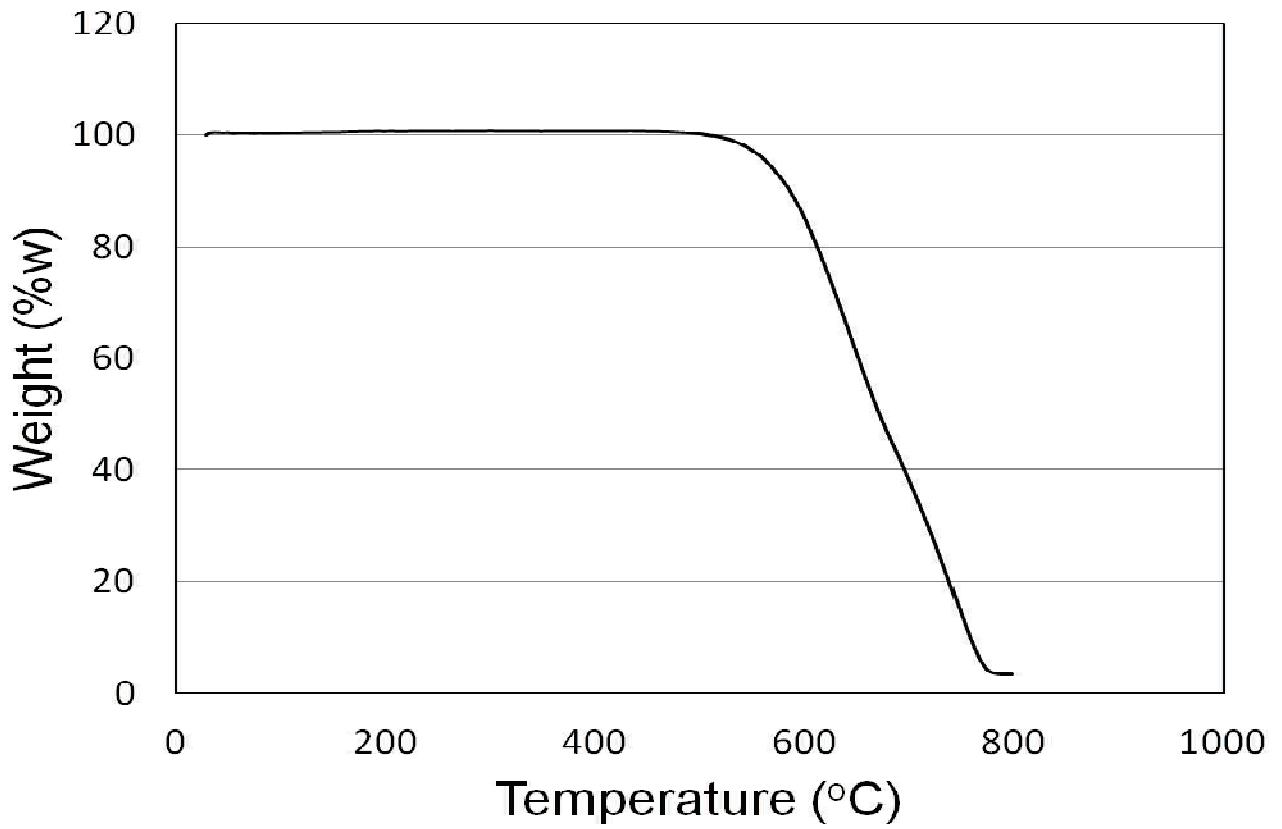
N2. 2 hours of batch time

Temp.°C	Mass/%	derivative (1/°C)	int temp
28.583	100	0.10131	31.083
33.583	100.50655	0.002214	36.083
38.583	100.51762	-0.010206	41.083
43.583	100.46659	0.009164	46.083
48.583	100.51241	-0.032082	51.083
53.583	100.352	0.023444	56.083
58.583	100.46922	-0.005094	61.083
63.583	100.44375	-0.002612	66.083
68.583	100.43069	-0.013382	71.083
73.583	100.36378	0.014918	76.083
78.583	100.43837	-0.00684	81.083
83.583	100.40417	0.002064	86.083
88.583	100.41449	-0.00174	91.083
93.583	100.40579	0.004514	96.083
98.583	100.42836	0.00528	101.083
103.583	100.45476	0.005304	106.083
108.583	100.48128	-0.002208	111.083
113.583	100.47024	-0.000882	116.083
118.583	100.46583	0.01327	121.083
123.583	100.53218	-0.007132	126.083
128.583	100.49652	0.00224	131.083
133.583	100.50772	0.004426	136.083
138.583	100.52985	0.00583	141.083
143.583	100.559	-0.000592	146.083
148.583	100.55604	0.000352	151.083
153.583	100.5578	0.008046	156.083
158.583	100.59803	0.008894	161.083
163.583	100.6425	0.005714	166.083
168.583	100.67107	0.001518	171.083
173.583	100.67866	0.009046	176.083
178.583	100.72389	-0.000716	181.083
183.583	100.72031	0.003372	186.083
188.583	100.73717	0.003538	191.083
193.583	100.75486	-0.010118	196.083
198.583	100.70427	0.011126	201.083
203.583	100.7599	-0.00566	206.083
208.583	100.7316	-0.000994	211.083
213.583	100.72663	-0.002398	216.083
218.583	100.71464	0.00831	221.083
223.583	100.75619	-0.003236	226.083
228.583	100.74001	0.004378	231.083
233.583	100.7619	-0.002728	236.083
238.583	100.74826	-0.001872	241.083
243.583	100.7389	0.000928	246.083
248.583	100.74354	0.003638	251.083
253.583	100.76173	0.005274	256.083
258.583	100.7881	-0.010888	261.083
263.583	100.73366	0.002744	266.083
268.583	100.74738	0.002894	271.083
273.583	100.76185	-0.003994	276.083
278.583	100.74188	0.00062	281.083
283.583	100.74498	0.003592	286.083

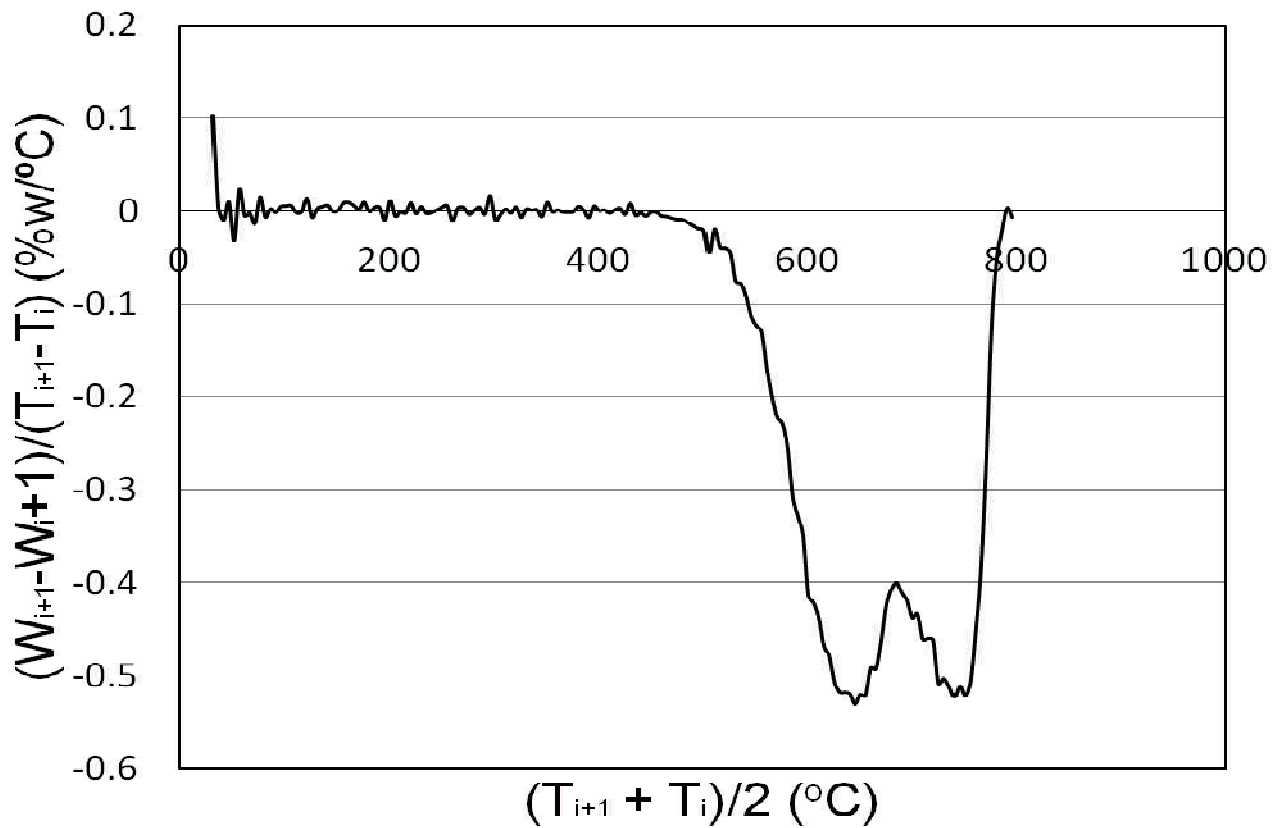
Temp.°C	Mass/%	derivative (1/°C)	int temp
288.583	100.76294	-0.003614	291.083
293.583	100.74487	0.016208	296.083
298.583	100.82591	-0.00949	301.083
303.583	100.77846	-0.004374	306.083
308.583	100.75659	0.002084	311.083
313.583	100.76701	-0.002502	316.083
318.583	100.7545	0.003844	321.083
323.583	100.77372	-0.007094	326.083
328.583	100.73825	0.00205	331.083
333.583	100.7485	0.000344	336.083
338.583	100.75022	0.001192	341.083
343.583	100.75618	-0.006168	346.083
348.583	100.72534	0.00884	351.083
353.583	100.76954	-0.001102	356.083
358.583	100.76403	0.000882	361.083
363.583	100.76844	-0.00129	366.083
368.583	100.76199	-0.001454	371.083
373.583	100.75472	-0.001016	376.083
378.583	100.74964	0.004504	381.083
383.583	100.77216	0.000964	386.083
388.583	100.77698	-0.007392	391.083
393.583	100.74002	0.004818	396.083
398.583	100.76411	-0.000136	401.083
403.583	100.76343	0.0009	406.083
408.583	100.76793	-0.002504	411.083
413.583	100.75541	0.00087	416.083
418.583	100.75976	0.002768	421.083
423.583	100.7736	-0.003914	426.083
428.583	100.75403	0.007726	431.083
433.583	100.79266	-0.004796	436.083
438.583	100.76868	-0.002146	441.083
443.583	100.75795	-0.005626	446.083
448.583	100.72982	-0.001332	451.083
453.583	100.72316	-0.001524	456.083
458.583	100.71554	-0.00552	461.083
463.583	100.68794	-0.006248	466.083
468.583	100.6567	-0.007934	471.083
473.583	100.61703	-0.009434	476.083
478.583	100.56986	-0.00939	481.083
483.583	100.52291	-0.012594	486.083
488.583	100.45994	-0.015596	491.083
493.583	100.38196	-0.01896	496.083
498.583	100.28716	-0.020928	501.083
503.583	100.18252	-0.044912	506.083
508.583	99.95796	-0.019504	511.083
513.583	99.86044	-0.039264	516.083
518.583	99.66412	-0.040256	521.083
523.583	99.46284	-0.045018	526.083
528.583	99.23775	-0.075962	531.083
533.583	98.85794	-0.078224	536.083
538.583	98.46682	-0.091446	541.083
543.583	98.00959	-0.11346	546.083

548.583	97.44229	-0.123774	551.083
553.583	96.82342	-0.129672	556.083
558.583	96.17506	-0.168556	561.083
563.583	95.33228	-0.199484	566.083
568.583	94.33486	-0.222106	571.083
573.583	93.22433	-0.228648	576.083
578.583	92.08109	-0.254238	581.083
583.583	90.8099	-0.30769	586.083
588.583	89.27145	-0.32862	591.083
593.583	87.62835	-0.34873	596.083
598.583	85.8847	-0.413594	601.083
603.583	83.81673	-0.42105	606.083
608.583	81.71148	-0.437466	611.083
613.583	79.52415	-0.468054	616.083
618.583	77.18388	-0.478248	621.083
623.583	74.79264	-0.50625	626.083
628.583	72.26139	-0.517242	631.083
633.583	69.67518	-0.517822	636.083
638.583	67.08607	-0.51933	641.083
643.583	64.48942	-0.529866	646.083
648.583	61.84009	-0.520062	651.083
653.583	59.23978	-0.521086	656.083
658.583	56.63435	-0.491728	661.083
663.583	54.17571	-0.492302	666.083
668.583	51.7142	-0.463026	671.083
673.583	49.39907	-0.42396	676.083
678.583	47.27927	-0.407142	681.083
683.583	45.24356	-0.400316	686.083
688.583	43.24198	-0.41066	691.083
693.583	41.18868	-0.41873	696.083
698.583	39.09503	-0.437308	701.083
703.583	36.90849	-0.43363	706.083
708.583	34.74034	-0.460118	711.083
713.583	32.43975	-0.459676	716.083
718.583	30.14137	-0.461158	721.083
723.583	27.83558	-0.508246	726.083
728.583	25.29435	-0.503128	731.083
733.583	22.77871	-0.511192	736.083
738.583	20.22275	-0.522288	741.083
743.583	17.61131	-0.511146	746.083
748.583	15.05558	-0.52142	751.083
753.583	12.44848	-0.506276	756.083
758.583	9.9171	-0.450552	761.083
763.583	7.66434	-0.384608	766.083
768.583	5.7413	-0.270414	771.083
773.583	4.38923	-0.128596	776.083
778.583	3.74625	-0.052216	781.083
783.583	3.48517	-0.021872	786.083
788.583	3.37581	0.00266	791.083
793.583	3.38911	-0.007	796.083
798.583	3.35411		

TPO - 2 hours



First derivative - 2 hours



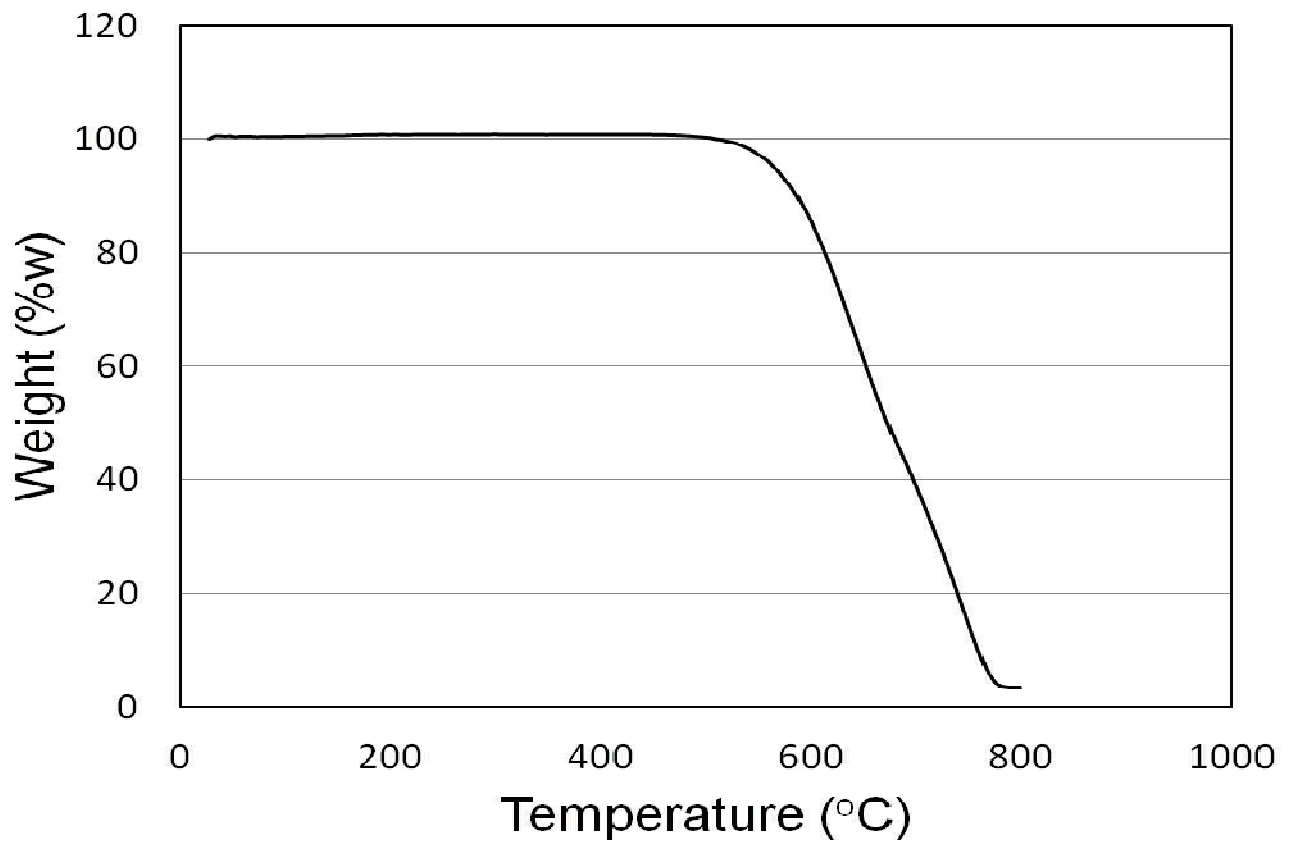
N3. 4 hours of batch time

Temp.°C	Mass/%	derivative (1/°C)	int temp
28.77	100	0.025442	31.27
33.77	100.12721	-0.01235	36.27
38.77	100.06546	0.00674	41.27
43.77	100.09916	-0.003304	46.27
48.77	100.08264	-0.00339	51.27
53.77	100.06569	0.000144	56.27
58.77	100.06641	-0.000696	61.27
63.77	100.06293	-0.007262	66.27
68.77	100.02662	0.003374	71.27
73.77	100.04349	-0.00029	76.27
78.77	100.04204	0.003122	81.27
83.77	100.05765	0.000964	86.27
88.77	100.06247	0.001	91.27
93.77	100.06747	0.001816	96.27
98.77	100.07655	0.002308	101.27
103.77	100.08809	1.4E-05	106.27
108.77	100.08816	0.00065	111.27
113.77	100.09141	0.001224	116.27
118.77	100.09753	0.002166	121.27
123.77	100.10836	0.003358	126.27
128.77	100.12515	0.003348	131.27
133.77	100.14189	-0.001346	136.27
138.77	100.13516	0.000964	141.27
143.77	100.13998	0.003668	146.27
148.77	100.15832	0.005198	151.27
153.77	100.18431	0.000504	156.27
158.77	100.18683	0.006482	161.27
163.77	100.21924	0.001966	166.27
168.77	100.22907	0.004374	171.27
173.77	100.25094	0.00323	176.27
178.77	100.26709	0.000866	181.27
183.77	100.27142	0.000386	186.27
188.77	100.27335	-0.000818	191.27
193.77	100.26926	-0.002006	196.27
198.77	100.25923	0.003536	201.27
203.77	100.27691	0.000918	206.27
208.77	100.2815	0.004332	211.27
213.77	100.30316	-0.00385	216.27
218.77	100.28391	0.00295	221.27
223.77	100.29866	-0.000202	226.27
228.77	100.29765	-0.007572	231.27
233.77	100.25979	0.010378	236.27
238.77	100.31168	-0.002864	241.27
243.77	100.29736	0.000912	246.27
248.77	100.30192	0.00073	251.27
253.77	100.30557	0.00616	256.27
258.77	100.33637	-0.003802	261.27
263.77	100.31736	0.000238	266.27
268.77	100.31855	-0.010572	271.27
273.77	100.26569	0.007254	276.27
278.77	100.30196	0.006402	281.27
283.77	100.33397	-0.006066	286.27

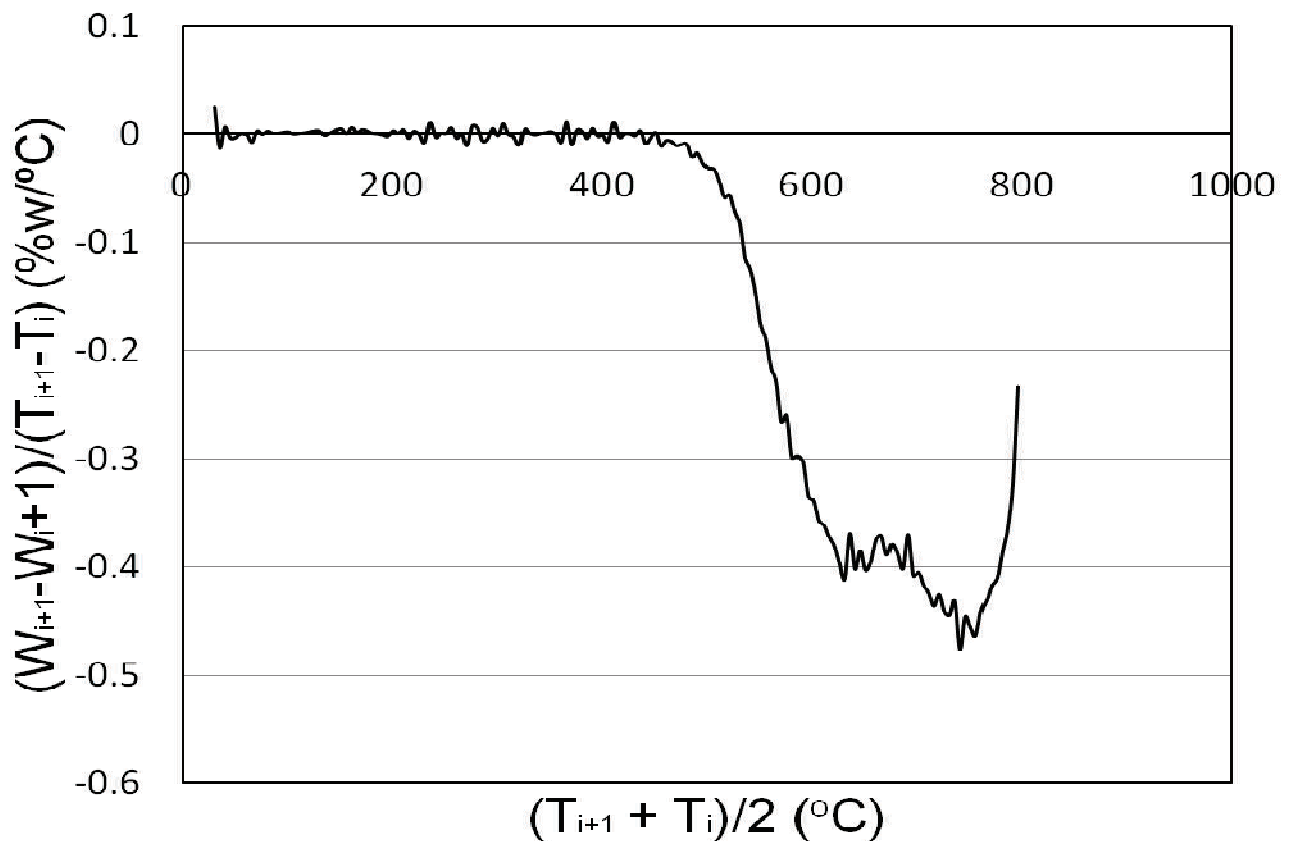
Temp.°C	Mass/%	derivative (1/°C)	int temp
288.77	100.30364	-0.004548	291.27
293.77	100.2809	0.005458	296.27
298.77	100.30819	-0.001424	301.27
303.77	100.30107	0.009626	306.27
308.77	100.3492	-0.00014	311.27
313.77	100.3485	-0.002372	316.27
318.77	100.33664	-0.01012	321.27
323.77	100.28604	0.004842	326.27
328.77	100.31025	0.00052	331.27
333.77	100.31285	-0.00077	336.27
338.77	100.309	0.000698	341.27
343.77	100.31249	0.001452	346.27
348.77	100.31975	0.002592	351.27
353.77	100.33271	-0.00046	356.27
358.77	100.33041	-0.00738	361.27
363.77	100.29351	0.011016	366.27
368.77	100.34859	-0.00986	371.27
373.77	100.29929	0.003806	376.27
378.77	100.31832	0.00322	381.27
383.77	100.33442	-0.003998	386.27
388.77	100.31443	0.005558	391.27
393.77	100.34222	-0.001746	396.27
398.77	100.33349	-0.001324	401.27
403.77	100.32687	-0.006648	406.27
408.77	100.29363	0.010554	411.27
413.77	100.3464	-0.002854	416.27
418.77	100.33213	0.000252	421.27
423.77	100.33339	0.00028	426.27
428.77	100.33479	-0.00168	431.27
433.77	100.32639	0.003544	436.27
438.77	100.34411	-0.008614	441.27
443.77	100.30104	-0.003634	446.27
448.77	100.28287	0.00166	451.27
453.77	100.29117	-0.01104	456.27
458.77	100.23597	-0.006024	461.27
463.77	100.20585	-0.006772	466.27
468.77	100.17199	-0.010588	471.27
473.77	100.11905	-0.009358	476.27
478.77	100.07226	-0.009378	481.27
483.77	100.02537	-0.02094	486.27
488.77	99.92067	-0.017148	491.27
493.77	99.83493	-0.026854	496.27
498.77	99.70066	-0.031152	501.27
503.77	99.5449	-0.032218	506.27
508.77	99.38381	-0.043202	511.27
513.77	99.1678	-0.058128	516.27
518.77	98.87716	-0.056072	521.27
523.77	98.5968	-0.071662	526.27
528.77	98.23849	-0.082882	531.27
533.77	97.82408	-0.114372	536.27
538.77	97.25222	-0.124634	541.27
543.77	96.62905	-0.1463	546.27

548.77	95.89755	-0.176052	551.27
553.77	95.01729	-0.188794	556.27
558.77	94.07332	-0.215344	561.27
563.77	92.9966	-0.22868	566.27
568.77	91.8532	-0.26608	571.27
573.77	90.5228	-0.259824	576.27
578.77	89.22368	-0.298368	581.27
583.77	87.73184	-0.297184	586.27
588.77	86.24592	-0.30339	591.27
593.77	84.72897	-0.334554	596.27
598.77	83.0562	-0.33878	601.27
603.77	81.3623	-0.356766	606.27
608.77	79.57847	-0.361372	611.27
613.77	77.77161	-0.371908	616.27
618.77	75.91207	-0.380436	621.27
623.77	74.00989	-0.396094	626.27
628.77	72.02942	-0.410902	631.27
633.77	69.97491	-0.368666	636.27
638.77	68.13158	-0.401512	641.27
643.77	66.12402	-0.384532	646.27
648.77	64.20136	-0.402394	651.27
653.77	62.18939	-0.39505	656.27
658.77	60.21414	-0.375304	661.27
663.77	58.33762	-0.37073	666.27
668.77	56.48397	-0.3881	671.27
673.77	54.54347	-0.378878	676.27
678.77	52.64908	-0.38748	681.27
683.77	50.71168	-0.401224	686.27
688.77	48.70556	-0.369682	691.27
693.77	46.85715	-0.407996	696.27
698.77	44.81717	-0.404586	701.27
703.77	42.79424	-0.41644	706.27
708.77	40.71204	-0.424166	711.27
713.77	38.59121	-0.435724	716.27
718.77	36.41259	-0.425072	721.27
723.77	34.28723	-0.440994	726.27
728.77	32.08226	-0.444544	731.27
733.77	29.85954	-0.43138	736.27
738.77	27.70264	-0.475774	741.27
743.77	25.32377	-0.445978	746.27
748.77	23.09388	-0.455456	751.27
753.77	20.8166	-0.462876	756.27
758.77	18.50222	-0.440442	761.27
763.77	16.30001	-0.430558	766.27
768.77	14.14722	-0.416862	771.27
773.77	12.06291	-0.410206	776.27
778.77	10.01188	-0.385608	781.27
783.77	8.08384	-0.364176	786.27
788.77	6.26296	-0.32219	791.27
793.77	4.65201	-0.23276	796.27
798.77	3.48821		

TPO - 4 hours



First derivative - 4 hours



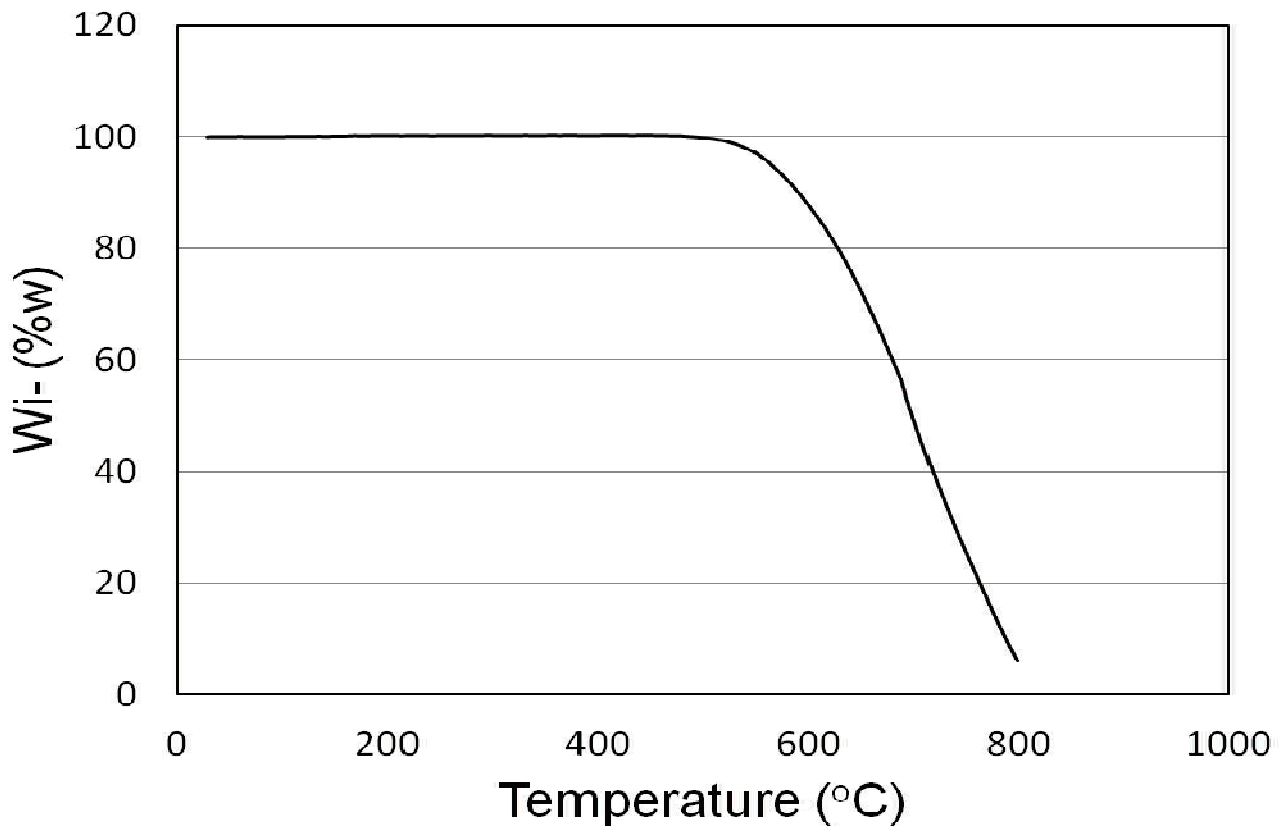
N4. 6 hours of batch time

Temp.°C	Mass/%	derivative (1/°C)	int temp
29.304	100	0.012552	31.804
34.304	100.06276	-0.003126	36.804
39.304	100.04713	0.000126	41.804
44.304	100.04776	-0.00101	46.804
49.304	100.04271	0.001878	51.804
54.304	100.0521	0.005666	56.804
59.304	100.08043	-0.00744	61.804
64.304	100.04323	-0.000902	66.804
69.304	100.03872	0.00226	71.804
74.304	100.05002	0.002016	76.804
79.304	100.0601	-0.007908	81.804
84.304	100.02056	0.005138	86.804
89.304	100.04625	-0.001752	91.804
94.304	100.03749	0.001096	96.804
99.304	100.04297	0.005562	101.804
104.304	100.07078	0.003858	106.804
109.304	100.09007	-0.000734	111.804
114.304	100.0864	-0.002754	116.804
119.304	100.07263	0.00656	121.804
124.304	100.10543	-0.004486	126.804
129.304	100.083	0.007762	131.804
134.304	100.12181	-0.004134	136.804
139.304	100.10114	0.001146	141.804
144.304	100.10687	0.00529	146.804
149.304	100.13332	-0.000248	151.804
154.304	100.13208	0.001574	156.804
159.304	100.13995	0.009028	161.804
164.304	100.18509	0.00861	166.804
169.304	100.22814	-0.006604	171.804
174.304	100.19512	0.001472	176.804
179.304	100.20248	0.001714	181.804
184.304	100.21105	0.009078	186.804
189.304	100.25644	-0.007518	191.804
194.304	100.21885	0.001586	196.804
199.304	100.22678	0.006972	201.804
204.304	100.26164	-0.006768	206.804
209.304	100.2278	-0.003958	211.804
214.304	100.20801	0.008636	216.804
219.304	100.25119	-0.005562	221.804
224.304	100.22338	0.002194	226.804
229.304	100.23435	-0.001384	231.804
234.304	100.22743	-0.002058	236.804
239.304	100.21714	-0.00162	241.804
244.304	100.20904	0.009382	246.804
249.304	100.25595	-0.00128	251.804
254.304	100.24955	-0.001254	256.804
259.304	100.24328	-0.00081	261.804
264.304	100.23923	-0.003714	266.804
269.304	100.22066	0.003852	271.804
274.304	100.23992	-0.002282	276.804
279.304	100.22851	0.007298	281.804
284.304	100.265	-0.003192	286.804

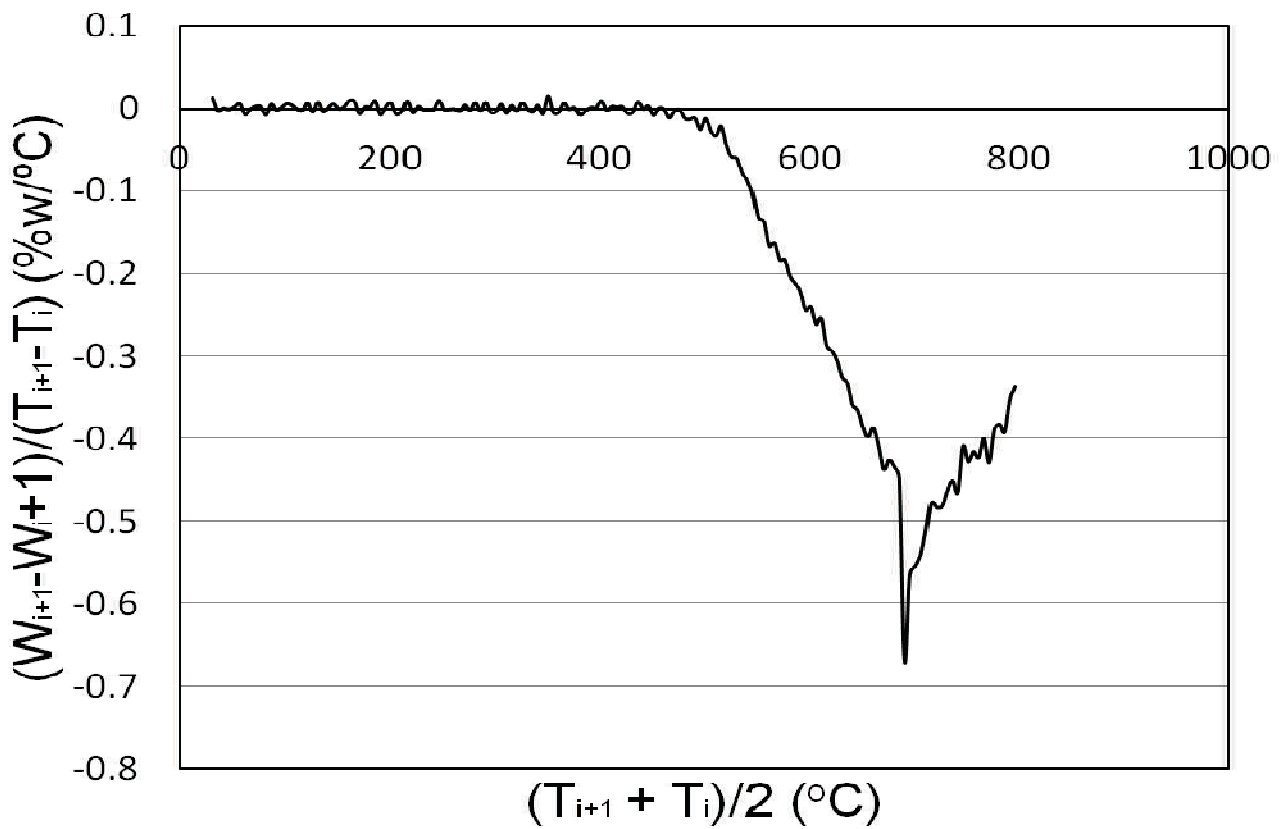
Temp.°C	Mass/%	derivative (1/°C)	int temp
289.304	100.24904	0.007536	291.804
294.304	100.28672	-0.004908	296.804
299.304	100.26218	-0.003934	301.804
304.304	100.24251	0.00514	306.804
309.304	100.26821	-0.005948	311.804
314.304	100.23847	0.003386	316.804
319.304	100.2554	-0.003458	321.804
324.304	100.23811	0.006994	326.804
329.304	100.27308	-0.000384	331.804
334.304	100.27116	-0.004666	336.804
339.304	100.24783	0.00374	341.804
344.304	100.26653	-0.006964	346.804
349.304	100.23171	0.014678	351.804
354.304	100.3051	-0.005246	356.804
359.304	100.27887	-0.005068	361.804
364.304	100.25353	0.006574	366.804
369.304	100.2864	-0.000786	371.804
374.304	100.28247	0.000832	376.804
379.304	100.28663	-0.007748	381.804
384.304	100.24789	-0.0026	386.804
389.304	100.23489	0.000994	391.804
394.304	100.23986	0.000784	396.804
399.304	100.24378	0.00896	401.804
404.304	100.28858	-0.002108	406.804
409.304	100.27804	0.002222	411.804
414.304	100.28915	0.001162	416.804
419.304	100.29496	0.001894	421.804
424.304	100.30443	-0.006176	426.804
429.304	100.27355	-0.004826	431.804
434.304	100.24942	0.008172	436.804
439.304	100.29028	-0.000514	441.804
444.304	100.28771	0.00276	446.804
449.304	100.30151	-0.008262	451.804
454.304	100.2602	0.00011	456.804
459.304	100.26075	-0.00101	461.804
464.304	100.2557	-0.011456	466.804
469.304	100.19842	-0.003584	471.804
474.304	100.1805	-0.00162	476.804
479.304	100.1724	-0.01171	481.804
484.304	100.11385	-0.012756	486.804
489.304	100.05007	-0.011788	491.804
494.304	99.99113	-0.025764	496.804
499.304	99.86231	-0.011942	501.804
504.304	99.8026	-0.027078	506.804
509.304	99.66721	-0.033828	511.804
514.304	99.49807	-0.021842	516.804
519.304	99.38886	-0.04461	521.804
524.304	99.16581	-0.059386	526.804
529.304	98.86888	-0.061274	531.804
534.304	98.56251	-0.077562	536.804
539.304	98.1747	-0.08787	541.804
544.304	97.73535	-0.104976	546.804

549.304	97.21047	-0.132806	551.804
554.304	96.54644	-0.137292	556.804
559.304	95.85998	-0.166798	561.804
564.304	95.02599	-0.162898	566.804
569.304	94.2115	-0.183334	571.804
574.304	93.29483	-0.183804	576.804
579.304	92.37581	-0.203876	581.804
584.304	91.35643	-0.212068	586.804
589.304	90.29609	-0.223166	591.804
594.304	89.18026	-0.244518	596.804
599.304	87.95767	-0.24021	601.804
604.304	86.75662	-0.26162	606.804
609.304	85.44852	-0.254002	611.804
614.304	84.17851	-0.287478	616.804
619.304	82.74112	-0.293748	621.804
624.304	81.27238	-0.304872	626.804
629.304	79.74802	-0.325906	631.804
634.304	78.11849	-0.33267	636.804
639.304	76.45514	-0.35958	641.804
644.304	74.65724	-0.366006	646.804
649.304	72.82721	-0.386354	651.804
654.304	70.89544	-0.398196	656.804
659.304	68.90446	-0.387108	661.804
664.304	66.96892	-0.408652	666.804
669.304	64.92566	-0.43773	671.804
674.304	62.73701	-0.42667	676.804
679.304	60.60366	-0.433772	681.804
684.304	58.4348	-0.44767	686.804
689.304	56.19645	-0.669078	691.804
694.304	52.85106	-0.564776	696.804
699.304	50.02718	-0.55471	701.804
704.304	47.25363	-0.542486	706.804
709.304	44.5412	-0.5124	711.804
714.304	41.9792	-0.47798	716.804
719.304	39.5893	-0.483546	721.804
724.304	37.17157	-0.481936	726.804
729.304	34.76189	-0.463478	731.804
734.304	32.4445	-0.45111	736.804
739.304	30.18895	-0.46601	741.804
744.304	27.8589	-0.409546	746.804
749.304	25.81117	-0.428474	751.804
754.304	23.6688	-0.41646	756.804
759.304	21.5865	-0.423748	761.804
764.304	19.46776	-0.400108	766.804
769.304	17.46722	-0.429468	771.804
774.304	15.31988	-0.389234	776.804
779.304	13.37371	-0.382834	781.804
784.304	11.45954	-0.391808	786.804
789.304	9.5005	-0.352958	791.804
794.304	7.73571	-0.3375	796.804
799.304	6.04821		

TPO - 6 hours



First derivative - 6 hours



Appendix O: Pore size distribution data

O1. Large scale test 4: 2 hours of t batch

Pore Diameter (Å)	Pore Volume (cm ³ /g·Å)	f(a)- f(b) (cm ³ /g·Å)	a - b (Å)	Area (cm ³ /g)
451.195	0.022797	0.0352089	139.704	4.918824166
311.491	0.0476208	0.04959915	72.377	3.58983768
239.114	0.0515775	0.04873845	45.407	2.213066799
193.707	0.0458994	0.0450626	30.481	1.373553111
163.226	0.0442258	0.0416524	22.113	0.921059521
141.113	0.039079	0.03876185	16.677	0.646431372
124.436	0.0384447	0.0374745	13.081	0.490203935
111.355	0.0365043	0.0348536	10.674	0.372027326
100.681	0.0332029	0.0323467	8.7874	0.284243392
91.8936	0.0314905	0.0299732	7.4128	0.222185337
84.4808	0.0284559	0.0276538	6.3333	0.175139812
78.1475	0.0268517	0.02695275	5.4835	0.147795405
72.664	0.0270538	0.02488925	4.8004	0.119478356
67.8636	0.0227247	0.02048355	4.2464	0.086981347
63.6172	0.0182424	0.0189734	3.7973	0.072047692
59.8199	0.0197044	0.1147937	1.6964	0.194736033
58.1235	0.209883	0.1134341	1.6912	0.19183975
56.4323	0.0169852	0.0151599	4.59	0.069583941
51.8423	0.0133346	0.0117979	3.7835	0.044637355
48.0588	0.0102612	0.0109611	2.3948	0.026249642
45.664	0.011661	0.122965	1.0866	0.133613769
44.5774	0.234269	0.119564205	1.0699	0.127921743
43.5075	0.00485941	0.00691612	3.0047	0.020780866
40.5028	0.00897283	0.101015415	1.6854	0.17025138
38.8174	0.193058	0.1277697	0.8792	0.11233512
37.9382	0.0624814	0.059165	2.4512	0.145025248
35.487	0.0558486	0.03822465	2.1611	0.082607291
33.3259	0.0206007	0.014561095	2.1318	0.031041342
31.1941	0.00852149	0.00651272	1.8104	0.011790628
29.3837	0.00450395	0.00497072	1.8268	0.009080511
27.5569	0.00543749	0.005690635	1.5865	0.009028192
25.9704	0.00594378	0.00538825	1.6368	0.008819488
24.3336	0.00483272	0.00804411	1.4252	0.011464466
22.9084	0.0112555	0.009580455	1.5175	0.01453834
21.3909	0.00790541	0.007970985	1.8782	0.014971104
19.5127	0.00803656	0.01108148	1.8423	0.020415411
17.6704	0.0141264			

Total area (cm³/g)	17.084	cm³/g
--------------------------------------	---------------	-------------------------

Appendix O: Pore size distribution data

Pore Diameter (Å)	Pore Volume (cm ³ /g·Å)	f(a)- f(b) (cm ³ /g·Å)	a - b (Å)	Area (cm ³ /g)
503.644	0.0315612	0.04685095	169.455	7.939127732
334.189	0.0621407	0.0640208	83.806	5.365327165
250.383	0.0659009	0.06392665	32.493	2.077168638
217.89	0.0619524	0.05992375	26.881	1.610810324
191.009	0.0578951	0.05644105	28.6	1.61421403
162.409	0.054987	0.05283335	21.312	1.125984355
141.097	0.0506797	0.0506787	16.244	0.823224803
124.853	0.0506777	0.04850705	12.947	0.628020776
111.906	0.0463364	0.0452701	10.536	0.476965774
101.37	0.0442038	0.04251625	8.7763	0.373135365
92.5937	0.0408287	0.0409563	7.3797	0.302245207
85.214	0.0410839	0.03751255	6.327	0.237341904
78.887	0.0339412	0.0332577	5.473	0.182019392
73.414	0.0325742	0.0315239	4.794	0.151125577
68.62	0.0304736	0.03020065	4.2557	0.128524906
64.3643	0.0299277	0.0274078	3.7806	0.103617929
60.5837	0.0248879	0.0233016	3.3894	0.078978443
57.1943	0.0217153	0.02091775	3.0768	0.064359733
54.1175	0.0201202	0.020953	2.8067	0.058808785
51.3108	0.0217858	0.0205839	2.5594	0.052682434
48.7514	0.019382	0.01780535	2.3391	0.041648494
46.4123	0.0162287	0.01645145	2.1573	0.035490713
44.255	0.0166742	0.01597445	2.0117	0.032135801
42.2433	0.0152747	0.0206479	1.8666	0.03854137
40.3767	0.0260211	0.07846505	1.698	0.133233655
38.6787	0.130909	0.122555	1.6123	0.197595427
37.0664	0.114201	0.07622345	2.3642	0.18020748
34.7022	0.0382459	0.02982	2.0482	0.061077324
32.654	0.0213941	0.01632285	2.0065	0.032751799
30.6475	0.0112516	0.01200285	1.7215	0.020662906
28.926	0.0127541	0.01272565	1.7504	0.022274978
27.1756	0.0126972	0.01247975	1.5242	0.019021635
25.6514	0.0122623	0.01241815	1.0333	0.012831674
24.6181	0.012574	0.01261785	1.551	0.019570285
23.0671	0.0126617	0.015305	1.9051	0.029157556
21.162	0.0179483	0.0179075	1.873	0.033540748
19.289	0.0178667	0.02140625	1.3061	0.027958703
17.9829	0.0249458	0.0230443	0.965	0.02223775
17.0179	0.0211428			

Total area (cm ³ /g)	24.354	cm ³ /g
---------------------------------	--------	--------------------

Appendix O: Pore size distribution data

Pore Diameter (Å)	Pore Volume (cm ³ /g·Å)	f(a)- f(b) (cm ³ /g·Å)	a - b (Å)	Area (cm ³ /g)
545.72	0.0562425	0.0771431	187.909	14.49588278
357.811	0.0980437	0.09769545	97.528	9.528041848
260.283	0.0973472	0.09751535	37.998	3.705388269
222.285	0.0976835	0.09368945	30.88	2.893130216
191.405	0.0896954	0.08920345	29.415	2.623919482
161.99	0.0887115	0.08639665	21.45	1.853208143
140.54	0.0840818	0.0826992	16.37	1.353785904
124.17	0.0813166	0.07816455	13.081	1.022470479
111.089	0.0750125	0.07239345	10.671	0.772510505
100.418	0.0697744	0.0689822	8.7207	0.601573072
91.6973	0.06819	0.06740365	7.3883	0.497998387
84.309	0.0666173	0.06274915	6.3804	0.400364677
77.9286	0.058881	0.05875335	5.4606	0.320828543
72.468	0.0586257	0.0581528	4.8151	0.280011547
67.6529	0.0576799	0.0571069	4.2852	0.244714488
63.3677	0.0565339	0.0551882	3.7904	0.209185353
59.5773	0.0538425	0.0502627	3.4095	0.171370676
56.1678	0.0466829	0.04760835	3.0853	0.146886042
53.0825	0.0485338	0.04840215	2.8034	0.135690587
50.2791	0.0482705	0.0474745	2.5602	0.121544215
47.7189	0.0466785	0.0452018	2.3473	0.106102185
45.3716	0.0437251	0.04522185	2.1677	0.098027404
43.2039	0.0467186	0.04421785	2.0187	0.089262574
41.1852	0.0417171	0.04860215	1.8647	0.090628429
39.3205	0.0554872	0.06859355	1.733	0.118872622
37.5875	0.0816999	0.09426395	1.621	0.152801863
35.9665	0.106828	0.0901568	1.5285	0.137804669
34.438	0.0734856	0.0661363	1.4547	0.096208476
32.9833	0.058787	0.0523058	2.1098	0.110354777
30.8735	0.0458246	0.04368115	1.8381	0.080290322
29.0354	0.0415377	0.0412785	1.2131	0.050074948
27.8223	0.0410193	0.04259625	1.1393	0.048529908
26.683	0.0441732	0.0431166	1.0921	0.047087639
25.5909	0.04206	0.0418286	1.0503	0.043932579
24.5406	0.0415972	0.04179435	1.0078	0.042120346
23.5328	0.0419915	0.0415249	0.9776	0.040594742
22.5552	0.0410583	0.03974645	0.9681	0.038478538
21.5871	0.0384346	0.03738935	0.9556	0.035729263
20.6315	0.0363441	0.0386106	0.9408	0.036324852
19.6907	0.0408771			

Total area (cm³/g)	42.842	cm³/g
--------------------------------------	---------------	-------------------------

Appendix P: Needs of electrical power

P1. Heating

Argon is considered as monoatomic perfect gas.

stage:

There is no work produced or employed.

Heating from 18 to 650°C at constant pressure (1 atm)

Gaseous current heating:

$$V_{\text{react}} := 10602.9 \text{ cm}^3 \quad Q_{\text{ArTotal}} := 375 \frac{\text{cm}^3}{\text{min}} \quad X_{\text{Ar}} := 1 \quad P_T := 1 \text{ atm} \quad MW_{\text{Ar}} = 0.04 \cdot \frac{\text{kg}}{\text{mole}}$$

$$C_{p\text{MAr}}(T) := \left(4.969 - 0.767 \cdot 10^{-5} \cdot \frac{T}{\text{K}} + 1.234 \cdot 10^{-8} \cdot \frac{T^2}{\text{K}^2} \right) \cdot \frac{\text{cal}}{\text{mole} \cdot \text{K}}$$

$$C_{p\text{Ar}}(T) := \frac{C_{p\text{MAr}}(T)}{MW_{\text{Ar}}}$$

$$C_{v\text{Ar}}(T) := \frac{C_{p\text{MAr}}(T) - R_{\text{GP}}}{MW_{\text{Ar}}}$$

Perfect gas:

$$h_{\text{Ar}}(T) := C_{p\text{Ar}}(T) \cdot T$$

$$u_{\text{Ar}}(T) := C_{v\text{Ar}}(T) \cdot T$$

$$F_{\text{Ar}}(T) := \rho_{\text{Ar}}(T) \cdot Q_{\text{ArTotal}}$$

First law of thermodynamics in open systems: $\Delta U = Q - W - H_{\text{outlets}} + H_{\text{inlets}}$

Energy balances (reactor as the control volume), applied for a transitory processes:

$$\frac{d}{dt} U = F_{\text{in}} \cdot h_{\text{in}} - F_{\text{out}}(t) \cdot h_{\text{out}}(t) + \frac{d}{dt} Q - \frac{d}{dt} W \quad W = 0$$

Integrating:

$$\Delta U_{12} = F_{\text{in}} \cdot h_{\text{in}} \cdot (t_f - t_0) - \int_{t_0}^{t_f} (F_{\text{out}}(t) \cdot h_{\text{out}}(t)) dt + Q_{12}$$

Inlet: constant properties (pure Ar at 18°C, 1 atm)

$$T_{\text{in}} := (18 + 273.13) \text{ K} \quad F_{\text{in}} := F_{\text{Ar}}(T_{\text{in}}) \quad F_{\text{in}} = 1.046 \times 10^{-5} \frac{\text{kg}}{\text{s}}$$

$$h_{\text{in}} := h_{\text{Ar}}(T_{\text{in}}) \quad h_{\text{in}} = 1.516 \times 10^5 \cdot \frac{\text{J}}{\text{kg}}$$

Outlet: temperature changes from 18°C to 650°C (20K/min)

$$\text{Temp}(t) := \left(T_{\text{in}} + 20 \frac{\text{K}}{\text{min}} \cdot t \right) \quad T_{\text{out}}(t) := \text{Temp}(t) \quad t_f := \frac{650 - 18}{20} \text{ min}$$

$$h_{\text{out}}(t) := h_{\text{Ar}}(T_{\text{out}}(t)) \quad F_{\text{out}}(t) := F_{\text{Ar}}(T_{\text{out}}(t)) \quad t_0 := 0 \text{ min}$$

Definition of the states:

$$\text{initial state (1): } T_1 := (18 + 273.13) \text{ K}$$

$$\text{final state (2): } T_2 := (650 + 273.13) \text{ K}$$

In the volume of control, the temperature changes according to the time:

$$m_{VC}(t) := V_{\text{reac}} \cdot \rho_{\text{Ar}}(\text{Temp}(t)) \quad u_{VC}(t) := u_{\text{Ar}}(\text{Temp}(t))$$

$$\text{Dado} \quad Q_{12} := 1000\text{J}$$

$$u_{VC}(t_f) \cdot m_{VC}(t_f) - u_{VC}(t_0) \cdot m_{VC}(t_0) = F_{\text{in}} \cdot h_{\text{in}} \cdot (t_f - t_0) - \int_{t_0}^{t_f} (F_{\text{out}}(t) \cdot h_{\text{out}}(t)) dt + Q_{12}$$

$$Q_{\text{theo}} := \text{Find}(Q_{12}) \quad Q_{\text{theo}} = 3.404\text{J}$$

$$\text{Power}_{\text{Heating_current}} := \frac{Q_{\text{theo}}}{t_f} \quad \text{Power}_{\text{Heating_current}} = 1.795 \times 10^{-3}\text{W}$$

Heat loss in heating stage:

The main heat loss is placed at the top and bottom part of the reactor, which consist of stainless discs of 15cm in diameter. It is considered throughout reactor, this zone is perfectly isolated.

$$T_{\text{ext}} := (18 + 273.13)\text{K} \quad T_{\text{max}} := (650 + 273)\text{K} \quad t_f = 31.6 \cdot \text{min}$$

$$\Delta x_{\text{lid}} := 0.3\text{cm} \quad D_{\text{lid}} := 14\text{cm} \quad D_{\text{ext}} := 11\text{cm}$$

$$k_{\text{air}}(T) := \left(0.2 + 1.538 \times 10^{-4} \cdot \frac{T}{\text{K}}\right) \cdot \frac{\text{W}}{\text{K} \cdot \text{m}} \quad \rho_{\text{Air}}(T) := \frac{0.0289 \left(\frac{\text{kg}}{\text{mole}}\right) \cdot P}{R_{\text{GP}} \cdot T}$$

$$A_{\text{in_out}} := 2 \cdot \left[\frac{D_{\text{lid}}^2}{4} \cdot \pi + \frac{D_{\text{lid}}^2 - (11\text{cm})^2}{4} \cdot \pi + 2\pi \cdot \frac{D_{\text{lid}}}{2} \cdot \Delta x_{\text{lid}} \right]$$

Convection coefficient calculation (empiric correlation):

$$\alpha(T) := \frac{k_{\text{air}}(T)}{\rho_{\text{Air}}(T) \cdot 1000 \frac{\text{J}}{\text{kg} \cdot \text{K}}} \quad \nu(T) := \frac{1.936 \cdot 10^{-5} \frac{\text{kg}}{\text{m} \cdot \text{sec}}}{\rho_{\text{Air}}(T)}$$

$$\text{Pr}(T) := \frac{\nu(T)}{\alpha(T)} \quad \text{Gr}(T) := \frac{2 \cdot g \cdot (T - T_{\text{ext}}) \cdot (0.9 \cdot D_{\text{lid}})^3}{\nu(T)^2 \cdot (T + T_{\text{ext}})} \quad C' := 0.0605 \quad n := \frac{1}{3}$$

$$\text{Nu}(T) := C' \cdot (\text{Pr}(T) \cdot \text{Gr}(T))^n \quad h_{\text{air}}(T) := \frac{\text{Nu}(T) \cdot k_{\text{air}}(T)}{0.9 D_{\text{lid}}} \quad \text{Convection coefficient depends on temperature:}$$

$$\text{Heat_loss}_{\text{Heating}} := \int_{t_0}^{t_f} [A_{\text{in_out}} \cdot h_{\text{air}}(\text{Temp}(t)) \cdot (\text{Temp}(t) - T_{\text{ext}})] dt \quad T_{VC} = \text{Temp}(t)$$

$$\text{Heat_loss}_{\text{Heating}} = 3.485 \times 10^5 \cdot \text{J} \quad \text{pot}_{\text{HeatLoss}} := \frac{\text{Heat_loss}_{\text{Heating}}}{t_f - t_0} \quad (\text{Average})$$

$$\text{pot}_{\text{HeatLoss}} = 183.817\text{W}$$

Heating to the reactor: $t_A := 5 \text{ sec}$ initialization value

$D_{\text{inner}} := 10 \text{ cm}$

$L_R := 135 \text{ cm}$

$$V_{\text{ceramic}} := \left[\frac{\pi}{4} \cdot (D_{\text{ext}}^2 - D_{\text{inner}}^2) \right] \cdot L_R \quad V_{\text{ceramic}} = 2.227 \times 10^3 \cdot \text{cm}^3$$

$$A_{\text{ext}} := 2 \cdot \pi \cdot \frac{D_{\text{ext}}}{2} \cdot L_R \quad A_{\text{ext}} = 0.467 \text{ m}^2 \quad k_{\text{ceramic}} := 0.46 \frac{\text{W}}{\text{K} \cdot \text{m}} \quad (\text{refractory ceramics})$$

$$\alpha_{\text{ceramic}} := 0.261 \cdot 10^{-6} \frac{\text{m}^2}{\text{sec}} \quad C_{\text{ceramic}} = \frac{k_{\text{ceramic}}}{\rho_{\text{ceramic}} \cdot \alpha_{\text{ceramic}}}$$

$$Q_{\text{HR}}(t) := V_{\text{ceramic}} \cdot \frac{k_{\text{ceramic}}}{\alpha_{\text{ceramic}}} \cdot (\text{Temp}(t) - T_{\text{ext}}) \quad \text{POWER}_{\text{heating_reactor}} := \frac{d}{dt} Q_{\text{HR}}(t_A)$$

$$\text{POWER}_{\text{heating_reactor}} = 1.308 \times 10^3 \text{ W}$$

Mean total electrical power necessary in heating stage:

$$\text{POT}_{\text{Heating}} := \text{Power}_{\text{Heating_current}} + \text{pot}_{\text{HeatLoss}} + \text{POWER}_{\text{heating_reactor}}$$

$$\text{POT}_{\text{Heating}} = 1.492 \times 10^3 \text{ W}$$

REFERENCES: ASHRAE 1997 FUNDAMENTS HANDBOOK PROPERTY DATA BANK

Fundamentals of heat transmission" F. Incropera. Ed. Pearson Prentice Hall, 1999.

"Transmisión de Calor", E. Torrella, J.M. Pinazo, R. Cabello, Servicio de Publicaciones, SPUPV 994128

P2. Reaction stage: Previously, hydrogen and ethane are considered as real substances. There is no work produced or employed. Stationary process. Reaction at constant pressure (1atm) and at 650°C. To evaluate the most unfavorable process, no heat produced by reactor is considered (assuming no conversion of reactants)

Gaseous current heating:

$$Q_{\text{Total}} := 1000 \frac{\text{cm}^3}{\text{min}} \quad X_{\text{H}_2} := \frac{3}{4} \quad X_{\text{C}_2\text{H}_6} := \frac{1}{4} \quad P_{\text{total}} := 1 \text{ atm}$$

$$MW_{\text{H}_2} := 0.002 \frac{\text{kg}}{\text{mole}} \quad MW_{\text{C}_2\text{H}_6} := 0.03 \frac{\text{kg}}{\text{mole}} \quad Q_{\text{C}_2\text{H}_6} := X_{\text{C}_2\text{H}_6} \cdot Q_{\text{Total}} \quad Q_{\text{H}_2} := X_{\text{H}_2} \cdot Q_{\text{Total}}$$

$$C_{P_H_2}(T) := \frac{1}{MW_{H_2}} \cdot \left(6.483 + 2.215 \cdot 10^{-3} \cdot \frac{T}{K} - 3.298 \cdot 10^{-6} \cdot \frac{T^2}{K^2} \right) \cdot \frac{\text{cal}}{\text{mole} \cdot K}$$

$$C_{P_C_2H_6}(T) := \frac{1}{MW_{C_2H_6}} \cdot \left(1.292 + 4.254 \cdot 10^{-2} \cdot \frac{T}{K} - 1.657 \cdot 10^{-5} \cdot \frac{T^2}{K^2} \right) \cdot \frac{\text{cal}}{\text{mole} \cdot K}$$

$$Z_{C_C_2H_6} := 0.285 \quad P_{C_C_2H_6} := 48.2 \text{ atm} \quad T_{C_C_2H_6} := 305.4 \text{ K}$$

Energetic balance:

$$\frac{d}{dt}U = - \sum_2 (F_{\text{out}} \cdot h_{\text{out}})_i + \sum_2 (F_{\text{in}} \cdot h_{\text{in}})_i + \frac{d}{dt}Q - \frac{d}{dt}W + \Delta H_{\text{reac}} \cdot r_{\text{reac}}$$

$$\frac{d}{dt}U = 0 \quad \frac{d}{dt}W = 0 \quad \Delta H_{\text{reac}} = 0$$

Stationary and with no work production or employment and considering null the released heat by reaction.

$$\frac{d}{dt}Q_{\text{MAX}} = - \sum_2 (F_{\text{in}} \cdot h_{\text{in}})_i + \sum_2 (F_{\text{out}} \cdot h_{\text{out}})_i = \text{Pot}_{\text{MAX}}$$

Ethane is calculated from grafics and data in ASHRAE 1997 FUNDAMENTALS HANDBOOK and in the chapter of properties of Data Bank :

$$P_{R_C_2H_6} := \frac{P_{\text{total}}}{P_{C_C_2H_6}} \quad P_{R_C_2H_6} = 0.021 \quad \text{In that zone ethane is like a ideal gas: check Z vs Pr table.}$$

Inlet: constant properties (250cm³/min of C₂H₆ and 750cm³/min of H₂) at 18°C, 1atm) $T_{\text{inlet}} := (18 + 273.13)K$ $T_{\text{inlet}} = 291.13 K$

$$\rho_{H_2_in} := \frac{MW_{H_2} \cdot P_{\text{total}}}{R_{GP} \cdot T_{\text{inlet}}} \quad F_{H_2_in} := Q_{H_2} \cdot \rho_{H_2_in} \quad h_{H_2_in} := C_{P_H_2}(T_{\text{inlet}}) \cdot T_{\text{inlet}}$$

$$T_{R_C_2H_6_in} := \frac{T_{\text{inlet}}}{T_{C_C_2H_6}} \quad T_{R_C_2H_6_in} = 0.953 \quad Z_{C_2H_6_in} := 0.98 \quad (\text{Ideal gas})$$

$$\rho_{C_2H_6_in} := \frac{MW_{C_2H_6} \cdot P}{R_{GP} \cdot T_{\text{inlet}} \cdot Z_{C_2H_6_in}} \quad F_{C_2H_6_in} := Q_{C_2H_6} \cdot \rho_{C_2H_6_in}$$

$$h_{C_2H_6_in} := C_{P_C_2H_6}(T_{\text{inlet}}) \cdot T_{\text{inlet}} \quad h_{C_2H_6_in} = 4.986 \times 10^5 \cdot \frac{J}{kg}$$

Outlet: constant properties (250cm³/min of C₂H₆ and 750cm³/min of H₂)
at 650°C, 1atm

$$T_{\text{outlet}} := (650 + 273.13) \cdot \text{K} \quad T_{\text{outlet}} = 923.13 \text{ K}$$

$$\rho_{\text{H}_2\text{out}} := \frac{\text{MW}_{\text{H}_2} \cdot P_{\text{total}}}{R_{\text{GP}} \cdot T_{\text{outlet}}} \quad F_{\text{H}_2\text{out}} := Q_{\text{H}_2} \cdot \rho_{\text{H}_2\text{out}} \quad h_{\text{H}_2\text{out}} := C_{\text{P_H}_2}(T_{\text{outlet}}) \cdot T_{\text{outlet}}$$

$$T_{\text{R_C}_2\text{H}_6\text{out}} := \frac{T_{\text{outlet}}}{T_{\text{C_C}_2\text{H}_6}} \quad T_{\text{R_C}_2\text{H}_6\text{out}} = 3.023 \quad Z_{\text{C}_2\text{H}_6\text{out}} := 0.99 \quad (\text{Ideal gas})$$

$$\rho_{\text{C}_2\text{H}_6\text{out}} := \frac{\text{MW}_{\text{C}_2\text{H}_6} \cdot P_{\text{total}}}{R_{\text{GP}} \cdot T_{\text{outlet}} \cdot Z_{\text{C}_2\text{H}_6\text{out}}} \quad F_{\text{C}_2\text{H}_6\text{out}} := Q_{\text{C}_2\text{H}_6} \cdot \rho_{\text{C}_2\text{H}_6\text{out}}$$

$$h_{\text{C}_2\text{H}_6\text{out}} := C_{\text{P_C}_2\text{H}_6}(T_{\text{outlet}}) \cdot T_{\text{outlet}} \quad h_{\text{C}_2\text{H}_6\text{out}} = 3.407 \times 10^6 \cdot \frac{\text{J}}{\text{kg}}$$

$$\text{Pot_max} = \sum_2 (F_{\text{out}} \cdot h_{\text{out}})_i - \sum_2 (F_{\text{in}} \cdot h_{\text{in}})_i$$

$$\text{Power_max} := h_{\text{H}_2\text{out}} \cdot F_{\text{H}_2\text{out}} + h_{\text{C}_2\text{H}_6\text{out}} \cdot F_{\text{C}_2\text{H}_6\text{out}} - (h_{\text{H}_2\text{in}} \cdot F_{\text{H}_2\text{in}} + h_{\text{C}_2\text{H}_6\text{in}} \cdot F_{\text{C}_2\text{H}_6\text{in}})$$

$$\text{Power_max} = 2.296 \text{ W} \quad \text{Heat_reaction}(t_{\text{batch}}) := \text{Power_max} \cdot t_{\text{batch}}$$

Heat loss in heating stage:

$$T_{\text{mean}} := \frac{T_{\text{ext}} + \text{Temp}(t_f)}{2} \quad T_{\text{mean}} = 607.13 \text{ K}$$

The main heat loss is placed at the top and bottom part of the reactor, which consist of stainless discs of 15cm in diameter. It is considered throughout reactor, this zone is perfectly isolated.

$$\text{Heat_loss}_{\text{Reaction}}(t_{\text{batch}}) := t_{\text{batch}} \cdot [2A_{\text{in_out}} \cdot h_{\text{air}}(T_{\text{mean}}) \cdot (\text{Temp}(t_f) - T_{\text{ext}})]$$

$$\text{pot}_R := 2A_{\text{in_out}} \cdot h_{\text{air}}(T_{\text{mean}}) \cdot (\text{Temp}(t_f) - T_{\text{ext}}) \quad \text{pot}_R = 753.081 \cdot \text{W}$$

Mean total electrical power necessary in heating stage:

$$\text{POT}_{\text{Reaction}} := \text{Power_max} + \text{pot}_R$$

$$\text{POT}_{\text{Reaction}} = 755.377 \text{ W} \quad \text{The energy employed depends on time of batch.}$$

REFERENCES: ASHRAE 1997 FUNDAMENTS HANDBOOK PROPERTY DATA BANK (APPENDIX H)
Fundamentals of heat transmission”F. Incropera. Ed. Pearson Prentice Hall, 1999.
“Transmisión de Calor”, E. Torrella, J.M. Pinazo, R. Cabello, Servicio de Publicaciones, SPUPV 994128